DEVELOPMENTAL TOXICITY OF GLYCERYL TRINITRATE

by
Ghalib Karim Bardai

Department of Pharmacology and Therapeutics
McGill University
Montreal, Quebec, Canada

A thesis submitted to the Faculty of Graduate Studies and Research, McGill University, in partial fulfillment of the requirements for the degree of Doctor of Philosophy

Submitted May 2017

This thesis is dedicated to Zain

ABSTRACT

Glyceryl trinitrate (GTN) is a therapeutic compound that has been shown to be embryotoxic. However, the paucity of current knowledge, with respect to both its activity as a developmental toxicant and the extent of its use during pregnancy, suggests that a detailed evaluation of GTN teratogenicity is warranted. Therefore, the central aim of the research in this thesis was to: (1) investigate the developmental toxicity of GTN in a biological model that is representative of mammalian development, the Japanese quail embryo (*Cotournix cotournix japonica*); (2) determine the ability of the embryo to biotransform the drug; and 3) elucidate the effects of GTN on global gene expression. Both *in-ovo* and ex-ovo quail embryo exposure models were used.

GTN exposure was embryotoxic to quail embryos, inducing developmental pathologies that included microphthalmia and cranio-facial, heart, and neural tube defects. Furthermore, GTN exposure induced an increase in nitrated proteins in these embryos; nitrated proteins may be involved in mediating developmental pathologies in quail embryos during organogenesis.

The increase in nitrated proteins after GTN exposure suggested that the embryo has the ability to metabolize this drug. GTN treatment of quail embryos resulted in an increase in nitrite, a decrease in total glutathione, and an increase in the ratio of NADP+/NADPH, indicating that redox balance may be compromised in exposed embryos. Indeed, alpha- and mu-type glutathione S-transferases (GSTs), purified from the whole embryo and the embryonic eye, had GTN-metabolizing activity. Co-treatment with N-acetyl cysteine, a glutathione precursor,

partially protected against the effects of GTN exposure. Thus, GTN denitration by quail embryo GSTs may represent a key initial step in the developmental toxicity of GTN.

Because the maintenance of redox homeostasis is critical in regulating proper and timely gene expression during embryo development, it was important to determine what perturbations in gene expression were occurring following GTN exposure. Ingenuity pathway analysis suggested that the EIF2, mTOR and WNT/β-CATENIN signaling pathways are most affected by GTN exposure.

In conclusion, GTN is a teratogen in quail embryos. One explanation as to the mechanism by which GTN induces these malformations is that the metabolism of GTN in the quail embryo results in a change in the redox status, which subsequently affects global gene expression. Thus, changes in redox status may dysregulate the expression of genes that are critical in pattern formation during embryo development.

RÉSUMÉ

Le trinitrate de glycéryle (GTN) est un composé thérapeutique pour lequel des effets embryotoxiques ont été observé. Cependant, il y a très peu de connaissances en ce qui concerne son activité toxique sur le développement embryonnaire. Étant donné son utilisation pendant la grossesse, une évaluation détaillée des effets tératogènes du GTN est necessaire. Par conséquent, l'objectif central de ce projet de recherche était de: (1) caractériser la toxicité du GTN sur le développement dans un modèle biologique représentatif du développement de mammifères : l'embryon de caille japonais (*Cotournix cotournix japonica*); (2) déterminer la capacité de biotransformation du GTN par l'embryon; et 3) élucider les effets de GTN sur l'expression des gènes de l'embryon. Des modèles d'exposition aux embryons de caille ont été utilisés à l'intérieur de l'œuf mais aussi ex-ovo.

Nous avons observé dque lexposition au GTN était toxique pour les embryons de cailles, induisant des pathologies de développement incluant des microphtalmies et des défauts cranio-faciaux, cardiaques et neurologiques. En outre, l'exposition au GTN a induit une augmentation des protéines nitrées dans ces embryons. Ces protéines nitrées pourraient être impliquées dans la médiation des pathologies du développement dans les embryons de cailles pendant l'organogenèse.

D’autre part, l'augmentation des protéines nitrées après l'exposition au GTN suggère que l'embryon a la capacité de métaboliser ce médicament. Nous avons mesuré que le traitement au GTN a entraîné une augmentation du nitrite, une diminution du glutathion total et une augmentation du rapport NADP + / NADPH dans les embryons de caille. Ceci indique que l'équilibre redox peut être compromis dans les embryons exposés. De plus, nous avons montré que les S-transferases (GST) de glutathion de type alpha- et mu, purifiées à partir de l'embryon entier et de l'œil embryonnaire, ont une activité métabolisant GTN. Finalement, le co-traitement avec du N-acétyl cystéine, un précurseur de glutathion, a partiellement protégé l’embryon contre les effets de l'exposition au GTN. Nos résultats suggèrent donc que la dénitration de GTN par les GST des embryons de cailles représente une première étape clé dans la toxicité pour le développement de GTN.

Étant donné que le maintien de l'homéostasie redox est essentiel pour réguler l'expression temporelle des gènes pendant des phasses clés du développement embryonnaire, nous avons chercher à déterminer les effets d’une exposition au GTN sur l'expression des gènes. L'analyse de la voie d'ingénierie a suggéré que les voies de signalisation EIF2, mTOR et WNT / β-CATENIN sont les plus affectées par l'exposition GTN.

En conclusion, le GTN est un tératogène dans les embryons de cailles. Une explication sur le mécanisme par lequel le GTN induit ces malformations est que le métabolisme du GTN dans l'embryon de caille donne lieu à une modification de

l'état redox affectant par la suite l'expression globale des gènes. Ainsi, les changements dans l'état redox peuvent déréguler l'expression de gènes qui sont essentiels à la formation de motifs lors du développement embryonnaire.

ACKNOWLEDGMENTS

I would like to thank my thesis supervisors, Drs. Barbara F. Hales and Geoffrey Sunahara for welcoming me into their laboratories, and for their patience, support, and direction throughout my studies.

I wish to express my gratitude to the FRQS for financial support over the course of my studies:

I would like to thank my fellow lab members over the years for their guidance and their support.

I would like to thank my parents. Especially my mother for her wisdom, love, and encouragement. A special thanks to my brother, Zahir Bardai, for his initial advice on my academic direction when I had none that led me down this path. To my sister, Narmin Bardai, for her kindness. She has been there through my joys and difficult times.

Finally, and most importantly, I would like to thank my wife for her patience and providing me the encouragement to see this work to its completion. To my children for having the patience and understanding when I could not be there.

TABLE OF CONTENTS

LIST OF TABLES

Chapter 2

Chapter 3

Chapter 4

LIST OF FIGURES

Chapter 1

Chapter 2

Chapter 3

LIST OF ABBREVIATIONS

1,2-GDN	- 1,2-glyceryl dinitrate
1,3-GDN	- 1,3-glyceryl dinitrate
mALDH2	- mitochondrial aldehyde dehydrogenase
BSA	- bovine serum albumin
BW	- body weight
cDNA	- complementary DNA
cRNA	- complementary RNA
CDNB	- 1-chloro-2,4-dinitrobenzene
CE	- crude extract
DPI	- diphenyliodonium chloride
EA	- ethacrynic acid
eIF2	- eukaryotic initiation factor 2
G	- grams
GSH	- glutathione
GSSG	- oxidized glutathione
GST	- glutathione *S*-transferase
GTN	- glyceryl trinitrate
HH	- Hamburger Hamilton
KOH	- potassium hydroxide
L	- liters
LC/MS	- liquid chromatography-mass spectrometry
Mg	- milligrams
Min	- minutes
mTOR	- mammalian target of rapamycin
NAC	- N-acetyl cysteine
NADP+	- oxidized nicotinamide adenine dinucleotide phosphate

NADPH	- reduced nicotinamide adenine dinucleotide phosphate
Ng	- nanograms
NO	- nitric oxide
NO_2^-	- nitrite
OCT	- optimal cutting temperature compound
pA	- picoamperes
PBS	- phosphate buffered saline
PVDF	- polyvinylidene difluoride
RP	-ribosomal proteins
SDS–PAGE	- Sodium dodecyl sulphate – polyacrylamide gel electrophoresis
TdT	- terminal deoxynucleotidyl transferase
TUNEL	- Terminal deoxynucleotidyl transferase–mediated nick-end labeling
Ug	- micrograms
WNT	- wingless-type MMTV integration site family

PREFACE – CONTRIBUTIONS OF AUTHOR

This thesis is written in manuscript form as permitted by the McGill University Graduate Studies and Research. It is comprised of three original research articles, as listed below, with the contribution(s) of each author.

1) Bardai GK., Hales BF., Sunahara GI. (2011). Developmental toxicity of glyceryl trinitrate in quail embryos. Birth Defects Res A Clin Mol Teratol. 2011 91:230-40.

The candidate conceived, designed, and performed all manipulations. Barbara Hales and Geoffrey Sunahara revised and edited the manuscript.

2) Bardai GK., Hales BF., Sunahara GI. (2013). Glyceryl trinitrate metabolism in the quail embryo by the glutathione S-transferases leads to a perturbation in redox status and embryotoxicity. Comp Biochem Physiol B Biochem Mol Biol. 165:153-64.

The candidate conceived, designed, and performed all manipulations. Barbara Hales and Geoffrey Sunahara revised and edited the manuscript.

3) Bardai GK., Hales BF., Sunahara GI. Global Gene Expression Changes in the Quail Embryo Following Treatment with Glyceryl trinitrate. In preparation.

The candidate conceived, designed, and performed all manipulations. Barbara Hales and Geoffrey Sunahara revised and edited the manuscript.

THESIS ORGANIZATION

To provide a detailed background and familiarize the reader with the current literature and the project, a review of the topics in this dissertation is presented in Chapter 1. Here, I provide a brief introduction to organic nitrates and their developmental toxicity with a detailed look at GTN as it relates to developmental toxicity. Also included is an overview of enzymatic systems that act on GTN, specifically focusing on the glutathione *S*-transferases (GSTs) and glutathione, their required co-factor and a critical regulator of redox status. Finally, I introduce the biological model studies in this thesis, the Japanese quail, and its use in toxicological studies. Chapter 2 describes the effects of GTN on the quail embryo in a dose-response study (Bardai et al. 2011). Chapter 3 presents the purification and characterization of the enzyme(s) capable of metabolising GTN in vitro (Bardai et al. 2013) and the effects of GTN metabolism on the metabolic status of the embryo. Chapter 4 examines the effects of exposure to GTN on global gene expression in the quail embryo. In Chapter 5, I summarize and discuss the implications of this work and further venues for research.

CHAPTER 1 - INTRODUCTION

NITRO-COMPOUNDS

Nitro-compounds are an important group of compounds that include a nitrite (NO_2^-) moiety within their chemical structure. The addition of the nitro group changes the physicochemical and electronic structure of the parent molecule, thereby allowing it to have multiple activities. Nitro based compounds are used in industrial, agricultural, and therapeutic applications. The organic nitrates (amyl nitrite, isosorbide mononitrate, isosorbide dinitrate, and glyceryl trinitrate) are an important group of nitro drugs that are prescribed for their anti-ischemic properties (Abrams, 1985).

ORGANIC NITRATES

Organic nitrates are polyol esters of nitric acid, whereas organic nitrites are esters of nitrous acid. Nitrate esters (-C-O-NO2) and nitrite esters (-C-O-NO) are characterized by a sequence of carbon-oxygen-nitrogen atoms, whereas nitro compounds possess carbon-nitrogen bonds (Fig. 1.1). Amyl nitrite, a highly volatile compound that is administered by inhalation, is of limited therapeutic value; other high molecular weight nitrate esters, such as isosorbide dinitrate and isosorbide mononitrate, are used in solid form. Glyceryl trinitrate (GTN), a low molecular mass organic nitrate, is moderately volatile and must be mixed with an inert carrier, such as lactose, to stabilize it. Of the organic nitrates, GTN is the most widely used pharmacological agent. GTN is structurally the simplest organic nitrate; its anti-ischemic effects are mediated by nitric oxide, formed via reduction of the NO_2^-.

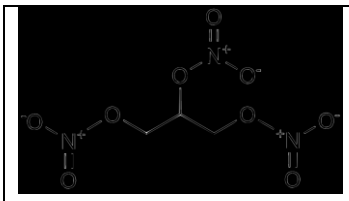

A

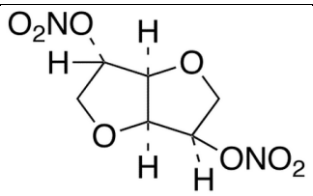

B

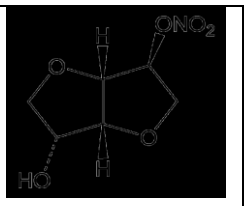

C

Figure.1.1 Structures of: A) glyceryl trinitrate, B) isosorbide dinitrate, C) and isosorbide-5-mononitrate.

PHARMACOLOGY AND CURRENT THERAPEUTIC USE OF GLYCERYL TRINITRATE

Pyroglycerine, the original name given to GTN by its inventor, Ascanio Sobrero (Marsh and Marsh, 2000), results from the nitration of glycerol using a mixture of nitric and sulphuric acids. This process creates an unstable compound; the reaction is highly exothermic and consequencely, GTN is an effective explosive. In addition to its commercially useful properties as a highly energetic material, William Murrell discovered that GTN dramatically and safely alleviated the symptoms of angina pectoris (Murrell, 1879).

GTN is a pro-drug that must be reduced to form gaseous nitric oxide (NO). It is generally accepted that NO is the primary molecule responsible for the relaxation of vascular smooth muscle. For more than a century, GTN has been used in the treatment of coronary artery disease and congestive heart failure because of its hemodynamic effects (Marsh and Marsh, 2000). GTN also has anti-aggregant properties. For example, NO is not only derived from the endothelium, it is also released from activated platelets. NO regulates cyclic guanosine-3,′5′-

monophosphate (cGMP) via activation of soluble guanylate cyclase and is the principal mechanism of negative control over platelet activity (Chirkov et al., 1999). Today, GTN remains the treatment of choice for angina, congestive heart failure, and acute myocardial infarction (Abrams, 1995; Ryan and Gibbons, 1996; Ferreira and Mochly-Rosen, 2012).

Angina pectoris pain, the primary symptom of the ischemic heart disease that affects more than 9 million Americans (Roger et al., 2012), is due to an imbalance in the oxygen supply-demand relationship within the cardiac muscle. GTN can alleviate this imbalance by dilating large conductance veins, arteries, and arterioles. At therapeutic concentrations (2.3 ±0.36 ng/ml) (Bashir et al. 1982; Armstrong et al. 1979) GTN preferentially causes peripheral venodilation that leads to a decrease in the venous return and a corresponding decrease in the sizes of both the left and right ventricular chambers (Abrams, 1996). This action results in a redistribution of circulating blood volume away from the heart and lungs to the splanchnic and mesenteric circulations of the body. This reduction in circulating blood volume results in a decrease in cardiac chamber size, ventricular filling pressure and wall tension, and systemic blood pressure (Abrams, 1985). At higher doses, GTN causes further venous pooling and arteriolar vasodilation. The simultaneous increased arterial conductance and decreased peripheral vascular resistance lessens cardiac work and lowers the myocardial oxygen requirements. This reaction enables the development of a favorable ratio of myocardial oxygen demand to myocardial oxygen supply, thereby preventing or alleviating ischemia.

GTN has additional uses in non-traditional settings, such as pain management (Lauretti et al., 2002) and osteoporosis treatment (Jamal et al., 2006) via modulation of cytokine (IL-1β, TNF-α, and IFN-γ)-induced effects on osteoblast function. Moderate induction of NO potentiates bone resorption, while constitutive production of NO at low concentrations promotes the proliferation of osteoblast-like cells (MacPherson et al., 1999). GTN has also been shown to disrupt signaling pathways (Bryan et al., 2005; Veselik et al., 2008), affecting the energy status of biological systems (Cao et al., 2009; Garcia et al., 2010), modifying proteins (Perlman et al., 2009), and forming both reactive oxygen and nitrogen species (Münzel et al., 1995).

Interestingly, GTN is also considered as a tocolytic therapy in preterm labor to reduce infant morbidity and mortality (Berkman et al., 2003; Black et al., 1999; Smith et al., 1999; Smith et al., 2007). GTN has been shown to cross the placenta (David et al., 2000) and to be metabolized (Bustard et al., 2002). Considering the emerging diverse possible uses of GTN, its therapeutic values during pregnancy, and the ability of GTN to disrupt critical signaling pathways, there is surprisingly little information on the developmental toxicology of GTN.

Mechanism of GTN action

The metabolic conversion of GTN to nitric oxide at or near the plasma membrane of the vascular smooth muscle cell represents the cellular basis for the vasodilatory action of GTN. Murad et al (1999) examined how various vasodilator molecules, including GTN, affected guanylate cyclase activity. They showed that

soluble guanylate cyclase (from rat liver and bovine tracheal smooth muscle) was stimulated by nitrite-containing compounds producing an increase in cGMP, which in turn, brought about vascular relaxation (Gruetter et al., 1981; Murad, 1999). Murad et al. (1999) suggested that cGMP activation may occur via the formation of NO because the gas also increased guanylate cyclase activity. This was the first time that NO was hypothesized to be involved in the mechanism of action of GTN.

There is a consensus today that GTN induces smooth muscle relaxation by supplementing the endogenous production of endothelial nitric oxide (NO) (Daiber et al., 2008). NO is an unstable and highly reactive diatomic molecule because of the presence of an unpaired electron in the π orbital, which allows for overlap with the Fe present in soluble guanylyl cyclase (sGC). The formation of an Fe(II) - NO complex results in the breaking of the His - Fe bond. This then leads to conformational changes that are communicated to the catalytic domain, which converts guanosine triphosphate to the second messenger cyclic 3'5'-guanosine monophosphate (cGMP), and activates cGMP-dependent protein kinase or protein kinase G (PKG) and cGMP-gated ion channels (Francis et al., 2010). The phosphorylation of target proteins by PKG causes a decrease in intracellular Ca^{2+} levels. The decreased Ca^{2+} in vascular smooth muscle, in turn, leads to a decrease in the phosphorylation of the myosin light chains in vascular smooth muscle cells. Because phosphorylation of the myosin light chains is required for tension to develop in smooth muscle cells, the decreased Ca^{2+} concentrations in vascular smooth muscle cells induces relaxation (Rapoport et al., 1983). For this sequence of events to occur, however, GTN must be biotransformed.

Biotransformation of GTN

GTN functions as a pro-drug; biotransformation to release NO_2^- is required to produce NO at its site of action in vascular smooth muscle. Data from cell culture and organ bath studies suggest that there are two pathways that operate in the biotransformation of GTN: (1) a mechanism-based and (2) a clearance based pathway (Hashimoto and Kobayashi, 2003). “Mechanism-based biotransformation” is distinguished from “clearance-based biotransformation” because nitric oxide (NO) is produced and contributes directly to vasodilation; this is accompanied by an excess of the 1,2-glyceryl dinitrate (GDN) metabolite relative to 1,3-GDN. The latter results in the production of biologically inactive metabolites and has no apparent cardiovascular effect. In the “clearance-based pathway,” equimolar amounts of both GTN metabolites, 1,2-GDN and 1,3-GDN, are produced, as well as nitrite and nitrate (Hashimoto and Kobayashi, 2003; Münzel et al., 2003). This metabolic pathway is catalyzed by glutathione reductase (GR) and glutathione-*S*-transferases (GSTs) (Kurz et al., 1993). The biotransformation of GTN can also occur via non-enzymatic reactions. Non-enzymatic reactions require very high concentrations (millimolar) of the thiol, L-cysteine; therefore, while the enzymatic biotransformation of GTN is well-documented (Münzel et al., 2005), the relevance of non-enzymatic biotransformation reactions for GTN *in-vivo* is questionable (Mayer and Beretta, 2008). The metabolites produced via the biotransformation of GTN, 1,2-GDN and 1,3-GDN, are capable of producing NO; however, they are less than one tenth as potent as GTN in inducingt relaxation of rabbit aortic strips (Salvemini et al., 1993; Wenzel et al., 2007).

Inorganic nitrite (NO_2^-) is the predominant nitrogen-oxide-containing species that has been demonstrated to be formed from GTN during incubation with vascular tissue (Bennett et al., 1994). Previously considered an oxidative product of NO metabolism, it is now clear that NO_2^- is an obligate intermediate in the generation of NO. The creation of NO_2^- from GTN occurs prior to NO generation, which indicates that NO_2^- is a precursor of NO and not its oxidation product (Kozlov et al., 2003). The known enzymes capable of metabolizing GTN to NO_2^- are as follows: glutathione *S*-transferases (GSTs), xanthine oxidoreductases, and mitochondrial aldehyde dehydrogenase (mtALDH) (Beretta et al., 2008; Chen et al., 2002; Mayer and Beretta, 2008). Of these enzymes, the GSTs are responsible for the largest proportion of enzymatic activity present in the cytoplasm (Board, 2007), where the highest rate of GTN biotransformation to NO_2^- occurs, and therefore represent the most important source of enzymatic GTN metabolizing activity and NO_2^- production (Lau and Benet, 1990).

GLUTATHIONE -*S*-TRANSFERASES

Living organisms have evolved different enzymatic systems to deal with toxic and xenobiotic products. These enzymes are found in Phase I (oxidation, reduction and hydrolysis); and Phase II (conjugation) reactions. Glutathione transferases (GST E.C. 2.5.1.18), a Phase II group of enzymes, are a family of dimeric enzymes that catalyze the nucleophilic attack of reduced glutathione (GSH) on the electrophilic centres of a wide variety of compounds (including therapeutic drugs). In mammals, there are three distinct GST families: the cytosolic

GSTs; the mitochondrial and peroxisomal “kappa” GSTs; and the microsomal GSTs, also known as MAPEGs (membrane-associated proteins in eicosanoid and glutathione metabolism) (Hayes et al., 2005). Studies on the subcellular localization of GSTs show that most GSTs are localized in the cytoplasm; GSTs represent up to 10% of cytosolic protein in the liver (Board, 2007). The cytosolic GST enzyme family, therefore, is one of the most important groups of isozymes participating in the catalytic biotransformation of xenobiotics.

Cytosolic GSTs

Mammalian cytosolic GSTs are homodimers with subunits ranging in molecular weight from 23 – 29 kDa (Hayes et al., 2005). Each subunit is 199-244 amino acids in length and contains one catalytic site. Based on amino acid sequence similarities, seven classes of cytosolic GST are recognized in mammalian species, and are designated as alpha, mu, pi, theta, sigma, zeta, and omega (Hayes and Pulford, 1995). GSTs are classified based on their primary structure at the N-terminus because, within the classes, this region tends to be better conserved than others and it includes an important part of the active site that is thought to be a key component in the catalytic activity of GSTs (Sheehan et al., 2001). It is generally accepted that GSTs share greater than 60% identity within a class, and that those with less than 30% shared identity are assigned to separate classes (Tew, 2007)

Catalytic activities of GSTs

GSTs catalyze the general reaction: GSH + R-X → GSR + HX. The function of the enzymatic reaction is to: (1) bring the substrate into proximity with glutathione (GSH) by binding both GSH and the electrophilic substrate to the active site of the protein, and (2) activate the sulfhydryl group on GSH, thereby allowing for nucleophilic attack of GSH on the electrophilic substrate that may be provided by a carbon, nitrogen or sulfur atom (Hayes and Pulford, 1995). Electrophilic groups are present in epoxides, aliphatic and aromatic halides, and in organic nitrate esters, such as GTN (Eaton and Bammler, 1999). The catalytic region of the enzyme contains an essential tyrosine, serine or cysteine residue that interacts with the thiol group of GSH, which then lowers its p*K*a to a value of approximately 6-7 (from its normal p*K*a value ~9). This is thought to be a key component of catalysis by the GSTs (Atkinson and Babbitt, 2009). The primary function of the N-terminal domain of GSTs is to provide a hydrophilic G-site (G for binding glutathione) for nucleophilic activation of the sulfhydryl group in GSH. This is done by the hydroxyl group of a conserved tyrosine that can establish a hydrogen bond with the GSH sulfur atom to form a highly reactive GSH thiol (GSH → GS•). This is the most conserved region in all the cytosolic GST enzymes, and is found in a cleft between the N- and C-terminal domains. The other site is an adjacent H-site that provides a hydrophobic environment for the binding of structurally diverse electrophilic xenobiotic substrates (Armstrong, 1997). Studies with the classical electrophilic substrate 1-chloro-2,4-dinitrobenzene (CDNB) show that the enzymatic activity of the enzyme occurs via positive cooperativity binding

throughout the C-terminal orientation. When GSH binds to the enzyme, conformational changes involving the C-terminal region are transmitted to the H-site, increasing the affinity for the electrophilic atom as well as the reaction rate of GS-X complex formation. This type of catalytic activity is thought to occur in the biotransformation of GTN (Stella et al., 1999).

Role of GST in the biotransformation of GTN

GTN has three electrophilic nitrogens. The involvement of GST in the biotransformation of GTN was initially demonstrated by Needleman and Hunter (Needleman and Hunter, 1965). This study showed that continuous perfusion of isolated rat livers with GTN resulted in a concentration dependent depletion of ATP and hepatic glutathione (GSH), a co-factor that is absolutely required for GST denitration activity. Furthermore, it was later shown that pretreatment of rats with bromobenzene caused a 70% reduction in hepatic GSH, which resulted in a marked inhibition (90% decrease) of GTN metabolism by the perfused liver (Needleman and Harkey, 1971). Additional biochemical studies using cytosolic fractions showed that GTN was denitrated to nitrous acid and glyceryl dinitrate by a GST type enzyme and that the reaction was GSH dependent (Keen et al., 1976). Further evidence for the involvement of GST type enzymes was provided using GST inhibitors, such as ethacrynic acid (EA) (Kurz et al., 1993).

GST isoforms showing activity towards GTN have been purified from human (Tsuchida et al., 1990), rabbit (Kurz et al., 1993), and rat aorta (Kenkare and Benet, 1996; Nigam et al., 1996; Primiano and Novak, 1993). In rat aorta, two alpha class,

one mu class, and one pi class GST were identified (Kashfi et al., 1994; Nigam et al., 1996). Nigam (Nigam et al., 1996) using class selective GST inhibitors, immunoprecipitation, and purified GST subunits to determine which rat vascular GSTs had biotransformation activity toward GTN. These studies suggested that GTN biotransformation in rat aorta can be attributed mainly to the class mu GSTs, while the alpha class isoforms, present at very low levels, were also shown to biotransform GTN (Singhal et al., 1996). The other isoforms (including the pi isoform, which is the most abundant) showed much lower activity towards GTN (Singhal et al., 1996). Tsuchida (Tsuchida et al., 1990) demonstrated that the mu class GST isoenzymes identified in human aorta biotransformed GTN, whereas the pi isoenzymes did not. The enzymatic activities of cytoplasmic alpha and mu class GSTs are, therefore, the critical and obligatory first steps in the biotransformation of GTN to NO_2^- and require the intracellular co-factor glutathione (GSH).

EMERGING ROLES OF GST

To date, all the functions ascribed to cytosolic GSTs show them to be primarily detoxifying enzymes (Sherratt and Hayes, 2001). However, GSTs have been found in other sub-cellular locations, such as the nuclei of many cells types. For example, GST alpha was detected in the nuclei of human hepatocytes (Campbell et al., 1991) and neurons (Johnson et al., 1993), microsomal GSTs have been in the nuclei of primary spermatocytes (Otieno et al., 1997), and class theta GSTs were discovered in the nuclei of mouse and human liver cells (Sherratt et al., 2002). In addition, an increased nuclear expression of GST pi (GSTP) was

found in many malignancies and cancer cell lines (Orlandi et al., 2009). Furthermore, studies with cell lines that are used to interrogate resistance to toxic chemicals have shown that resistant cell lines have high GSTP1-1 protein expression and nuclear sublocalization (Lo et al., 2008). The cDNA-directed expression of GSTP1-1 in such cell lines can increase resistance to cytotoxic agents (Board, 2007). Other studies have established that the nuclear expression of GSTP increases in response to treatment with anticancer drugs (Goto et al., 2002; Tew and Townsend, 2011). Mechanistic studies of the regulation of GSTP, in association with carcinogenesis, suggest that the dimeric form of GSTP has the capacity to interact specifically with the C-terminus region of the mitogen-activated protein kinase (MAPK) JNK complex (Gildenhuys et al., 2010; Wang et al., 2001). The activation of this kinase cascade via JNK phosphorylation, and the subsequent transactivation of c-JUN transcription factors linked to cell proliferation (Shaulian and Karin, 2001) occurs following destabilization of the GSTP-JNK complex during oxidative stress (Adler et al., 1999). Lastly, the alpha class GST, GSTA1-1 has been associated with the outer nuclear membrane and compartmentalized in the nucleus of hepatocytes (Stella et al., 2007). Therefore, it is evident that besides the detoxification role that has been classically ascribed to GSTs, they also play an important role in regulating the stress response.

GLUTATHIONE

Glutathione (GSH), discovered in 1888 by Rey Pailhade, was originally termed an “organic hydrogenate of sulphur” (Mora 2011). Glutathione (GSH), a tripeptide of glutamic acid, cysteine, and glycine, an important co-factor in the enzymatic reactions involving GST, is the most abundant non-protein thiol (up to 10 mM) (Tateishi et al., 1974). GSH is found in the cytosol (90%), mitochondria (10%), endoplasmic reticulum, and the nucleus (Meister, 1991). As a tripeptide, GSH is less prone to oxidation than cysteine itself, making it an ideal compound for maintaining intracellular redox potential. One approach to determine the cellular redox status is to quantify GSH and GSSG and calculate the half-cell redox potential (Eh, expressed in mV) of the GSSG/2GSH couple with the Nernst equation (Flohé, 2013). Using this equation, intracellular Eh values ranging from -165 (oxidized) to -258 mV (reduced) have been measured in various cell types and cell states (Schafer and Buettner, 2001).

Functions of GSH

Traditionally, the role of GSH has been related mainly to the protection of macromolecules against oxidative stress, defined as “an imbalance in prooxidants and antioxidants with associated disruption of redox circuitry and macromolecular damage” (Go and Jones, 2010). This early definition was derived from the physiological functions ascribed to GSH that included regulation of enzymatic activity (Ernst et al., 1978; Ziegler, 1985), amino acid transport (Viña et al., 1989), control of cytoskeleton assembly (Burchill et al., 1978), and protection against electrophilic insult via GST (Boyland and Chasseaud, 1969). Therefore, the abundance of GSH, its redox properties, and its lack of toxicity make it an ideal cellular thiol “redox buffer” to maintain a given thiol/disulfide redox potential (Sies, 1999), and a crucial molecule in protecting the cell against oxidants and electrophilic insult.

As the role of GSH in the maintenance of cellular redox homeostasis was being pursued, studies on cellular proliferation showed that tumor cells demonstrated higher GSH levels during the exponential growth phase than during a non-dividing state (Harris and Patt, 1969; Post et al., 1983); a decrease in GSH biosynthesis in vivo inhibited tumor growth rate (Kosower and Kosower, 1978). While these studies showed a causal relationship between cellular proliferation and GSH levels, Atazori et al. (Atzori et al., 1990) reported that GSH must reach certain critical levels before proliferation can be initiated, and that variations in the protein sulfhydryl redox status may relate directly to regulation of cell growth. This critical study showed that GSH is directly involved in cell proliferation and growth.

The link between the redox status of a cell and the ability of the cell to undergo proliferation was demonstrated by Nkabyo et al. (2002), who concluded that each phase in the life of the cell is characterized by its cellular redox state, as determined by the glutathione (GSH)/glutathione disulfide (GSSG) ratio. Proliferating cells are in the most reduced state, with Eh values between -260mV and -230mV (Schafer and Buettner, 2001). Upon a growth arrest caused by differentiation (Nkabyo et al., 2002) or contact inhibition (Schafer and Buettner, 2001), cells are 40 mV more oxidized (-220mV to -190mV), whereas the apoptotic process is accompanied by further oxidation, up to -165mV.

Therefore, when the cell progresses from proliferation, through contact inhibition, differentiation, and finally apoptosis, there is a change from a reduced to an oxidized cellular redox environment. Because this model also applies universally to cells from different organisms (Schafer and Buettner, 2001), a hypothesis was put forward by Schafer and Buettner (Schafer and Buettner, 2001). This hypothesis was that thiols and disulfides, via the GSSG/2GSH couple, may function as nano-switches that move the cell from proliferation through differentiation towards programmed cell death if the redox environment cannot be maintained, or necrosis when the oxidative insult is too severe. This hypothesis led to further studies unravelling novel roles of GSH in cells.

Novel Cellular Roles of GSH

The hypothesis put forward by Schafer and Buettner (Schafer and Buettner, 2001) led to research into new roles of GSH. An important result of this research was a redefinition of the redox status. Classically, the redox status was defined based upon the ratio of GSH to its disulfide, GSSG (Flohé, 2013). However, redox homeostasis is now also defined by the GSH content that is utilized by proteins themselves. For example, large-scale analysis of the proteome has identified the disulfide proteome (i.e., proteins containing a redox sensitive cysteine) as being made up of two subproteomes, a structural group and a redox-sensitive group (Fan et al., 2009). On exposure to nitrosative stress, the redox sensitive group can undergo post-translational modification through disulfide linkages between GSH and redox-sensitive cysteine residues within proteins (Mieyal et al., 2008). This adds a tripeptide and a net negative charge that can lead to both structural and functional changes in the target protein. This process, termed *S*-glutathionylation, is reversible and therefore has the potential to act as an integral biological switch in a number of critical signaling events (Townsend, 2007). Menon et al. (2003) demonstrated the requirement for an oxidative event in early G1 phase for cells to proceed to S phase. Conour et al. (2004) have shown that a significant increase in GSH, combined with static ROS production, indicates an overall re-reduction of the intracellular environment as cells progress from G1 to G2/M phase. These studies suggest the potential for an oscillating intracellular redox environment within the nucleus to regulate cell cycle progression.

Role of nuclear GSH

Markovic et al (Markovic et al., 2010) showed that cells concentrate GSH in the nucleus during early phases of cell growth when most of the cells are in an active division phase. GSH then redistributes uniformly between the nucleus and the cytoplasm when cells reach confluence. This suggests that GSH concentrations cannot be regarded as static, and that differing concentration levels within the nucleus may be critical to the regulation of the cell cycle.

The current model of cell-cycle regulation incorporates a redox cycle, whereby prior to initiation of the cell cycle (Fig. 1.2A), GSH is equally distributed between the cytoplasm and nucleus. Low levels of cellular oxidation combined with low GSH levels are required early in the G1-phase of the cell cycle (Menon et al., 2003) (Fig. 1.2B).

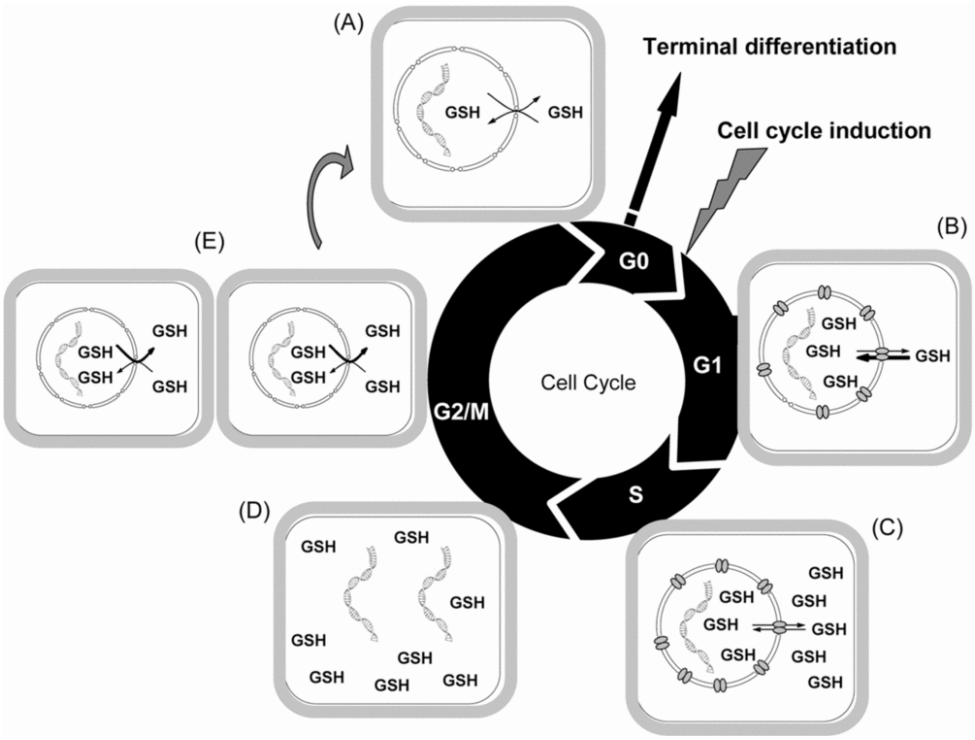

Figure 1.2. The glutathione cycle within the eukaryotic cell cycle. (Diaz Vivancos et al., 2010)

For cells to then progress from the G1- to the S- phase, an increase in total GSH is necessary (Conour et al., 2004) (Fig 1.2C). The discovery that GSH is recruited into the nucleus from the cytoplasm during the cell cycle in animal cells (Markovic et al., 2007; Pallardó et al., 2009) is perhaps one of the most important findings in understanding how changes in GSH play a role in mediating developmental toxicity. For example, the depletion of cytoplasmic GSH decreases the oxidative defense capacity of the cell, as indicated first by the transcriptome profile, which shows a decreased abundance of antioxidant and defense transcripts (Diaz Vivancos et al., 2010). A second major consequence of a depletion of the cytoplasmic GSH pool could be an impairment of the signaling

pathways that up-regulate cellular defense in response to xenobiotic insults, which have a direct requirement for cytosolic GSH.

Role of GSH in the developing embryo

Embryo development proceeds from fertilization to birth. Interspersed within this period are stages during which the embryo goes through dramatic changes beginning with cleavage and blastulation. This is then followed by implantation, gastrulation and early organogenesis, organogenesis and fetal growth and development, cumulating in the establishment of normal anatomical structure and function in the embryo or fetus (Ufer et al., 2010). Key times of susceptibility to xenobiotics include the period of organogenesis, when organs are developing, and the fetal period. Exposure during the embryonic period may result in embryonic death or structural birth defects.

The progression through the developmental stages involves dramatic changes in programmed cell proliferation and differentiation. While the master control of these signaling events ultimately resides in the genetic code, the signaling events that ultimately lead to changes in cellular proliferation, differentiation and symmetry are dependent upon redox dependent transcription factors and signaling maintained by GSH (Harvey et al., 2002). Transcription factors require a reduced environment to bind to DNA and are involved directly in transcription, nucleotide metabolism, (de)phosphorylation, or (de)ubiquitinylation, all essential processes for cell cycle progression and normal embryo development. For example, during cleavage and blastulation, the transcription factor p65 (RelA),

belonging to the nuclear factor κB (NF-κB) family of transcription factors consisting of five members, p50 (NF-κB1), p52 (NF-κB2), c-Rel, and RelB, is essential for embryo development (Yan and Hales, 2005; Beg et al., 1995). Other redox sensitive transcription factors expressed during the embryonic period are Activator Protein-1 (AP1) (Shaulian and Karin, 2002), while nuclear factor (erythroid-derived 2)-like 2 (Nrf2) is a transcription factor which binds with high affinity to the antioxidant response element (AREs) and, thus, are of major importance for regulation of the expression of gene products containing this cis-regulatory element in their promoters.

Therefore, the disruption of redox homeostasis during susceptible periods of embryonic development by endogenous or xenobiotics can result in developmental pathologies as has been shown to occur by the well documented teratogen, thalidomide.

Thalidomide: A developmental teratogen

Thalidomide, a known developmental toxicant causing limb reduction malformations after exposure *in utero*, was initially shown to have no adverse developmental effects in rats during pre-clinical testing of the drug (Janer et al., 2008). The role of nuclear glutathione in the deleterious effects of thalidomide was investigated using a thalidomide-resistant (rat) and a thalidomide-sensitive (rabbit) species (Hansen et al., 2002) to compare potential differences among limb bud cells. These studies revealed that glutathione distribution was different in these cell types, with thalidomide inducing cytosolic GSH depletion in both cell lines. In the thalidomide resistant species, however, nuclear GSH levels remained high;

this was not observed in the rabbit thalidomide-sensitive cells. A more recent study (Knobloch et al., 2008) using mouse embryo fibroblasts to delineate the basis for the species susceptibility to thalidomide, suggested that mouse embryo fibroblasts (MEFs) are resistant to the effects of thalidomide. This was due to approximately five-fold higher levels of GSH in mouse embryo fibroblast compared with sensitive species. Furthermore, pharmacological depletion of GSH sensitizes MEFs to thalidomide-initiated superoxide anion formation and apoptosis that is observed both in human and chick embryo fibroblasts.

Given these data, GSH is intimately linked to the dramatic changes in oxidative status that occur in the nucleus during the cell cycle, thereby influencing genetic and possibly epigenetic changes.

DEVELOPMENTAL TOXICITY OF ORGANIC NITRATES

Data regarding the developmental effects of GTN in humans comes from The Collaborative Perinatal Project, a study that described the health of four children with physical disabilities (from a group of 15 patients) who were exposed to a combination of GTN and amyl nitrite during the first-trimester of pregnancy, along with eight patients who had been exposed to other vasodilators (as cited in Briggs et al., 2008). Furthermore, published data, according to TERIS, an automated teratology resource, indicate that GTN has a “non-determined” rating of risk due to the lack of data (Friedman et al., 1990).

The few animal studies conducted using other organic nitrates show contradictory results. In rats, doses of 500 mg/kg/day of isosorbide mononitrate caused significant increases in the prolongation of gestation, prolonged parturition, stillbirth, and neonatal death (Wyeth-Ayerst Laboratories, 1993a). Isosorbide dinitrate, at doses 35 and 150 times the maximum recommended human dose, produced dose-related embryo toxicity in rabbits (Wyeth-Ayerst Laboratories, 1993b). Studies conducted with GTN in rats and rabbits, however, showed no adverse fetal effects. Taken together, these studies suggest that current data regarding the developmental toxicity of GTN are incomplete and ambiguous. Furthermore, the developmental toxicity data regarding GTN’s predominant metabolite, nitrite, suggest that a detailed teratological evaluation of GTN is needed (Kociba and Sleight, 1970; Veselik et al., 2008). To gather more comprehensive information, as described in the present thesis, we performed a

series of experiments to better understand the developmental toxicology of GTN using a classical and widely accepted animal model.

THE AVIAN SPECIES AS A BIOLOGICAL MODEL IN TOXICITY TESTING

Presently, model systems used for developmental biology and toxicology studies include the nematode (*Caenorhabditis elegans*), the fruit fly (*Drosophila melanogaster*), the zebrafish (*Danio rerio*), the South African clawed toad frog (*Xenopus laevis*), the mouse (*Mus musculus*), and the chicken (*Gallus gallus*). Of these model organisms, the chicken embryo has the longest continuous history as an experimental model for studies in developmental biology (Stern, 2004) and across various disciplines within the biological sciences (Vorster and Lizamore, 2001). Another avian species that is often overlooked is the Japanese quail (*Coturnix coturnix japonica*) (Huss et al., 2008).

The Japanese quail embryo: *Coturnix coturnix japonica* is our model system

The Japanese quail is a member of the pheasant family. In comparison to the chicken egg, Japanese quail eggs are small, measuring about 30 mm in length and weighing approximately 10 g. The incubation period of the Japanese quail is approximately 16.5 d, and the embryos are hardy with a low mortality rate (Ainsworth et al., 2010; Huss et al., 2008; Sellier et al., 2006). When compared to the chicken, the rapid advancement to sexual maturity and prodigious egg production of the Japanese quail all combine to substantially shorten the time

needed to carry out toxicology and developmental studies (Ainsworth et al., 2010; Huss et al., 2008).

The Japanese quail has been well described as a research model by Padgett and Ivey (1959). A detailed developmental atlas of the quail (Padgett and Ivey, 1960), based on the 1951 chicken staging system of Hamburger and Hamilton (Hamburger and Hamilton, 1951), also exists. These staging studies, while helpful at the time, were incomplete, and variations in descriptions, stages, and incubation timings make comparison to the chick model difficult. In addition, the accelerated ontogeny of quail embryos at mid to late stages of development means that an equitable comparison to the chick is ineffective. However, Sellier et al. (2006) produced a detailed study looking at the first 72 h of development of Japanese quail, chick, turkey, duck, goose, and guinea fowl. An online quail developmental atlas is also available (Ruffins et al., 2007). Ainsworth et al. (2010) produced a detailed developmental staging atlas for the quail by studying 400 embryos at earlier incubation ages, when developmental differences between each hour time-point are more pronounced. These results clearly indicate that there are minimal differences between the rate of quail embryonic development and chick embryos up to HH stage 28. However, the quail embryo, from stage 29 onwards, develops at an accelerated rate, reaching HH stage 46 approximately 100 h earlier than the chick. Therefore, up to this period (stage 28), chick and quail embryos can be directly compared using either the descriptive details or stages of development (Ainsworth et al., 2010) (Fig. 1.3). Given this recent comparative

study, comparisons between the Japanese quail and the well-described chicken embryo are possible.

Additionally, another piece of evidence that allows comparisons between the two species is based on integrated linkage map analysis of 1,050 quail from three independent F2 populations (Kayang et al., 2006). Although the quail and the chicken have a divergence that goes back to 35 million years (Pereira and Baker, 2006), studies performed by alignment of microsatellite data with the Amplified Fragment Length Polymorphism map together with Fluorescence In Situ Hybridization, reveal very high similarities between the two species for eight macrochromosomes and the 14 microchromosomes (Kayang et al., 2006) The high conservation of gene order between the two species suggests that information from the chicken model can reliably be used for genome analyses in quail.

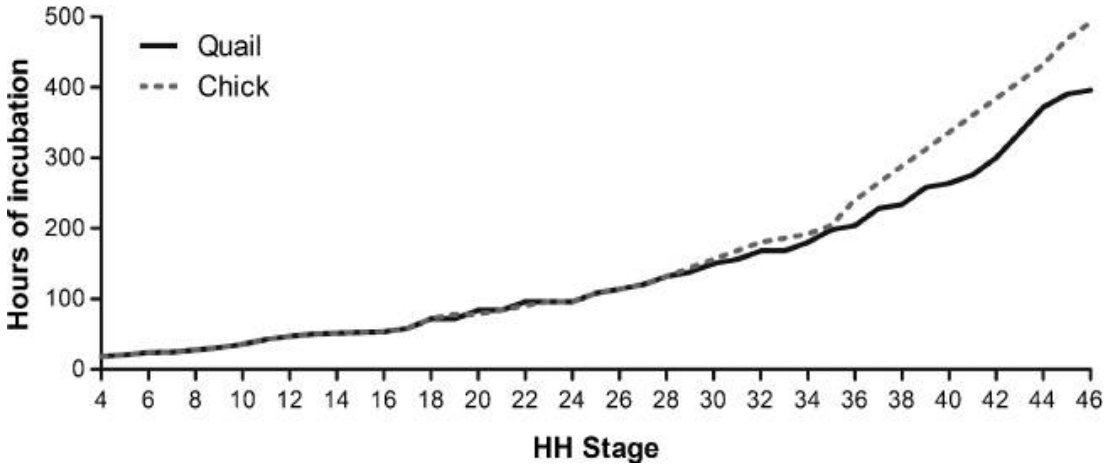

Figure 1.3. Graph showing the average developmental rate (hours of incubation) for Japanese quail and chick embryos, related to HH stages. (Ainsworth et al., 2010)

Use of Japanese quail in biological studies

While originally used for studies in developmental biology, the Japanese quail and the Japanese quail embryo are also used to investigate the reproductive toxicology of chemical compounds and the effects of environmental endocrine disruptors (Gregus et al., 1983; Ottinger et al., 2005). Other practical advantages of using quail (aside from those described above) are that, unlike the embryo of a rodent, quail embryos are easily accessible and manipulated during normal development. Toxicants can be administered readily to the embryo *in ovo* using well-developed techniques (Drake et al., 2006; Stephens, 2009). The ability to harvest and grow the embryo *ex ovo* has been extensively documented (Chapman et al., 2001) and used to investigate basic mechanisms in developmental biology and the mechanisms of action of toxicants. Another major advantage to using this model in elucidating the mechanisms of action of a drug is that the quail embryo lacks a placental system, which might be a hindrance to understanding what drugs do at the embryonic stage in mammalian models. The lack of a placental system in the quail allows the evaluation of the direct action of a drug on the embryo and the determination of whether the embryo contains all the necessary enzymes to metabolize or detoxify the drug.

STUDY RATIONALE

The organic nitrates, due to their mechanisms of action, are excellent anti-ischemic drugs with widespread use; other novel therapeutic uses of GTN include pain management (Lauretti et al., 2002), osteoporosis (Jamal et al., 2006) and as a tocolytic therapy in preterm labor to reduce infant morbidity and mortality (Berkman et al., 2003; Black et al., 1999; Smith et al., 1999; Smith et al., 2007). Given their widespread use and the paucity of toxicological data, there is a need for a detailed teratological evaluation of organic nitrates.

Of the organic nitrates, GTN is widely used, well studied, and simple in terms of chemical structure (i.e., it has three nitrates linked by an ester bond to a glycerol backbone). These properties make this compound an ideal molecule to study the developmental toxicity of organic nitrates. GTN, a pro-drug, is metabolized by many enzymatic systems, including the glutathione S-transferases (Bennett et al., 1994). During the metabolism of GTN via GSTs, glutathione (GSH) is utilized and nitrite (NO_2^-) is released. GSH is the major intracellular regulator of redox status in the mammalian cell and is critical to normal embryo development. In the developing embryo, GSH availability is limited and therefore perturbation in the redox status may disrupt embryonic development (Gardiner and Reed, 1995; Shi et al., 2000). GTN also induces the formation of reactive oxygen species, such as superoxide (Münzel et al., 1995), causes post-translational protein modifications (Perlman et al., 2009), and alters pyrimidine nucleotide ratios (Garcia et al., 2010), all of which are critical biochemical processes to normal embryo development. Nitrite, the metabolite of GTN, activates second messenger

pathways (Bryan et al., 2005) and is understood to be a developmental teratogen (Fan and Steinberg 1996). Despite the extensive use of GTN in therapeutics, its unique metabolism, and the known biological reactivity of its metabolites, relatively little is known about the developmental toxicity of GTN.

HYPOTHESIS

I hypothesize that GTN is a developmental toxicant in the quail embryo. I propose that the embryo metabolizes GTN via a GST type enzyme. This GST metabolism of GTN utilizes GSH, resulting in a disruption of redox status. Disturbances in redox homeostasis during embryo development will result in the aberrant activation of transcription factors and changes in gene expression that may explain the embryo dysmorphogenesis that is observed.

To test this hypothesis, I investigated, for the first time, the developmental toxicity of GTN in the quail embryo. I first determined at what point during development, the embryo was most sensitive to GTN exposure. My next goal was to characterize the types of malformations induced at this stage of development. I investigated the role of metabolism in the developmental toxicity of GTN by characterizing the enzymes in the quail embryo that are capable of metabolizing GTN. The consequences of this metabolic activity, both in terms of the redox and metabolic status of the embryo, were examined. Finally, I explored the molecular basis for the adverse effects of GTN on quail embryo development by elucidating the effects of this drug on global gene expression.

OBJECTIVES

I investigated the developmental teratogenicity of GTN by: (1) treating quail embryos, a biologically relevant embryo model, with GTN during various windows of development to determine the most sensitive period of exposure; (2) characterizing and purifying the enzymes capable of metabolizing GTN in the embryo; (3) executing a series of *ex ovo* and *in ovo* supplementation studies to examine the effects of GTN on the redox and metabolic status of the embryo; and, (4) measuring the effects of GTN exposure *in vivo* on gene expression using a global array approach.

References

Abrams, J. (1985). Hemodynamic effects of nitroglycerin and long-acting nitrates. Am Heart J *110*, 216-224.

Abrams, J. (1995). The role of nitrates in coronary heart disease. Archives of Internal Medicine *155*, 357-364.

Abrams, J. (1996). Beneficial actions of nitrates in cardiovascular disease. Am J Cardiol *77*, 31C-37C.

Adler, V., Yin, Z., Fuchs, S.Y., Benezra, M., Rosario, L., Tew, K.D., Pincus, M.R., Sardana, M., Henderson, C.J., and Wolf, C.R. (1999). Regulation of JNK signaling by GSTp. The EMBO journal *18*, 1321-1334.

Ainsworth, S.J., Stanley, R.L., and Evans, D.J. (2010). Developmental stages of the Japanese quail. J Anat *216*, 3-15.

Armstrong, P.W., Armstrong, J.A., and Marks, G.S. (1979). Blood levels after sublingual nitroglycerin. Circ *59*, 585-588.

Armstrong, R.N. (1997). Structure, catalytic mechanism, and evolution of the glutathione transferases. Chem Res in Tox *10*, 2-18.

Atkinson, H.J., and Babbitt, P.C. (2009). Glutathione transferases are structural and functional outliers in the thioredoxin fold. Biochem *48*, 11108-116

Atzori, L., Dypbukt, J.M., Sundqvist, K., Cotgreave, I., Edman, C.C., Moldéus, P., and Grafström, R.C. (1990). Growth-associated modifications of low-molecular-weight thiols and protein sulfhydryls in human bronchial fibroblasts. J Cell Physiol *143*, 165-171.

Bashir, A., Lewis, M.J., and Henderson, A.H. (1982). Pharmacokinetic studies of various preparations of glyceryl trinitrate. Br.J.Clin.Pharmac *14*, 779-784.

Beg, A.A., Sha, W.C., Bronson, R.T., Ghosh, S., and Baltimore, D. (1995). Embryonic lethality and liver degeneration in mice lacking the RelA component of NF-kappa B. Nature *376*, 167-170.

Bennett, B.M., McDonald, B.J., Nigam, R., and Simon, W.C. (1994). Biotransformation of organic nitrates and vascular smooth muscle cell function. Trends Pharmacol Sci *15*, 245-249.

Beretta, M., Gruber, K., Kollau, A., Russwurm, M., Koesling, D., Goessler, W., Keung, W.M., Schmidt, K., and Mayer, B. (2008). Bioactivation of nitroglycerin by purified mitochondrial and cytosolic aldehyde dehydrogenases. J Biol Chem *283*, 17873-17880.

Berkman, N.D., Thorp, J.M., Lohr, K.N., Carey, T.S., Hartmann, K.E., Gavin, N.I., Hasselblad, V., and Idicula, A.E. (2003). Tocolytic treatment for the management of preterm labor: a review of the evidence. Am J Obstet Gynecol *188*, 1648-1659.

Black, R.S., Lees, C., Thompson, C., Pickles, A., and Campbell, S. (1999). Maternal and fetal cardiovascular effects of transdermal glyceryl trinitrate and intravenous ritodrine. Obstet Gynecol *94*, 572-576.

Board, P.G. (2007). The use of glutathione transferase-knockout mice as pharmacological and toxicological models. Expert Opin Drug Metab Toxicol *3*, 421-433.

Boyland, E., and Chasseaud, L.F. (1969). Glutathione S-aralkyltransferase. Biochem J *115*, 985-991.

Bryan, N.S., Fernandez, B.O., Bauer, S.M., Garcia-Saura, M.F., Milsom, A.B., Rassaf, T., Maloney, R.E., Bharti, A., Rodriguez, J., and Feelisch, M. (2005). Nitrite is a signaling molecule and regulator of gene expression in mammalian tissues. Nat Chem Biol *1*, 290-297.

Burchill, B.R., Oliver, J.M., Pearson, C.B., Leinbach, E.D., and Berlin, R.D. (1978). Microtubule dynamics and glutathione metabolism in phagocytizing human polymorphonuclear leukocytes. J Cell Biol *76*, 439-447.

Bustard, M.A., Farley, A.E., and Smith, G.N. (2002). The pharmacokinetics of glyceryl trinitrate with the use of the in vitro term human placental perfusion setup. Am J Obstet Gynecol *187*, 187-190.

Campbell, J.A.H., Corrigall, A.V., Guy, A., and Kirsch, R.E. (1991). Immunohistologic localization of alpha, Mu, and Pi class glutathione S-transferases in human tissues. Cancer *67*, 1608-1613.

Cao, Z., Bell, J.B., Mohanty, J.G., Nagababu, E., and Rifkind, J.M. (2009). Nitrite enhances RBC hypoxic ATP synthesis and the release of ATP into the vasculature: a new mechanism for nitrite-induced vasodilation. Am J Physiol Heart Circ Physiol *297*, H1494-H1503.

Chapman, S.C., Collignon, J., Schoenwolf, G.C., and Lumsden, A. (2001). Improved method for chick whole-embryo culture using a filter paper carrier. Dev Dyn *220*, 284-289.

Chen, Z., Zhang, J., and Stamler, J.S. (2002). Identification of the enzymatic mechanism of nitroglycerin bioactivation. Proc Natl Acad Sci U S A *99*, 8306-8311.

Chirkov, Y.Y., Holmes, A.S., Chirkova, L.P., and Horowitz, J.D. (1999). Nitrate resistance in platelets from patients with stable angina pectoris. Circulation *100*, 129-134.

Conour, J.E., Graham, W.V., and Gaskins, H.R. (2004). A combined in vitro/bioinformatic investigation of redox regulatory mechanisms governing cell cycle progression. Physiol Genomics *18*, 196-205.

Daiber, A., Wenzel, P., Oelze, M., and Münzel, T. (2008). New insights into bioactivation of organic nitrates, nitrate tolerance and cross-tolerance. Clin Res Cardiol *97*, 12-20.

David, M., Walka, M.M., Schmid, B., Sinha, P., Veit, S., and Lichtenegger, W. (2000). Nitroglycerin application during cesarean delivery: plasma levels, fetal/maternal ratio of nitroglycerin, and effects in newborns. Am J Obstet Gynecol *182*, 955-961.

Diaz Vivancos, P., Wolff, T., Markovic, J., Pallardó, F.V., and Foyer, C.H. (2010). A nuclear glutathione cycle within the cell cycle. Biochem J *431*, 169-178.

Drake, V.J., Koprowski, S.L., Lough, J.W., and Smith, S.M. (2006). Gastrulating chick embryo as a model for evaluating teratogenicity: a comparison of three approaches. Birth Defects Res A Clin Mol Teratol *76*, 66-71.

Eaton, D.L., and Bammler, T.K. (1999). Concise review of the glutathione S-transferases and their significance to toxicology. Toxicol Sci *49*, 156-164.

Ernst, V., Levin, D.H., and London, I.M. (1978). Inhibition of protein synthesis initiation by oxidized glutathione: activation of a protein kinase that phosphorylates the alpha subunit of eukaryotic initiation factor 2. Proc Natl Acad Sci U S A *75*, 4110-4114.

Fan, A.M., and Steinberg, V.E. (1996). Health Implications of Nitrate and Nitrite in Drinking Water: An Update on Methemoglobinemia Occurrence and Reproductive and Developmental Toxicity. Reg Tox and Pharm *23*, 35-43.

Fan, S.W., George, R.A., Haworth, N.L., Feng, L.L., Liu, J.Y., and Wouters, M.A. (2009). Conformational changes in redox pairs of protein structures. Protein Sci *18*, 1745-1765.

Ferreira, J. C. B., & Mochly-Rosen, D. (2012). Nitroglycerin Use in Myocardial Infarction Patients: Risks and Benefits. Circulation Journal : Official Journal of the Japanese Circulation Society, *76*, 15–21.

Flohé, L. (2013). The fairytale of the GSSG/GSH redox potential. Biochim Biophys Acta *1830*, 3139-3142.

Francis, S.H., Busch, J.L., Corbin, J.D., and Sibley, D. (2010). cGMP-dependent protein kinases and cGMP phosphodiesterases in nitric oxide and cGMP action. Pharmacol Rev *62*, 525-563.

Friedman, J.M., Little, B.B., Brent, R.L., Cordero, J.F., Hanson, J.W., and Shepard, T.H. (1990). Potential human teratogenicity of frequently prescribed drugs. Obstet Gynecol *75*, 594-599.

Garcia, J.I., Seabra, A.B., Kennedy, R., and English, A.M. (2010). Nitrite and nitroglycerin induce rapid release of the vasodilator ATP from erythrocytes:

Relevance to the chemical physiology of local vasodilation. J Inorg Biochem *104*, 289-296.

Gardiner, C.S., and Reed, D.J. (1995). Synthesis of glutathione in the preimplantation mouse embryo. Arch Biochem Biophys *318*, 30-36.

Gildenhuys, S., Wallace, L.A., Burke, J.P., Balchin, D., Sayed, Y., and Dirr, H.W. (2010). Class Pi glutathione transferase unfolds via a dimeric and not monomeric intermediate: Functional implications for an unstable monomer. Biochemistry *49*, 5074-5081.

Go, Y.M., and Jones, D.P. (2010). Redox control systems in the nucleus: mechanisms and functions. Antioxid Redox Signal *13*, 489-509.

Goodman, L.S., Brunton, L.L., Chabner, B., and Knollmann, B.C. (2010). Goodman & Gilman's pharmacological basis of therapeutics (New York: McGraw-Hill Prof Med/Tech).

Goto, S., Kamada, K., Soh, Y., Ihara, Y., and Kondo, T. (2002). Significance of nuclear glutathione S-transferase π in resistance to anti-cancer drugs. Cancer Science *93*, 1047-1056.

Gregus, Z., Watkins, J.B., Thompson, T.N., Harvey, M.J., Rozman, K., and Klaassen, C.D. (1983). Hepatic phase I and phase II biotransformations in quail and trout: comparison to other species commonly used in toxicity testing. Toxicology and Applied Pharmacology *67*, 430-441.

Gruetter, C.A., Gruetter, D.Y., Lyon, J.E., Kadowitz, P.J., and Ignarro, L.J. (1981). Relationship between cyclic guanosine 3':5'-monophosphate formation and relaxation of coronary arterial smooth muscle by glyceryl trinitrate,

nitroprusside, nitrite and nitric oxide: effects of methylene blue and methemoglobin. J Pharmacol Exp Ther *219*, 181-186.

Hamburger, V., and Hamilton, H.L. (1951). A series of normal stages in the development of the chick embryo. Journal of Morphology *88*, 49-92.

Hansen, J.M., Harris, K.K., Philbert, M.A., and Harris, C. (2002). Thalidomide modulates nuclear redox status and preferentially depletes glutathione in rabbit limb versus rat limb. J Pharmacol Exp Ther *300*, 768-776.

Harris, J.W., and Patt, H.M. (1969). Non-protein sulfhydryl content and cell-cycle dynamics of Ehrlich ascites tumor. Exp Cell Res *56*, 134-141.

Harvey, A.J., Kind, K.L., and Thompson, J.G. (2002). REDOX regulation of early embryo development. Reproduction *123*, 479-486.

Hashimoto, S., and Kobayashi, A. (2003). Clinical pharmacokinetics and pharmacodynamics of glyceryl trinitrate and its metabolites. Clin Pharmacokinet *42*, 205-221.

Hayes, J.D., and Pulford, D.J. (1995). The glutathione S-transferase supergene family: regulation of GST and the contribution of the isoenzymes to cancer chemoprotection and drug resistance. Crit Rev Biochem Mol Biol *30*, 445-600.

Hayes, J.D., Flanagan, J.U., and Jowsey, I.R. (2005). Glutathione transferases. Annu Rev Pharmacol Toxicol *45*, 51-88.

Huss, D., Poynter, G., and Lansford, R. (2008). Japanese quail (*Coturnix japonica*) as a laboratory animal model. Lab Anim (NY) *37*, 513-519.

Jamal, S.A., Hamilton, C.J., Black, D., and Cummings, S.R. (2006). The effects of organic nitrates on osteoporosis: a randomized controlled trial [ISRCTN94484747]. Trials *7*, 10.

Janer, G., Slob, W., Hakkert, B.C., Vermeire, T., and Piersma, A.H. (2008). A retrospective analysis of developmental toxicity studies in rat and rabbit: what is the added value of the rabbit as an additional test species? Regul Toxicol Pharmacol *50*, 206-217.

Johnson, J.A., el Barbary, A., Kornguth, S.E., Brugge, J.F., and Siegel, F.L. (1993). Glutathione S-transferase isoenzymes in rat brain neurons and glia. The Journal of Neuroscience *13*, 2013-2023.

Kashfi, K., Rimarachin, J.A., Weksler, B.B., and Dannenberg, A.J. (1994). Differential induction of glutathione S-transferase in rat aorta versus liver. Biochem Pharmacol *47*, 1903-07.

Kayang, B.B., Fillon, V., Inoue-Murayama, M., Miwa, M., Leroux, S., Fève, K., Monvoisin, J.L., Pitel, F., Vignoles, M., et al. (2006). Integrated maps in quail (*Coturnix japonica*) confirm the high degree of synteny conservation with chicken (Gallus gallus) despite 35 million years of divergence. BMC Genomics *7*, 101.

Keen, J.H., Habig, W.H., and Jakoby, W.B. (1976). Mechanism for the several activities of the glutathione S-transferases. J Biol Chem *251*, 6183-88.

Kenkare, S.R., and Benet, L.Z. (1996). Tolerance to nitroglycerin in rabbit aorta. Investigating the involvement of the mu isozyme of glutathione S-transferases. Biochem Pharmacol *51*, 1357-363.

Knobloch, J., Reimann, K., Klotz, L.O., and Rüther, U. (2008). Thalidomide resistance is based on the capacity of the glutathione-dependent antioxidant defense. Mol Pharm *5*, 1138-144.

Kociba, R.J., and Sleight, S.D. (1970). Nitrite toxicosis in the ascorbic acid-deficient guinea pig. Toxicol Appl Pharmacol *16*, 424-29.

Kosower, N.S., and Kosower, E.M. (1978). The glutathione status of cells. Int Rev Cytol *54*, 109-160.

Kozlov, A.V., Dietrich, B., and Nohl, H. (2003). Various intracellular compartments cooperate in the release of nitric oxide from glycerol trinitrate in liver. Br J Pharmacol *139*, 989-997.

Kurz, M.A., Boyer, T.D., Whalen, R., Peterson, T.E., and Harrison, D.G. (1993). Nitroglycerin metabolism in vascular tissue: role of glutathione S-transferases and relationship between NO. and NO2- formation. Biochem J *292 (Pt 2)*, 545-550.

Lau, D.T., and Benet, L.Z. (1990). Nitroglycerin metabolism in subcellular fractions of rabbit liver. Dose dependency of glyceryl dinitrate formation and possible involvement of multiple isozymes of glutathione S-transferases. Drug Metab Dispos *18*, 292-97.

Lauretti, G.R., Perez, M.V., Reis, M.P., and Pereira, N.L. (2002). Double-blind evaluation of transdermal nitroglycerine as adjuvant to oral morphine for cancer pain management. J Clin Anesth *14*, 83-86.

Lo, H.W., Stephenson, L., Cao, X., Milas, M., Pollock, R., and Ali-Osman, F. (2008). Identification and functional characterization of the human

glutathione S-transferase P1 gene as a novel transcriptional target of the p53 tumor suppressor gene. Mol Cancer Res *6*, 843-850.

MacPherson, H., Noble, B.S., and Ralston, S.H. (1999). Expression and functional role of nitric oxide synthase isoforms in human osteoblast-like cells. Bone *24*, 179-185.

Markovic, J., Borrás, C., Ortega, A., Sastre, J., Viña, J., and Pallardó, F.V. (2007). Glutathione is recruited into the nucleus in early phases of cell proliferation. J Biol Chem *282*, 20416-424.

Markovic, J., Gimeno, A., Burguete, C., Pallardó, F.V., García-Gimenez, J.L., and Mora, M. (2011). The nuclear compartmentation of glutathione: effect on cell cycle progression. In CC Chen, ed, Selected Topics in DNA Repair. InTech, Rijeka, Croatia, pp 271–292

Markovic, J., García-Gimenez, J.L., Gimeno, A., Viña, J., and Pallardó, F.V. (2010). Role of glutathione in cell nucleus. Free Radic Res *44*, 721-733.

Marsh, N., and Marsh, A. (2000). A short history of nitroglycerine and nitric oxide in pharmacology and physiology. Clin Exp Pharmacol Physiol *27*, 313-19.

Mayer, B., and Beretta, M. (2008). The enigma of nitroglycerin bioactivation and nitrate tolerance: news, views and troubles. Br J Pharmacol *155*, 170-184.

Meister, A. (1991). Glutathione deficiency produced by inhibition of its synthesis, and its reversal; applications in research and therapy. Pharmacol Ther *51*, 155-194.

Menon, S.G., Sarsour, E.H., Spitz, D.R., Higashikubo, R., Sturm, M., Zhang, H., and Goswami, P.C. (2003). Redox regulation of the G1 to S phase transition in the mouse embryo fibroblast cell cycle. Cancer Res *63*, 2109-117.

Mieyal, J.J., Gallogly, M.M., Qanungo, S., Sabens, E.A., and Shelton, M.D. (2008). Molecular mechanisms and clinical implications of reversible protein S-glutathionylation. Antioxid Redox Signal *10*, 1941-1988.

Murad, F., (1999). Discovery of some of the biological effects of nitric oxide and its role in cell signaling. Biosci Rep 19, pp 133-154.

Murrell, W. (1879). Nitro-glycerine as a remedy for angina pectoris. The Lancet *113*, 225-227.

Münzel, T., Daiber, A., and Mülsch, A. (2005). Explaining the phenomenon of nitrate tolerance. Circ Res *97*, 618-628.

Münzel, T., Feil, R., Mülsch, A., Lohmann, S.M., Hofmann, F., and Walter, U. (2003). Physiology and pathophysiology of vascular signaling controlled by guanosine 3',5'-cyclic monophosphate-dependent protein kinase [corrected]. Circulation *108*, 2172-2183.

Münzel, T., Sayegh, H., Freeman, B.A., Tarpey, M.M., and Harrison, D.G. (1995). Evidence for enhanced vascular superoxide anion production in nitrate tolerance. A novel mechanism underlying tolerance and cross-tolerance. J Clin Invest *95*, 187-194.

Needleman, P., and Harkey, A.B. (1971). Role of endogenous glutathione in the metabolism of glyceryl trinitrate by isolated perfused rat liver. Biochem Pharmacol *20*, 1867-876.

Needleman, P., and Hunter, F.E. (1965). The transformation of glyceryl trinitrate and other nitrates by glutathione-organic nitrate reductase. Mol Pharmacol *1*, 77-86.

Nigam, R., Anderson, D.J., Lee, S.F., and Bennett, B.M. (1996). Isoform-specific biotransformation of glyceryl trinitrate by rat aortic glutathione S-transferases. J Pharmacol Exp Ther *279*, 1527-1534.

Nkabyo, Y.S., Ziegler, T.R., Gu, L.H., Watson, W.H., and Jones, D.P. (2002). Glutathione and thioredoxin redox during differentiation in human colon epithelial (Caco-2) cells. Am J Physiol Gastrointest Liver Physiol *283*, G1352-G1359.

Orlandi, A., Costantini, S., Campione, E., Ferlosio, A., Amantea, A., Bianchi, L., Chimenti, S., and Spagnoli, L.G. (2009). Relation between animal-type melanoma and reduced nuclear expression of glutathione S-transferase pi. Archives of dermatology *145*, 55-62.

Otieno, M.A., Baggs, R.B., Hayes, J.D., and Anders, M.W. (1997). Immunolocalization of microsomal glutathioneS-transferase in rat tissues. Drug Metabolism and Disposition *25*, 12-20.

Ottinger, M.A., Quinn, M.J., Lavoie, E., Abdelnabi, M.A., Thompson, N., Hazelton, J.L., Wu, J.M., Beavers, J., and Jaber, M. (2005). Consequences of endocrine disrupting chemicals on reproductive endocrine function in birds: establishing reliable end points of exposure. Domest Anim Endocrinol *29*, 411-419.

Padgett, C.A., and Ivey, W.D. (1959). Coturnix quail as a laboratory research animal. Science *129*, 267-268.

Padgett, C.S., and Ivey, W.D. (1960). The normal embryology of the Coturnix quail. The Anatomical Record *137*, 1-11.

Pallardó, F.V., Markovic, J., García, J.L., and Viña, J. (2009). Role of nuclear glutathione as a key regulator of cell proliferation. Mol Aspects Med *30*, 77-85.

Pereira, S.L., and Baker, A.J. (2006). A molecular timescale for galliform birds accounting for uncertainty in time estimates and heterogeneity of rates of DNA substitutions across lineages and sites. Molecular Phylogenetics and Evolution *38*, 499 - 509.

Perlman, D.H., Bauer, S.M., Ashrafian, H., Bryan, N.S., Garcia-Saura, M.F., Lim, C.C., Fernandez, B.O., Infusini, G., McComb, M.E., et al. (2009). Mechanistic insights into nitrite-induced cardioprotection using an integrated metabolomic/proteomic approach. Circ Res *104*, 796-804.

Post, G.B., Keller, D.A., Connor, K.A., and Menzel, M. (1983). Effect of culture conditions on glutathione content in A549 cells. Biochem Biophys Res Commun *114*, 737 - 742.

Primiano, T., and Novak, R.F. (1993). Purification and characterization of class mu glutathione S-transferase isozymes from rabbit hepatic tissue. Arch Biochem Biophys *301*, 404-410.

Rapoport, R.M., Draznin, M.B., and Murad, F. (1983). Endothelium-dependent vasodilator-and nitrovasodilator-induced relaxation may be mediated

through cyclic GMP formation and cyclic GMP-dependent protein phosphorylation. Trans Assoc Am Physicians *96*, 19-30.

Roger, V.L., Go, A.S., Lloyd-Jones, D.M., Benjamin, E.J., Berry, J.D., Borden, W.B., Bravata, D.M., Dai, S., Ford, E.S., et al. (2012). Heart disease and stroke statistics--2012 update: a report from the American Heart Association. Circulation *125*, e2-e220.

Ruffins, S.W., Martin, M., Keough, L., Truong, S., Fraser, S.E., Jacobs, R.E., and Lansford, R. (2007). Digital three-dimensional atlas of quail development using high-resolution MRI. ScientificWorldJournal *7*, 592-604.

Ryan, T.J., and Gibbons, R.J. (1996). 1999 Update: ACC/AHA guidelines for the management of patients with acute myocardial infarction. J Am Coll Cardiol *28*, 1328-1428.

Salvemini, D., Pistelli, A., and Anggard, E. (1993). Vascular and anti-platelet actions of 1,2- and 1,3-glyceryl dinitrate. Br J Pharmacol *110*, 937-942.

Schafer, F.Q., and Buettner, G.R. (2001). Redox environment of the cell as viewed through the redox state of the glutathione disulfide/glutathione couple. Free Radic Biol Med *30*, 1191-1212.

Sellier, N., Brillard, J.P., Dupuy, V., and Bakst, M.R. (2006). Comparative staging of embryo development in chicken, turkey, duck, goose, guinea fowl, and Japanese quail assessed from five hours after fertilization through seventy-two hours of incubation. Journal of Applied Poultry Research *15*, 219-228.

Shaulian, E., and Karin, M. (2001). AP-1 in cell proliferation and survival. Oncogene *20*, 2390-2400.

Shaulian, E., and Karin, M. (2002). AP-1 as a regulator of cell life and death. Nat Cell Biol *4*, E131-E136.Sheehan, D., Meade, G., Foley, V.M., and Dowd, C.A. (2001). Structure, function and evolution of glutathione transferases: implications for classification of non-mammalian members of an ancient enzyme superfamily. Biochem J *360*, 1-16.

Sherratt, P.J., and Hayes, J.D. (2001). Enzyme systems that metabolise drugs and other xenobiotics (John Wiley & Sons).

Sherratt, P.J., Williams, S., Foster, J., Kernohan, N., Green, T., and Hayes, J.D. (2002). Direct comparison of the nature of mouse and human GST T1-1 and the implications on dichloromethane carcinogenicity. Toxicology and Applied Pharmacology *179*, 89-97.

Shi, Z.Z., Osei-Frimpong, J., Kala, G., Kala, S.V., Barrios, R.J., Habib, G.M., Lukin, D.J., Danney, C.M., Matzuk, M.M., and Lieberman, M.W. (2000). Glutathione synthesis is essential for mouse development but not for cell growth in culture. Proc Natl Acad Sci U S A *97*, 5101-5106.

Sies, H. (1999). Glutathione and its role in cellular functions. Free Radical Biology and Medicine *27*, 916-921.

Singhal, S.S., Piper, J.T., Srivastava, S.K., Chaubey, M., Bandorowicz-Pikula, J., Awasthi, S., and Awasthi, Y.C. (1996). Rabbit aorta glutathione S-transferases and their role in bioactivation of trinitroglycerin. Toxicol Appl Pharmacol *140*, 378-386.

Smith, G.N., Walker, M.C., and McGrath, M.J. (1999). Randomised, double-blind, placebo controlled pilot study assessing nitroglycerin as a tocolytic. Br J Obstet Gynaecol *106*, 736-39.

Smith, G.N., Walker, M.C., Ohlsson, A., O'Brien, K., Windrim, R., and Canadian Preterm Labour Nitroglycerin Trial Group (2007). Randomized double-blind placebo-controlled trial of transdermal nitroglycerin for preterm labor. Am J Obstet Gynecol *196*, 37.e1-e8.

Stella, L., Nicotra, M., Ricci, G., Rosato, N., and Di Iorio, E.E. (1999). Molecular dynamics simulations of human glutathione transferase P1-1: analysis of the induced-fit mechanism by GSH binding. Proteins *37*, 1-9.

Stella, L., Pallottini, V., Moreno, S., Leoni, S., De Maria, F., Turella, P., Federici, G., Fabrini, R., Dawood, K.F., et al. (2007). Electrostatic association of glutathione transferase to the nuclear membrane. Evidence of an enzyme defense barrier at the nuclear envelope. J Biol Chem *282*, 6372-6379.

Stephens, T.D. (2009). The effect of thalidomide in chicken embryos. Birth Defects Res A Clin Mol Teratol *85*, 725-731.

Stern, C.D. (2004). The chick embryo--past, present and future as a model system in developmental biology. Mech Dev *121*, 1011-1013.

Tateishi, N., Higashi, T., Shinya, S., Naruse, A., and Sakamoto, Y. (1974). Studies on the regulation of glutathione level in rat liver. J Biochem *75*, 93-103.

Tew, K.D. (2007). Redox in redux: Emergent roles for glutathione S-transferase P (GSTP) in regulation of cell signaling and S-glutathionylation. Biochem Pharmacol *73*, 1257-1269.

Tew, K.D., and Townsend, D.M. (2011). Regulatory functions of glutathione S-transferase P1-1 unrelated to detoxification. Drug Metab Rev *43*, 179-193.

Townsend, D.M. (2007). S-glutathionylation: indicator of cell stress and regulator of the unfolded protein response. Mol Interv *7*, 313-324.

Tsuchida, S., Maki, T., and Sato, K. (1990). Purification and characterization of glutathione transferases with an activity toward nitroglycerin from human aorta and heart. Multiplicity of the human class Mu forms. J Biol Chem *265*, 7150-7157.

Ufer, C., Wang, C.C., Borchert, A., Heydeck, D., and Kuhn, H. (2010). Redox control in mammalian embryo development. Antioxid Redox Signal *13*, 833-875.

Veselik, D.J., Divekar, S., Dakshanamurthy, S., Storchan, G.B., Turner, J.M., Graham, K.L., Huang, L., Stoica, A., and Martin, M.B. (2008). Activation of estrogen receptor-alpha by the anion nitrite. Cancer Res *68*, 3950-3958.

Viña, J.R., Palacin, M., Puertes, I.R., Hernandez, R., and Viña, J. (1989). Role of the gamma-glutamyl cycle in the regulation of amino acid translocation. Am J Physiol *257*, E916-E922.

Vorster, W., and Lizamore, D.J. (2001). The avian embryo: a developmental research tool. Netherlands Journal of Zoology *51*, 135-153.

Wang, T., Arifoglu, P., Ronai, Z., and Tew, K.D. (2001). Glutathione S-transferase P1--1 (GSTP1--1) inhibits c-Jun N-terminal kinase (JNK1) signaling through interaction with the C terminus. Journal of Biological Chemistry *276*, 20999-21003.Wenzel, P., Hink, U., Oelze, M., Seeling, A., Isse, T., Bruns, K.,

Steinhoff, L., Brandt, M., Kleschyov, A.L., et al. (2007). Number of nitrate groups determines reactivity and potency of organic nitrates: a proof of concept study in ALDH-2-/- mice. Br J Pharmacol *150*, 526-533.

Wyeth-Ayerst Laboratories: Product information. Ismo. 1993a.

Wyeth-Ayerst Laboratories: Product information. Isordil. 1993b

Yan, J., and Hales, B.F. (2005). Activator protein-1 (AP-1) DNA binding activity is induced by hydroxyurea in organogenesis stage mouse embryos. Toxicol Sci *85*, 1013-1023.

Ziegler, D.M. (1985). Role of reversible oxidation-reduction of enzyme thiols-disulfides in metabolic regulation. Annu Rev Biochem *54*, 305-329.

CHAPTER 2: The Developmental Toxicity of Glyceryl Trinitrate in Quail Embryos

Ghalib K. Bardai, Barbara F. Hales and Geoffrey I. Sunahara

Published in: *Birth Defects Research Part A: Clinical and Molecular Teratology*

Birth Defects Res A Clin Mol Teratol. (2011) 91, 230-240.

Preamble

There is conflicting and inconsistent data in the literature regarding the developmental toxicity of the organic nitrate, GTN. Therefore a detailed teratological evaluation of the organic nitrate GTN is needed.

GTN induces the formation of reactive oxygen species such as superoxide, activates second messenger pathways, induces post-translational protein modifications, and alters pyrimidine nucleotide ratios. Since GTN has been shown to perturb these pathways that play a role in embryo development, we hypothesized that GTN is a developmental toxicant using a quail embryo model of embryo development.

ABSTRACT

Background: Although glyceryl trinitrate (GTN) is used extensively to treat angina and heart failure, little is known about its effects on the conceptus during organogenesis. The goal of these studies was to investigate the effects of GTN in a model organism, the quail (*Coturnix coturnix japonica*) embryo.

Methods: To identify the effects of GTN on quail embryo development, fertilized quail eggs (n=10-12 eggs/group) were injected with GTN (0, 4.4, 44 or 440 μM) at Hamburger-Hamilton (HH) stage 0, 9 or 19 and examined 7 days later. Next, HH9 eggs were injected with GTN (0, 0.88, 4.4, 8.8, 44, 88, and 440 μM, in 20 μl per egg) and examined 24-, 48- or 72-h post injection. Finally, one side of the developing eye was exposed to GTN (44 μM) *ex ovo* and the tissue was probed for the presence of nitrated proteins.

Results: *In ovo* GTN exposure induced a dose dependent increase in the number of malformed viable quail embryos with a maximal effect in HH 9 embryos. Microphthalmia, craniofacial, heart, and neural tube defects were elevated in GTN exposed embryos. An increase in nitrated proteins was observed in the developing eye region of embryos exposed e*x ovo* to GTN.

Conclusions: GTN treatment induced a variety of malformations in quail embryos. The presence of nitrated proteins suggests that organic nitrates such as GTN generate reactive nitrogen species. We hypothesize that GTN perturbations in the redox status of the embryo may underlie its developmental toxicity.

Key Words: Organic nitrate, quail embryo, microphthalmia, reactive nitrogen species, redox status

INTRODUCTION

Organic nitrates (amyl nitrite, isosorbide mononitrate, isosorbide dinitrate, and glyceryl trinitrate) are used as anti-ischemic drugs; as well, they have been found to be effective therapeutic agents in osteoporosis (Jamal et al., 2006) and cancer pain management (Lauretti et al., 2002). These compounds are considered pro-drugs since they require bioactivation to nitric oxide (NO) and nitrite (NO_2^-) to mediate their pharmacological effects; both nitric oxide and nitrite adversely affect embryo development *in-vitro* (Inoue et al., 2004; Barroso et al., 1998). Given the widespread use of these compounds in cardiovascular diseases and their possible use in other therapeutic settings, it is important to determine the role of the parent compounds and metabolites in mediating any effects on the developing embryo.

The data from animal studies in which the effects of exposure to organic nitrates were determined are inconsistent in the literature. For example, treatment with isosorbide mononitrate in rats prolonged gestation and parturition and increased stillbirth and neonatal death without an increase in embryotoxicity (Wyeth-Ayerst Laboratories, 1993a), whereas isosorbide dinitrate in rabbits produced dose-related embryotoxicity (Wyeth-Ayerst Laboratories, 1993b). Treatment with GTN did not produce adverse fetal effects in studies conducted with rats and rabbits. There is also some ambiguity with respect to the effects of organic nitrates in humans. The Collaborative Perinatal Project recorded four malformed children from a group of 15 patients exposed to GTN and amyl nitrite during the first trimester and eight other patients exposed to vasodilators (as cited in Briggs et al., 2008). Due to the lack of data, GTN has a “non determined” rating

of risk in TERIS, an automated teratology resource, and carries a FDA warning level of “C”, signifying that a risk cannot be ruled out (Friedman et al., 1990). Thus, a detailed teratological evaluation of organic nitrates is needed.

GTN is a structurally simple compound containing three nitrates linked by an ester bond to a glycerol backbone. The metabolic breakdown products of GTN are the di (1,2 – 1,3 glyceryl) and mono (1, 2 glyceryl) nitrates of the parent compound, as well as NO and NO_2^- (Hashimoto and Kobayashi, 2003). GTN induces the formation of reactive oxygen species such as superoxide (Münzel et al., 1995), activates second messenger pathways (Bryan et al., 2005), induces post-translational protein modifications (Perlman et al., 2009), and alters pyrimidine nucleotide ratios (Garcia et al., 2010).

The quail embryo is an excellent model system for developmental biology, embryology, and teratology studies since it is accessible and easily manipulated during embryonic stages. This embryo undergoes rapid organogenesis; the availability of a comprehensive description of quail embryo development (Huss et al., 2008; Padgett and Ivey, 1959; Padgett and Ivey, 1960) permits the use of experimental exposures that target specific developmental stages (Drake et al., 2006). In this *in-ovo* model, maternal metabolism is absent, allowing the ascertainment of the direct effects of drugs on the embryo. Furthermore, this embryo can be cultured *ex-ovo*, allowing an examination of the effects of exposing specific areas of embryos at one stage of development. Thus, the quail embryo model provides a convenient model system in which to ascertain how a teratogen may interfere with organogenesis in the absence of the mother.

A series of *in-ovo* and *ex-ovo* dose response experiments were done to determine the effects of GTN on quail embryo development. Furthermore, the impact of GTN on protein nitration was investigated.

MATERIALS AND METHODS

Chemicals and reagents: A stock solution of GTN (99.9% purity) (CAS 118-96-7) in corn oil was supplied by General Dynamics Ordnance and Tactical Systems - Canada (Valleyfield, QC, Canada) at a concentration of 0.2 g/ml. Authentic standard solutions of 1,2 and 1,3 glyceryl dinitrate solutions in acetonitrile (1 g/L) were purchased from Cerilliant Corporation (Round Rock, TX). Sodium nitrite (1000 mg/L) standards were obtained from Alltech (Deerfield, IL). Acetonitrile and acetone (high performance liquid chromatography, HPLC grade) were obtained from EM Science (Darmstadt, Germany). All other reagents were from the Sigma Chemical Co. (St. Louis, MO).

GTN determinations: GTN determinations were done using a previously described method (Groom et al., 2002) modified for GTN determinations. Briefly, GTN determinations were done using a Waters (Milford, MA) HPLC-UV chromatographic system composed of a Model 600 pump, a Model 717 Plus injector, a Model 2996 Photodiode-Array Detector, and a temperature control module. A Supelcosil LC-CN column (250 x 4.6 mm, 5 µm particles; Supelco, Bellefonte, PA) was used for separation with a column heater set at 35°C. The isocratic mobile phase consisted of methanol/water (30/70, v/v) delivered at 1.5 ml/min for 8 min. A linear gradient was then run from 30% to 65% methanol, v/v over 12 min; following this, the solvent ratio was returned to initial isocratic conditions over 5 min. These initial conditions were then held for another 5 min.

The sample volume injected was 50 μl with a total run time of 25 min. The detector was set to scan from 200 to 325 nm with extraction of chromatograms at 205 nm. A calibration curve using known concentrations of GTN was run prior to analysis. The limit of quantification was 0.05 mg/L. Relative standard deviation for the instrument precision was < 1.3% for concentrations equal or higher than 0.5 mg/L, and 7.5% for a concentration of 0.05 mg /L.

Preparation of test solutions: Dilutions of the stock GTN solution (0.2 g/ml) were made in corn oil to achieve nominal concentrations of 0, 0.88, 4.4, 8.8, 44, 88, and 440 μM (0, 0.1, 0.5, 1, 5, 10, and 50 μg/μl) of GTN. Concentrations of dissolved GTN in the corn oil vehicle were analyzed for the presence of GTN and its metabolites using HPLC, as described above. Actual respective concentrations of GTN (μg/μl) were found to be 0.09 ± 0.03 (SE; n=3), 0.64 ± 0.05 (n=3), 1.3 ± 0.1 (n=3), 5.5 ± 0.48 (n=3), 9.8 ± 0.8 (n=3), 54.8 ± 2.5 (n=3), and 102±1.2 (n=3). HPLC analysis revealed the absence of known GTN metabolites in the test solutions on the day of injection.

***Handling and preparation of Japanese quail embryos*:** All animal studies were carried out in accordance with the established protocols of the National Research Council of Canada, Biotechnology Research Institute for the use of animals. Fertilized Japanese quail (*Coturnix coturnix japonica*) eggs (n= 120 for Study 1, and n= 1050 for Study 2) were obtained from a local breeder (Couvoir Simetin, Mirabel, QC, Canada) on the day of laying. Eggs that showed signs of physical

stress (cracks or dented) were discarded; the remaining eggs were incubated at 22°C for 2 h, horizontally on their long axis to allow the germ cells to be positioned close to the topmost point on the yolk and to avoid trauma from the introduction of the needle. During this time embryo development ceases. Following 2 h incubation, eggs were placed in an environment-controlled incubator (Octagon 40 forced draft incubator; Brinsea, Titusville, FL) set at 37 ± 1°C and 60± 5% relative humidity. All embryos were staged according to the criteria of Hamburger and Hamilton (HH) (Hamburger and Hamilton, 1951).

Glyceryl trinitrate (GTN) injection procedure: GTN in corn oil was injected directly into the center of the egg yolk using an established protocol that does not cause developmental anomalies in control embryos (Drake et al., 2006). Prior to injection the blunt end of the egg was wiped with sterile gauze moistened with 70% ethanol; a small hole (1 mm) was made using a Dremel™ (USA) tool without penetrating the membrane. Eggshell residue remaining after the drilling was brushed away. Vehicle (corn oil) or test substance was slowly injected into the center of the yolk using a Hamilton glass syringe with a 0.8 x 40 21GA 11/2 needle. Following a single injection of GTN, the hole was sealed with paraffin wax and the eggs were placed into a forced draft incubator, as described above.

Experimental Design**:** The temporal and concentration dependency of the developmental toxicity of GTN were investigated in separate studies. The objective for Study 1 was to identify the effects of GTN during critical periods of development

(Fig. 2.1A). Eggs were randomly divided into control (corn oil) and GTN treated groups and allowed to incubate to HH stage 0, 9 or 19. In our laboratory, quail embryos reached HH 9 and HH 19 in an incubation time of 25 and 70h, respectively. Since quail eggs are highly mottled and colored, making windowing unreliable, a subset (n=5) of eggs was removed to check that embryos had developed to the desired stage (Bellairs and Osmond, 2005; Padgett and Ivey, 1960). Each HH group was then injected with a constant volume of 10 µl GTN solution (n=10 eggs/group) to give final concentrations, based upon the volume of the egg (10 ml), of 4.4, 44, and 440 µM per egg and examined following incubation for 7 d. The objective for Study 2 (Fig. 2.1B) was to increase the range of treatment concentrations, based upon our observations in Study 1. HH9 embryos were injected with a constant volume of 20 µl GTN solution to give a final concentration of 0, 0.88, 4.4, 8.8, 44, 88 or 440 µM per egg; embryos were examined 24-, 48- or 72-h post injection.

***Analysis of embryos treated in ovo*:** Following incubation, the eggs were removed from the incubator. Embryonic survival was determined after carefully removing the shell from a 1 to 2 cm area directly over the embryo and observing the presence of a beating heart. Live embryos were kept at 4°C for 2 h; this was sufficient to arrest all physiological function. Body lengths were measured following embryo harvest. Craniofacial development was compared in treated and control embryos harvested 48 h post-treatment in the following manner. We first assessed the presence of a meso-metencephalic fold; this fold delineates the hindbrain from

the mesencephalon (Fig 2.4A; #1, #2). The mesencephalon was then evaluated to ensure that it was a completely rounded and closed. We next evaluated both the diencephalon and telencephalon (Fig 2.4A; #5, #6) to ensure that these were present as discrete structures divided by a well-defined fold. The eye and its size and position relative to the telencephalon and the diencephalon were examined. Cardiac development was also assessed in comparison to control embryos. The position of the developing heart inside the body cavity and proper looping, as well as the conus arteriosus, ventricle and atrium, were examined. For neural tube defects, embryos were examined from the dorsal view. Indications of failure of the neural tube to close were considered as neural tube defects. Following assessment of embryos as described above, photomicrographs of the craniofacial region of the embryos were taken using a stereomicroscope. In these photomicrographs both the eye and mesencephalon were present as well-defined discrete structures that allowed for tracing using the program ImageJ. Briefly, the entire craniofacial area was traced in the following manner: a perimeter was traced, using ImageJ, starting at the meso-metencephalic fold, over the mesencephalon, diencephalon, around the telencephalon and ending at the first pharyngeal arch. A direct line was then traced from the first pharyngeal arch to join the starting point (meso-metencephalic fold).

***Histological analysis*:** Embryos were cut away from the vitelline and allantoic circulatory system, rinsed with isotonic saline, weighed and a gross evaluation was done. Embryos were then fixed overnight in 4% paraformaldehyde. Embryos destined for ossified bone and cartilaginous double staining, including viable

embryos from all dose groups and those embryos displaying microphthalmia, were fixed according to the method described by Nakane (1999) for 7d old embryos. Briefy, embryos were simultaneously fixed and stained for 2d at 37°C in freshly prepared 95% ethanol containing 20mL acetic acid, and 15mg Alcian blue 8GX. Following this, embryos were dehydrated in a fresh solution of 95% ethanol. Embryos were then transferred to 0.002% alizarin red S/0.2% KOH solution for 1d and cleared in increasing concentrations (25, 50 and 75%) of glycerin/H_2O solutions for 7d and then stored in 100% glycerin.

Embryos for cryosectioning were processed as described below. Following overnight incubation in 4% paraformaldehyde, specimens were rinsed in phosphate buffered saline (PBS), placed in a 25% sucrose-PBS solution overnight, and then transferred to a 35% sucrose-PBS solution. Following this, half of the sucrose-PBS solution was removed and replaced with optimum cutting temperature (OCT) compound. Embryos remained in the OCT solution for 2 h before being transferred into 100% OCT for 1 h at 40°C. Embryo heads were then dissected and immersed into OCT compound® (Shandon Scientific Ltd., Pittsburgh, PA, USA) and frozen at -80°C until use. Pre-frozen samples equilibrated to -15°C in a Leica 1900 cryostat were placed into the cryostat chamber. The cryostat and knife temperatures were set to -18°C and -25°C, respectively. Tissue sections (8 μm thick) were cut and placed onto slides for storage at -80°C until required.

Paraffin processing of quail embryos was carried out as previously described (Simard et al., 2006). Briefly, embryos were collected and fixed in a 3.7% formaldehyde/60% ethanol/30% water solution for 1 h, washed twice in 70% ethanol for 15 min, and stored at -20°C. Embryos were dehydrated through a series of ethanol washes and washed twice for 30 min in xylene before being embedded in paraffin. Embryos were then sectioned at 10 µm and sections were placed on Fisherbrand™ Superfrost™ Plus glass slides.

***Terminal deoxynucleotidyl transferase–mediated nick-end labeling (TUNEL) assay*:** Apoptosis was assessed by the terminal deoxynucleotidyl transferase (TdT)-mediated deoxy-UTP nick end labeling (TUNEL) assay using ApopTag® Peroxidase *In Situ* Apoptosis Detection kit (S7100, Chemicon International Inc., Temecula, CA), according to the manufacturer's instructions. Following TUNEL staining, sections were counterstained with methyl green and mounted under glass coverslips with Permount™ (Fisher Scientific Inc., Montreal, QC).

***Preparation of ex-ovo embryo cultures*:** Following incubation at 37.7 ± 0.5°C and 55-60% relative humidity, eggs were processed according to Chapman et al. (2001) at HH9 when primary optic vesicle development occurs. Briefly, the yolk was placed into a glass Petri dish and the albumen over the blastoderm was removed. A filter paper (2 cm x 2 cm) with a small hole (5 mm diameter) punched in the middle was placed over the embryo. After cutting through the vitelline membranes, the filter paper with attached blastoderm was placed ventral side up

into a Petri dish with an agar-albumen substrate. Any remaining yolk adhering to the filter paper was gently washed away. Using a stereomicroscope, a filter paper soaked in 88 μM GTN in corn oil was placed next to the left eye, while another filter paper soaked in the corn oil vehicle was placed next to the opposite eye. The embryos were placed in a humidified, heated chamber for 18 h. Embryos were then removed, photographed and processed as required.

***Western Blot Analysis*:** Protein concentration was determined with bicinchoninic acid protein assay kit from Pierce Chemical Company (Rockford, IL) using bovine serum albumin as the standard. Samples were loaded on 10% gels using a BioRad Mini Protean® II electrophoresis system and run at room temperature for 2 h at 110 V. Separated proteins were electrophoretically transferred onto a PVDF membrane overnight at 4°C; membranes were developed with One-Step Western Advanced Kit for mouse primary antibody (Genscript Corporation, Piscataway, NJ). Primary anti–nitrotyrosine mouse monoclonal antibody (clone 1A6, Millipore Canada, Etobicoke, ON) and anti-beta actin mouse monoclonal antibody, as an internal standard (V10178, Genescript Corporation), were used at 200- and 10,000-fold dilutions, respectively.

Statistical Analysis: Measurements of embryo were done from photomicrographs using ImageJ v1.43 software (National Institutes of Health, Bethesda, MD). The data were expressed as mean ± SD and were evaluated by

Chi square for linear trends, one-way or two-way analysis of variance (ANOVA) or Spearman on ranks, where appropriate. The *a priori* level of significance was $p \leq 0.05$. Differences between exposure groups and their respective controls were considered significant when $p \leq 0.05$ using the Dunnett's post-hoc test. Statistical analysis was done using GraphPad Prism version 5.0 for Macintosh, GraphPad Software (San Diego, CA).

RESULTS

Developmental toxicity induced by GTN treatment (Study 1)

The effects of GTN treatment (0, 4.4, 44 or 440 μM) on HH 0, 9 or 19 stage quail embryos were assessed according to the exposure protocol shown in Fig 2.1 (Study 1). GTN treatment produced a dose-dependent increase in embryo mortality (Table 2.1). GTN was highly embryotoxic to HH 0 embryos while HH 9 and 19 embryos were more resistant. HH 19 embryos were least susceptible to GTN insult, as seen by the increased number of surviving embryos across dose groups when compared to the HH 0 and 9 groups. Embryo growth, as assessed by crown rump lengths (Table 2.1), was not significantly affected except at 44 μM ($p \leq 0.05$) in the HH 0 group. An ANOVA two-way 4 (dose) X 3 (groups) factorial design between subjects was conducted to analyze the effects of GTN treatment on embryo weights. Developmental stage did not have a significant impact ($F[2,83] = 2.99$, $p = 0.05$). However, the interaction effect (Dose x Stage) and GTN treatment both had significant effects ($F[6,83] = 2.85$, $p = 0.01$) and ($F[3,83] = 8.91$, $p \leq 0.001$), respectively. Post hoc comparisons of embryo weights within dose groups was performed using the Dunnett's multiple comparison test. The HH 0 group showed a significant difference ($p \leq 0.001$) between control and the 44 μM GTN concentration. However, post hoc analysis of the highest concentration tested in this dose group was not possible due to the low number of survivors (n=3). In the HH 9 group significant differences were observed between controls, the 4.4 μM ($p \leq 0.05$) and 440 μM concentration tested ($p \leq 0.001$). Multiple comparison testing showed significant differences ($p \leq 0.05$) between control and the highest

concentration tested in the HH19 treatment group. An increased incidence of microphthalmia was observed in the 44 μM treatment groups in both HH 9 (40% incidence) and HH 19 (22% incidence) treated-embryos. The absence of microphthalmia in the HH9 embryos exposed to the highest dose of GTN (440 μM) may be a consequence of embryo mortality. Skeletal anomalies were not observed in combined Alcian Blue-Alizarin red stained embryos (data not shown). Taken together, these data indicate that GTN treatment was embryotoxic to early stage embryos (HH 0), retarded embryo growth in a dose dependent manner independent of the stage and induced microphthalmia.

***Histological analysis*:**

A histological analysis was performed on the embryos presenting with microphthalmia (Fig. 2.2A). Embryos presenting with microphthalmia had upper beaks that were slightly bent towards the micropthalmic eye (Fig. 2.2A). A cross sectional analysis through the sagittal plane (Fig. 2.2B) clearly showed that the affected eye (designated as ae) was decreased in volume and had a small round lens compared to the oval lens of the unaffected eye (ue). In a higher magnification view of the ae region (Fig. 2.2C), the neural retinal (nr) cell layer was smaller and detached from the retinal-pigmented epithelium (rpe) compared to the ue region (Fig. 2.2D); the rpe of the ae was thin and highly disorganized.

Because the underlying matrix is critical to normal organ growth and development, we investigated the matrix of connective tissue surrounding both the unaffected and affected eye. The deposition of glycosaminoglycans was investigated using the Alcian blue staining technique while cells undergoing apoptosis were detected with the TUNEL technique (Fig. 2.3). A uniform distribution of glycosaminoglycans in the ue (Fig. 2.3A) and an absence of apoptosis (Fig. 2.3B) were observed in the ue. In contrast, there was an abnormal, enlarged amount of glycosaminoglycan staining in the ae (Fig. 2.3C); furthermore, TUNEL staining revealed increased apoptosis at the periphery of this glycosaminoglycan staining (Fig. 2.3D; arrow). These data demonstrate that the underlying matrix was affected in the microphthalmic eye, coinciding with an increase in the presence of apoptotic cells in comparison to the unaffected eye.

Detailed dose-response study (Study 2)

A detailed dose-response study was conducted at HH 9 to characterize embryos treated with GTN. Fertile quail eggs (n=1050) were injected with GTN (0, 0.88, 4.4, 8.8, 44, 88 or 440 μM; n = 50 eggs/concentration) at HH 9 of development; following treatment with GTN, eggs were returned to the incubator and examined 24 (n=350), 48 (n=350), and 72-h (n=350) post dose (pd) for body length, craniofacial development (mesencephalon, metencephalon, prosencephalon, telencephalon, optic vesicle, and eye), heart (atrium, ventricle) and neural tube defects compared to timed-matched controls. Figure 2.4 shows examples of the types of defects observed. A normal 48-h post dose individual is

shown in Fig 2.4A with a well developed hindbrain, mesencephalon, eye, heart, and forebrain. Fig. 2.4B shows a GTN (44 μM) exposed embryo 48-h post-dose in which there is a failure of cranial neural tube closure, absence of mesencephalon, and an underdeveloped hind and forebrain when compared to control (Fig. 2.4A). The heart and the developing vessels are protruding from the body cavity. Fig. 2.4C depicts failure of complete neural tube closure after GTN (440 μM) exposure in an embryo 48-h post dose, seen from the dorsal view. Fig. 2.4D shows a GTN (44 μM) exposed embryo with microphthalmia 72-h post treatment.

All viable embryos (normal and malformed) (Table 2.2) in the 24- and 72-h post dose groups were subjected to a one-way between subjects ANOVA to compare the effects of GTN treatment on embryo growth as assessed by body length. There was a significant effect of treatment on embryo length at the $p \leq 0.05$ level for the seven concentrations tested in both the 24- and 72-h pd groups [$F(6, 241) = 17$, $p = 0.0002$] and [$F(6,230) = 4$, $p = 0.0003$], respectively (Table 2.2). Post hoc comparisons using Dunnett's multiple comparison test for the 24-h pd group showed significant differences ($p \leq 0.001$) across all dose groups when compared to control at $p \leq 0.05$; however, in the 72-h pd group significant differences were seen between control and the 4.4 ($p \leq 0.05$), 44 ($p \leq 0.01$) and 440 μM ($p \leq 0.05$) GTN concentrations. Survival of embryos across all dose groups was not significantly affected, with only the highest dose (440 μM) showing an increase in embryo mortality at 72-h post treatment. Taken together, these results suggest that the exposure of early embryos to GTN decreased embryo growth;

embryos displayed substantial recovery from the effects of treatment by 72-h post-treatment.

Viable embryos with craniofacial (mesencephalon, metencephalon, prosencephalon, telencephalon, optic vesicle and eye), heart (atrium, ventricle) and neural tube defects were observed in all GTN-treatment groups. The dose-response relationship for malformed embryos with craniofacial, heart, and neural tube defects is illustrated in Fig. 2.5A (48-h pd) and Fig. 2.5B (72-h pd). The EC_{50}s (concentrations at which GTN induced malformations in 50% of the exposed embryos) in the 48- and 72-h pd treatment groups were 10 and 16 μM, respectively (Fig. 2.5A,B).

A Spearman correlation matrix showed a significant correlation between craniofacial defects and heart and neural tube defects in the 48-h pd (r = 0.99, p=0.0004 ; r = 0.97, p=0.0028) embryos with EC_{50}'s of 12 and 29, respectively. A significant correlation was also observed between craniofacial and heart defects in the 72-h pd (r = 0.87, p=0.012) group with EC_{50}'s of 7.3 and 50, respectively (Fig. 2.5B). In contrast, there was not a significant correlation between craniofacial defects and microphthalmia (r = 0.65, p=0.39) (EC_{50} > 100). Thus, the GTN treatment induced dose dependent increase in craniofacial defects was strongly correlated with both cardiac and neural tube defects in the 48- and 72-h pd groups, suggesting a common mechanism. Microphthalmia was not correlated with these defects, suggesting a different mechanism of toxicity.

Since craniofacial defects were one of the predominant malformations that we observed we measured craniofacial size by tracing the perimeter of the

craniofacial structure using ImageJ in embryos 24-, 48-, and 72-h pd. A trend towards a decrease in craniofacial size was significant for the seven GTN concentrations tested at the $p \leq 0.05$ level [$F(6,241) = 13.7$, $p = 0.02$], [$F(6,261) = 6.1$, $p = 0.002$], and [$F(6,255 = 11.1$, $p = 0.002$] (Table 2.2). Post hoc comparisons using Dunnett's multiple comparison test was done for all the pd groups at $p \leq 0.05$. While the 24-h pd group showed a significant difference across all dose groups when compared to control, in the 48-h pd group and the 72h pd group craniofacial size was significantly reduced compared to control in the highest dose groups tested.

To determine the relative contributions of discrete structures that contribute to craniofacial size, the mesencephalon and the eye, we undertook an examination of the sizes of these structures in both the 48- and 72-h pd GTN treatment groups (Table 2.2) by tracing these discrete structures within the craniofacial area as described in Materials and Methods. Measurements were done only in embryos that had apparently normal eyes. Examination of embryos 48-h pd showed significant effects of GTN exposure on both the mescencephalon and eye across treatment groups ($p = 0.0064$ and $p = 0.001$, respectively). The increase in eye circumference in the 0.88 μM GTN treatment group may reflect increased growth or be a consequence of edema. Dunnett's post-hoc comparisons of the size of the mesencephalon showed a significant difference between control and the highest dose group ($p \leq 0.01$) in the 48-h pd group. Measurements of mesencephalon and eye circumference performed on the 72-h pd treatment group showed significant treatment related effects ($p = 0.009$ and $p = 0.03$, respectively). Dunnett's multiple

comparison test showed a difference between the control group and the highest concentration tested ($p \leq 0.01$) for mesencephalon measurements. Differences were seen between control and the 44 ($p \leq 0.001$) and 440 ($p \leq 0.001$) GTN-treatment groups for eye diameter measurements. Taken together, these results suggest that GTN had an early effect on embryo growth and craniofacial size (24-h pd) and that this effect persisted in the embryos examined 72-h pd. Since the mesencephalon and the eye contribute to the overall size of the craniofacial area, the decrease in craniofacial size may be attributed to decreases in the size of these structures.

Effects of GTN treatment of ex ovo embryo cultures

The *ex-ovo* culture method was used to analyze the effects of GTN exposure on the development of the optic vesicle in more detail. Using this method, localized GTN exposure to one side of the developing eye field is possible while the other eye field serves as a control. Figure 2.6A shows the developing optic vesicle. On the non-treated side, two very distinct dark banding patterns (dashed lines) are observed when compared to the treated side. These darker banding patterns on the treated side are a developing lens and the regressing presumptive neural retina and retinal pigmented epithelium, as seen in a cross section of this area (Fig. 2.6B). The GTN treated side shows the presence of an optic vesicle, devoid of a lens, neural retina, and retinal pigmented epithelium. Taken together, these data demonstrate that localized GTN exposure to embryos *ex ovo* arrested the development of the eye, specifically by inhibiting the development of the neural retinal and retinal pigment epithelium.

GTN has been shown to posttranslationally modify proteins by nitrating amino-acids (Perlman et al., 2009). To determine if GTN treatment results in the nitration of embryonic proteins, we determined the levels of nitrated proteins in embryo homogenates from vehicle and GTN-exposed embryos using western blot analysis with a monoclonal antibody to nitrotyrosine (anti-NT). While nitrated embryonic proteins were detected in control embryos, a dose dependent increase in the amounts of these nitrated proteins was observed in GTN-exposed embryos (Fig. 2.7) with predominant bands appearing in the 216 and 16 kDa regions.

DISCUSSION

The paucity of data on the toxicological effects of organic nitrates prompted us to carry out studies with a well-characterized organic nitrate, GTN, and the quail embryo, a biological model representative of mammalian development. Our studies demonstrate that GTN is highly embryotoxic to early stage quail embryos; the embryo lethality of GTN was greater in HH0 embryos than in HH 9 and 19 stage embryos (Table 2.1). Significant decreases in embryo weight were observed in GTN exposed embryos at all three HH stages. In addition, GTN exposure resulted in numerous malformations, including craniofacial, heart, and neural tube defects, as well as microphthalmia. Localized *ex-ovo* treatment of GTN also led to ocular malformations.

GTN exposure may result in the generation of pro-oxidative reactive nitrogen species (Fig. 2.7) or reactive oxygen species (Haqqani et al., 2002; Münzel et al., 1995). Such free radicals would perturb redox homeostasis or the equilibrium between pro- and anti-oxidative processes. Anti-oxidative defenses consist of small molecules (GSH, ascorbic acid, and tocopherols) and the enzymatic activities of antioxidant enzymes (GSH peroxidases, GSH reductase), which are generally reduced in embryos compared to the adult (Wilson et al., 1992; Winn and Wells, 1999; Parman et al., 1999). Disturbances in redox homeostasis may also affect cellular energy metabolism (Wentzel and Eriksson, 2005; Akazawa, 2005; Eriksson and Borg, 1991) and redox sensitive transcription factors.

One of the predominant malformations observed in GTN-exposed quail embryos is microphthalmia. At HH 9 in avian development, the optic vesicles (OV), symmetrical bilateral evaginations from the diencephalon, expand through the mesenchyme to contact the surface ectoderm at which point the ectoderm thickens into a lens placode, which then begins to invaginate (Bellairs and Osmond, 2005). This invagination generates two distinct cellular layers, an internal layer, the neural retina and an external layer, the retinal pigment epithelium, while the ventral portion of the optic vesicle forms the optic nerve (Adler and Canto-Soler, 2007; Chow and Lang, 2001). Our histological data of the sagittal cross sections shows the affected eye, with a small round lens and an undeveloped optic nerve (Fig 2.2B). However, at a higher magnification, it is apparent that the neural retina of the affected eye is thin, disorganized and detached from the retinal-pigmented epithelium (Fig. 2.2C, D). The effects of GTN exposure on early stages of eye development, when optic vesicle is in contact with the surface ectoderm, may reflect an effect on the specification of the neural retina and retinal pigmented epithelium by inductive signals originating in the surface ectoderm via FGF-8 (Vogel-Höpker et al., 2000) and in the extra-ocular mesenchyme through an activin-like signal (Fuhrmann et al., 2000).

Using whole embryo cultures, Fantel and colleagues (Fantel et al., 1986; Greenaway et al., 1986) demonstrated that the nitro based compound niridazole (l-(5‘-nitro-2’thiazolyl)-2 imidazolidinone) induced microphthalmia. The conclusions drawn in these studies were related to the reactive species of the parent structure (nitro anion radical, nitroso and hydronitroxide radical) generated

under relatively hypoxic conditions, rather than to the covalent binding of nitro compounds or their denitrated metabolites to proteins (Fantel et al., 1988; Fantel et al., 1989), However, new data show that the nitrite anion is a biologically active molecule (Bryan et al., 2005; Garcia et al., 2010) under both hypoxic and normoxic conditions (Cao et al., 2009), suggesting an alternate hypothesis that implicates the nitrite anion. Niridazole-induced microphthalmia was positively correlated with the formation of the denitrated metabolite of niridazole, 1-thiocarbamoyl-2-imidazolidinon; 4'-methylniridazole (MNDZ), a structural analogue of niridazole without a nitro group, did not induce this specific malformation. These data suggest that release of the nitro moiety was critical in inducing microphthalmia. While GTN and nirizidole are different structures, and therefore have differing chemistries, nitrite is a by-product of GTN metabolism and should not be ruled out. Therefore, the extent to which the embryo metabolizes GTN to release nitrite may be a decisive factor in the developmental toxicity of this chemical.

Since the extracellular matrix serves as a source of morphogenetic factor and facilitates complex tissue interactions, movements, and shape changes during early stages of lens and optic vesicle morphogenesis (Peterson et al., 1995), we examined the regional distribution of this component as assessed by Alcian blue staining. Regional differences in staining patterns (Fig. 2.3A, C) were found that correlated with increased apoptosis (Fig. 2.3B, D), suggesting that glycoprotein deposition was perturbed. A possible explanation for this may be that signaling between the cellular layers of the developing eye (neural retina and retinal pigmented epithelium) was perturbed since both these cellular structures were

affected in the microphthalmic eye.

GTN exposure induced a dose dependent increase in the number of malformed embryos (Fig 2.5A, B). Interestingly, there was a significant positive correlation between craniofacial and heart defects in both the 48 and 72-h post-dose groups (r = 0.99, p=0.0004 and r = 0.87, p=0.012, respectively) (Fig. 2.5A, B). This positive correlation suggests that GTN affects a pathway that is common to craniofacial and heart development. The neural crest cells may represent such a "shared" pathway. Neural crest cells give rise to many structures in the craniofacial region and a subpopulation of neural crest cells, the cardiac neural crest cells, migrate from discrete areas in the hindbrain into the developing aortic arch arteries (Hutson and Kirby, 2003; Kirby et al., 1983). Most of the heart defects we observed included aortic arch anomalies (Fig. 2.4B). It is interesting to speculate on how GTN may affect neural crest cells. Retinoic acid, generated from retinol by retinaldehyde dehydrogenases, constitutes the most important signaling pathway in neural crest cell migration (VanGelder et al., 2010). GTN can irreversibly inactivate mitochondrial aldehyde dehydrogenase (Beretta et al., 2008), an enzyme that shares 83% sequence similarity with retinaldehyde dehydrogenase (Yoshida et al., 1998). Therefore, it is possible that GTN inhibits retinaldehyde dehydrogenase, resulting in decreased retinoic acid, which has been shown to result in neural crest related malformations (Wilson et al., 1953)

The observation that the induction of microphthalmia by GTN was not correlated to craniofacial or heart defects (r = 0.65, p=0.39) suggests a different mechanism of action. This is surprising since abnormal neural crest cell

differentiation and distribution have been implicated in ocular anomalies, including microphthalmia (Warburg and Friedrich, 1987; Warburg, 1992). However, since the eye is derived from three different tissues, the anterior neuroectoderm, the neuroepithelium, and the periocular mesenchyme, with the neuroepithelium giving rise to both the neural retina and the pigment retinal epithelium while the periocular mesenchyme originates from both the head mesoderm and the cranial neural crest (Creuzet et al., 2005; Gage et al., 2005), it is possible that GTN or its metabolites specifically affect the neuroepithelium, resulting in abnormal development of the retinal pigment epithelium or neural retina, as observed in our first study (Fig. 2.2C, D).

GTN exposure localized to the ocular region arrested eye development (Fig. 2.6A, B), and caused an increase in nitrated proteins (Fig. 2.7). GTN may be metabolized to release nitrite, which then reacts with tyrosine containing amino acids, increasing nitrated proteins. Interestingly, recent *in-vitro* studies have shown that physiological levels of GTN or nitrite cause a increase in extracellular ATP levels (Cao et al., 2009; Garcia et al., 2010); purine mediated signaling by ATP has been suggested to trigger, once converted to ADP by nucleases, both the expression of eye field transcription factors and eye development in *Xenopus* (Massé et al., 2007). Further studies are needed to elucidate the role of protein nitration in the embryotoxicity of organic nitrates such as GTN.

Acknowledgments. We thank Dr. Aimee K. Ryan for helpful discussions and assistance with the ex-ovo quail embryo cultures, and Annamaria Halasz and Louise Paquet (Biotechnology Research Institute, National Research Council of Canada) for GTN and nitrite analyses. Financial support was received from the US Strategic Environmental Research and Development Program (SERDP Project). Ghalib Bardai is the recipient of a PhD stipend from the FRQS.

REFERENCES

Adler R, Canto-Soler MV. 2007. Molecular mechanisms of optic vesicle development: Complexities, ambiguities and controversies. Dev Biol 305:1-13.

Akazawa S. 2005. Diabetic embryopathy: studies using a rat embryo culture system and an animal model. Congenit Anom (Kyoto) 45:73-79.

Barroso RP, Osuamkpe C, Nagamani M, Yallampalli C. 1998. Nitric oxide inhibits development of embryos and implantation in mice. Mol Hum Reprod 4:503-507.

Bellairs R, Osmond M. 2005. The atlas of chick development. 2nd ed. London: Elsevier Academic Press.

Beretta M, Sottler A, Schmidt K, Mayer B, Gorren AC. 2008. Partially irreversible inactivation of mitochondrial aldehyde dehydrogenase by nitroglycerin. J Biol Chem 283: 30735-30744.

Briggs GB, Freedman RF, Sumner YS. 2008. Drugs in pregnancy and lactation: a reference guide to fetal and neonatal risk. Lippincott Williams and Wilkins.

Bryan NS, Fernandez BO, Bauer SM, Garcia-Saura MF, Milsom AB, Rassaf T, Maloney RE, Bharti A, Rodriguez J, Feelisch M. 2005. Nitrite is a signaling molecule and regulator of gene expression in mammalian tissues. Nat Chem Biol 1: 290-297.

Cao Z, Bell JB, Mohanty JG, Nagababu E, Rifkind JM. 2009. Nitrite enhances RBC hypoxic ATP synthesis and the release of ATP into the vasculature: a new mechanism for nitrite-induced vasodilation. Am J Physiol Heart Circ Physiol 297: H1494-H1503.

Chapman SC, Collignon J, Schoenwolf GC, Lumsden A. 2001. Improved method for chick whole-embryo culture using a filter paper carrier. Dev Dyn 220: 284-289.

Chow RL, Lang RA. 2001. Early eye development in vertebrates. Annu Rev Cell Dev Biol 17: 255-296.

Creuzet S, Vincent C, Couly G. 2005. Neural crest derivatives in ocular and periocular structures. Int J Dev Biol 49: 161-171.

Drake VJ, Koprowski SL, Lough JW, Smith SM. 2006. Gastrulating chick embryo as a model for evaluating teratogenicity: a comparison of three approaches. Birth Defects Res A Clin Mol Teratol 76: 66-71.

Eriksson UJ, Borg LA. 1991. Protection by free oxygen radical scavenging enzymes against glucose-induced embryonic malformations in vitro. Diabetologia 34: 325-331.

Fantel AG, Greenaway JC, Walker E, Juchau MR. 1986. The toxicity of niridazole in rat embryos in vitro. Teratology 33: 105-112.

Fantel AG, Juchau MR, Tracy JW, Burroughs CJ, Person RE. 1989. Studies of mechanisms of niridazole-elicited embryotoxicity: Evidence against a major role for covalent binding. Teratology 39: 63-74.

Fantel AG, Person RE, Tracy JW, Juchau MR. 1988. Niridazole metabolism by rat embryos in vitro. Teratology 37: 213-221.

Friedman JM, Little BB, Brent RL, Cordero JF, Hanson JW, Shepard TH. 1990. Potential human teratogenicity of frequently prescribed drugs. Obstet Gynecol 75: 594-599.

Fuhrmann S, Levine EM, Reh TA. 2000. Extraocular mesenchyme patterns the optic vesicle during early eye development in the embryonic chick. Development 127: 4599-4609.

Gage PJ, Rhoades W, Prucka SK, Hjalt T. 2005. Fate maps of neural crest and mesoderm in the mammalian eye. Invest Ophthalmol Vis Sci 46: 4200-4208.

Garcia JI, Seabra AB, Kennedy R, English AM. 2010. Nitrite and nitroglycerin induce rapid release of the vasodilator ATP from erythrocytes: relevance to the chemical physiology of local vasodilation. J Inorg Biochem 104: 289-296.

Greenaway JC, Fantel AG, Juchau MR. 1986. On the capacity of nitroheterocyclic compounds to elicit an unusual axial asymmetry in cultured rat embryos. Toxicol Appl Pharmacol 82: 307-315.

Groom CA, Halasz A, Paquet L, Morris N, Olivier L, Dubois C, Hawari J. 2002. Accumulation of HMX (Octahydro-1,3,5,7-tetranitro-1,3,5,7-tetrazocine) in

indigenous and agricultural plants grown in HMX-contaminated anti-tank firing-range soil. Environ. Sci. Technol 36: 112-118

Hamburger V, Hamilton HL. 1951. A series of normal stages in the development of the chick embryo. Journal of Morphology 88: 49-92.

Haqqani AS, Kelly JF, Birnboim HC. 2002. Selective nitration of histone tyrosine residues in vivo in mutatect tumors. J Biol Chem 277: 3614-3621.

Hashimoto, S. and Kobayashi, A. 2003. Clinical pharmacokinetics and pharmacodynamics of glyceryl trinitrate and its metabolites. Clin Pharmacokinet 42: 205-221.

Hsu LC, Tani K, Fujiyoshi T, Kurachi K, Yoshida A. 1985. Cloning of cDNAs for human aldehyde dehydrogenases 1 and 2. Proc Natl Acad Sci U S A 82:3771-3775.

Huss D, Poynter G, Lansford R. 2008. Japanese quail (*Coturnix japonica*) as a laboratory animal model. Lab Anim 37: 513-519.

Hutson MR, Kirby ML. 2003. Neural crest and cardiovascular development: a 20-year perspective. Birth Defects Res C Embryo Today 69: 2-13.

Inoue T, Kaibara M, Sakurai-Yamashita Y, Kawano M, Ishimaru T, Taniyama K. 2004. Increases in serum nitrite and nitrate of a few-fold adversely affect the outcome of pregnancy in rats. J Pharmacol Sci 95: 228-233.

Jamal SA, Hamilton CJ, Black D, Cummings SR. 2006. The effects of organic nitrates on osteoporosis: A randomized controlled trial [ISRCTN94484747]. Trials 7: 1-14.

Kirby ML, Gale TF, Stewart DE. 1983. Neural crest cells contribute to normal aorticopulmonary septation. Science 220: 1059-1061.

Lauretti GR, Perez MV, Reis MP, Pereira NL. 2002. Double-Blind evaluation of transdermal nitroglycerine as adjuvant to oral morphine for cancer pain management. J Clin Anesth 14: 83-86.

Massé K, Bhamra S, Eason R, Dale N, Jones EA. 2007. Purine-mediated signalling triggers eye development. Nature 449: 1058-1062.

Münzel T, Sayegh H, Freeman BA, Tarpey MM, Harrison DG. 1995. Evidence for enhanced vascular superoxide anion production in nitrate tolerance. a novel

mechanism underlying tolerance and cross-tolerance. J Clin Invest 95: 187-194.

Nakane Y, Tsudzuki M. 1999. Development of the skeleton in Japanese quail embryos. Development Growth and Differentiation 41: 523-534.

Padgett CA, Ivey WD. 1959. Coturnix quail as a laboratory research animal. Science 129: 267-268.

Padgett CS, Ivey WD. 1960. The normal embryology of the coturnix quail. The Anatomical Record 1371: 1-11

Parman T, Wiley MJ, Wells PG. 1999. Free radical-mediated oxidative DNA damage in the mechanism of thalidomide teratogenicity. Nat Med 5: 582-585.

Perlman DH, Bauer SM, Ashrafian H, Bryan NS, Garcia-Saura MF, Lim CC, Fernandez BO, Infusini G, McComb ME, Costello CE, Feelisch M. 2009. Mechanistic insights into nitrite-induced cardioprotection using an integrated metabolomic/proteomic approach. Circ Res 104: 796-804.

Peterson PE, Pow CS, Wilson DB, Hendrickx AG. 1995. Localisation of glycoproteins and glycosaminoglycans during early eye development in the macaque. J Anat 186: 31-42.

Simard A, Di Pietro E, Young CR, Plaza S, Ryan AK. 2006. Alterations in heart looping induced by overexpression of the tight junction protein claudin-1 are dependent on its c-terminal cytoplasmic tail. Mech Dev 123: 210-227.

van Gelder MM, van Rooij IA, Miller RK, Zielhuis GA, de Jong-van den Berg LT, Roeleveld N. 2010. Teratogenic mechanisms of medical drugs. Hum Reprod Update 16: 378-394.

Vogel-Höpker A, Momose T, Rohrer H, Yasuda K, Ishihara L, Rapaport DH. 2000. Multiple functions of fibroblast growth factor-8 (FGF-8) in chick eye development. Mech Dev 94: 25-36.

Warburg M. 1992. Update of sporadic microphthalmos and coloboma. Non-Inherited anomalies. Ophthalmic Paediatr Genet 13: 111-122.

Warburg M, Friedrich U. 1987. Coloboma and microphthalmos in chromosomal aberrations. Chromosomal aberrations and neural crest cell developmental field. Ophthalmic Paediatr Genet 8: 105-118.

Wentzel P, Eriksson UJ. 2005. A diabetes-like environment increases malformation rate and diminishes prostaglandin E(2) in rat embryos: reversal by administration of vitamin E and folic acid. Birth Defects Res A Clin Mol Teratol 73: 506-511.

Wilson JG, Roth CB, Warkany J. 1953. An analysis of the syndrome of malformations induced by maternal vitamin A deficiency. Effects of restoration of vitamin A at various times during gestation. Am J Anat 92:189 - 217.

Wilson JX, Lui EM, Del Maestro RF. 1992. Developmental profiles of antioxidant enzymes and trace metals in chick embryo. Mech Ageing Dev 65: 51-64.

Winn LM, Wells PG. 1999. Maternal administration of superoxide dismutase and catalase in phenytoin teratogenicity. Free Radic Biol Med 26: 266-274.

Wyeth-Ayerst Laboratories: Product information. Ismo. 1993a.

Wyeth-Ayerst Laboratories: Product information. Isordil. 1993b.

Tables

Table 2.1. Effects of *in-ovo* GTN exposure after 7 d incubation: Study 1.

Stage (HH)	GTN (μM)	Eggs (n)[a]	Fertile Eggs (n)[b]	Mortality (%)	Crown Rump (mm)[c]	Weight (g)[c]	Microphthalmia (%)
0	0	10	7	0	20.4 ±2.7	0.81 ± 0.13	0
	4.4	10	9	22	19.4 ± 1.4	0.76 ± 0.17	0
	44	10	9	44	16.5 ±2.5[*]	0.48 ± 0.33[***]	0
	440	10	10	70	19.5 ± 1.4	0.84 ± 0.01	0
9	0	11	10	0	20.6 ± 1.8	0.94 ± 0.07	0
	4.4	11	10	10	18.2 ± 2.4	0.76 ± 0.15[*]	20
	44	11	10	20	19.8 ± 2.2	0.79 ± 0.15	40
	440	11	9	56	18.3 ±3.5	0.68 ± 0.16[**]	0
19	0	11	10	0	20.8 ± 2.1	0.93 ± 0.08	0
	4.4	11	10	10	19.4 ± 2.0	0.81 ± 0.09	0
	44	11	9	11	19.5 ± 1.7	0.78 ± 0.10	22
	440	11	11	18	19.2 ± 1.8	0.76 ± 0.06[*]	9

[a] number of eggs treated
[b] number of fertile eggs
[c] Mean ± S.D
[*]Significantly different from control (***$p \leq 0.0001$; **$p \leq 0.001$; *$p \leq 0.05$) when examined using Dunnett's post-hoc test

Table 2.2. Effects of *in-ovo* GTN treatment on body length, cranio-facial circumference, mescencephalon circumference and eye diameter; Study 2.

Post-dose (h)	GTN (μM)	(n)[a]	Body length (mm)[b]	Craniofacial circumference (mm)	Mescencephalon circumference (mm)	Eye diameter (mm)
24	0	37	6.6 ± 0.72	1.3 ± 0.26	n/d	n/d
	0.88	32	5.7±0.76***	1.1 ± 0.19**	n/d	n/d
	4.4	44	5.5±0.58***	1.0 ± 0.18***	n/d	n/d
	8.8	29	5.5±0.59***	0.97 ± 0.19***	n/d	n/d
	44	38	5.8±0.65***	1.0 ± 0.21***	n/d	n/d
	88	36	5.3±0.70***	0.91 ± 0.16***	n/d	n/d
	440	32	5.1 ± 1.1***	0.96 ± 0.27***	n/d	n/d
48	0	35	n/d	3.6 ± 0.63	1.0 ± 0.28	0.39±0.13
	0.88	43	n/d	4.1 ± 1.0	1.1 ± 0.30	0.52±0.17***
	4.4	36	n/d	3.9 ± 1.2	1.0 ± 0.32	0.45 ± 0.21
	8.8	40	n/d	3.4 ± 0.68	0.93 ± 0.21	0.35 ± 0.09
	44	39	n/d	3.6 ± 1.0	0.97 ± 0.26	0.40 ± 0.14
	88	36	n/d	3.6 ± 0.91	0.90 ± 0.22	0.38 ± 0.12
	440	39	n/d	2.9 ± 0.91*	0.80 ± 0.25**	0.32 ± 0.14
72	0	35	15.9 ± 0.84	12.0 ± 1.8	3.7 ± 0.54	2.4 ± 0.71
	0.88	46	15.6 ± 0.76	12.9 ± 1.8	3.9 ± 0.57	2.4 ± 0.56
	4.4	46	14.9 ± 1.6*	13.5 ± 2.2	3.9 ± 0.74	2.7 ± 0.73
	8.8	35	15.6 ± 1.0	13.9 ± 2.6*	4.1 ± 0.90	2.6 ± 0.68
	44	48	14.8±1.0**	10.9 ± 2.4	3.3 ± 0.79	1.6 ± 0.85***
	88	43	15.2 ± 1.2	11.9 ± 2.7	3.5 ± 1.0	2.1 ± 0.82
	440	24	14.6 ± 1.8*	9.8 ± 2.1*	3.0 ± 0.58**	1.3 ± 0.50***

[a]number of viable individuals
[b]Mean ± SD
*Significantly different from control (***$p \leq 0.0001$; **$p \leq 0.001$; *$p \leq 0.05$) when examined using Dunnett's post-hoc test
n/d = not done

Figures and Legends

Figure 2.1 Treatment protocol for glyceryl trinitrate (GTN) exposure studies: Study 1 and Study 2. For Study 1, three groups of eggs (n=10-12/group) were incubated to the desired stage of development (HH stages 0, 9 and 19), GTN was then administered to the eggs and embryos were assessed 7 d later. For Study 2, GTN was administered at HH stage 9 and embryos were assessed 24, 48 and 72-h post-dose.

Figure 2.1

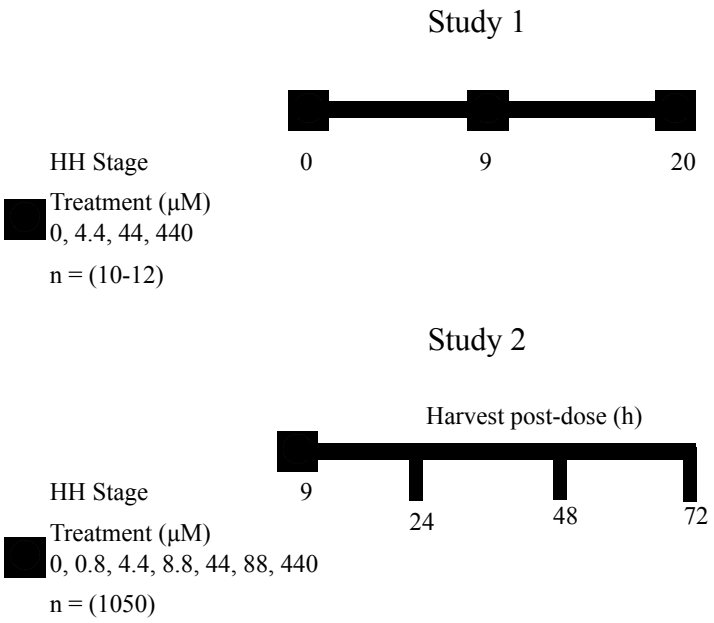
Study 1
HH Stage
0
9
20
Treatment (μM)
0, 4.4, 44, 440
n = (10-12)
Study 2
Harvest post-dose (h)
HH Stage
9
24
48
72
Treatment (μM)
0, 0.8, 4.4, 8.8, 44, 88, 440
n = (1050)

Figure 2.2 Effects of GTN on eye development. A) A stereomicroscope representation of a seven-day-old embryo treated at HH 9 with 440 μM GTN presenting with unilateral microphthalmia. Line represents where a sagittal cross section was taken; (B) is a hematoyxylin and eosin stained cross section of A (ae) affected eye; (ue) unaffected eye; (le) lens; (nr) neural retina; (rpe) retinal pigment epithelium. C and D) are higher magnification (40X) views of the ae and ue. The ae shows a thin and highly disorganized nr detached from the rpe.

Figure 2.2

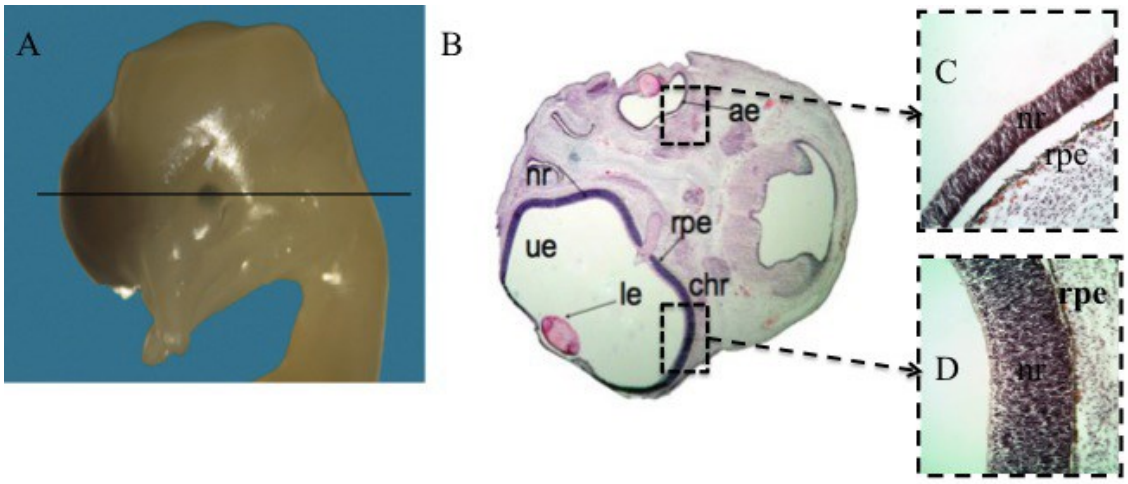

Figure 2.3 Alcian blue and TUNEL staining in the underlying supporting matrix of both the Unaffected and Affected eye (40X). Alcian blue staining for glycosaminoglycans (GAG) in the unaffected eye (A) clearly shows an even distribution of staining when compared to the affected eye (C), which shows increased, abnormal glycosaminoglycan distribution. TUNEL staining shows increased apoptosis in the choroid (chr) of the affected (D) compared to the unaffected eye (C) at the periphery of the abnormal GAG distribution of the affected (D, arrow) eye

Figure 2.3

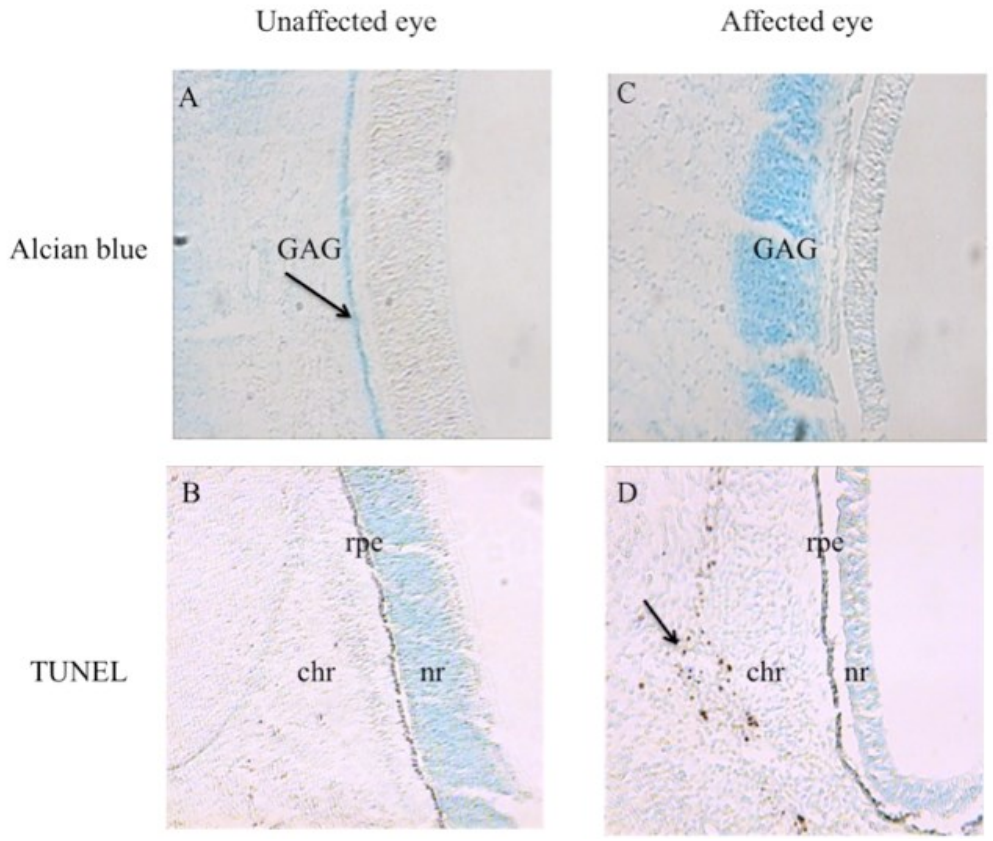
Unaffected eye
Affected eye
Alcian blue
TUNEL
A
GAG
C
GAG
B
rpe
chr
nr
D
rpe
chr
nr

Figure 2.4 Effects of GTN treatment on quail embryo development. Embryos were observed under a stereomicroscope. (A) control embryo 48-h post-dose; (1) hindbrain, (2) mesencephalon, (3) eye, (4) heart, (5) diencephalon and (6) telencephalon. B) GTN-exposed embryo (44 μM) 48-h post-dose showing failure of the cranial neural tube (1) to close, absence of mesencephalon, and an underdeveloped hind and forebrain; the eye is still oval and craniofacial distance is reduced when compared to the control embryo. The heart (2) is protruding from the body cavity. C) GTN-exposed embryo 48-h post dose (440 μM), seen from the dorsal view, showing incomplete closure of neural tube (*). D) GTN-exposed embryo 72-h pd (44 μM) with microphthalmia (#).

Figure 2.4

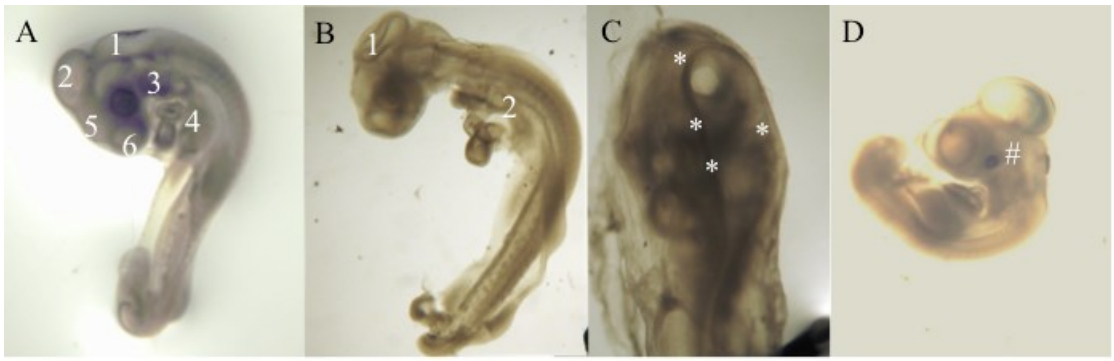

Figure 2.5 Dose-response analysis of the malformations observed in GTN-exposed embryos from Study 2 at 48-h (A) and 72-h (B) post-dose. Symbols indicate viable malformed embryos (-▽-), craniofacial (-□-), heart (-△-), neural tube (-○-) and microphthalmic (- ◇ -) defects. Data have been normalized on the Y-axis from 0 – 100%.

Figure 2.5

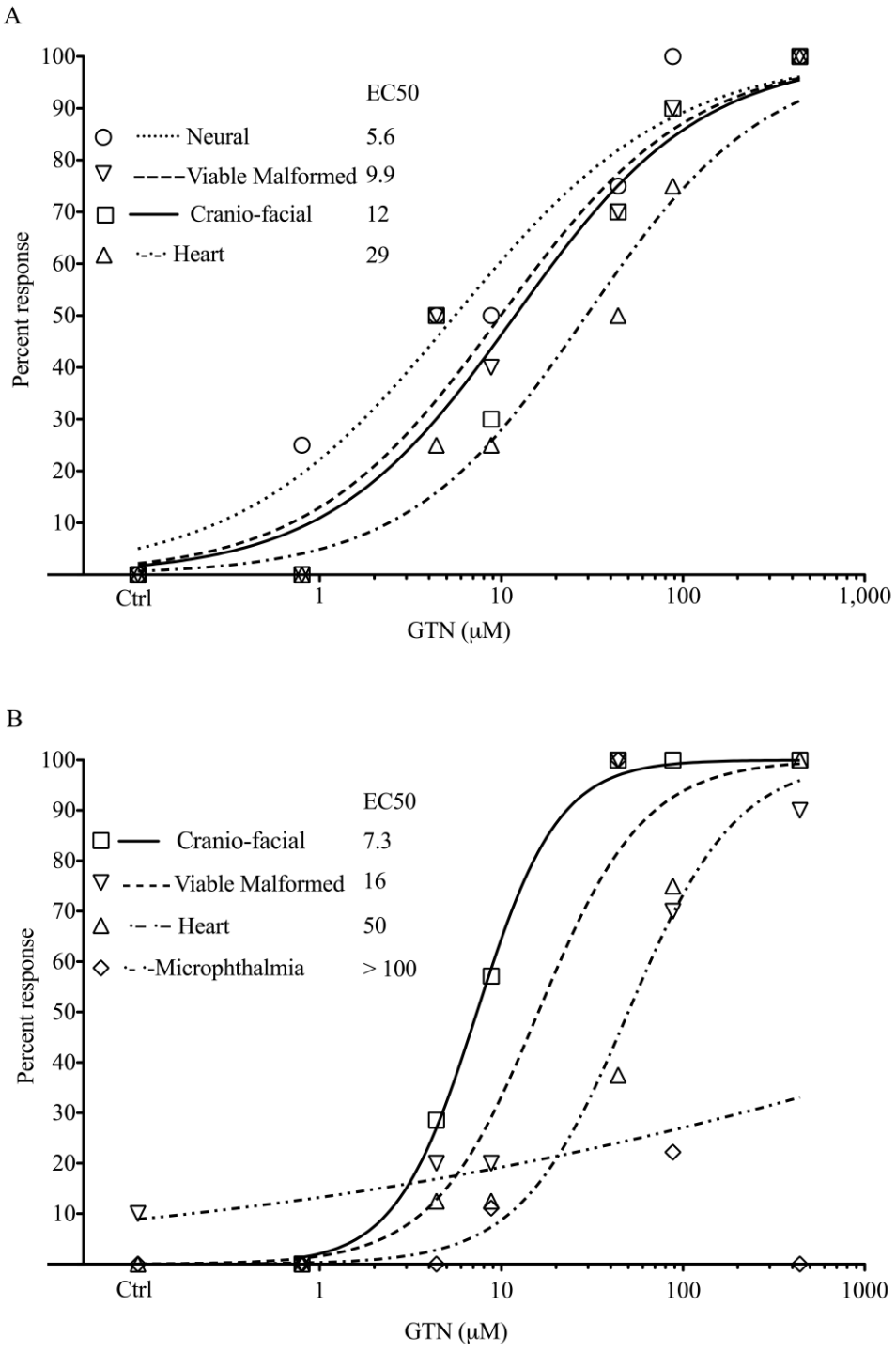
A
EC50
Neural 5.6
Viable Malformed 9.9
Cranio-facial 12
Heart 29
Percent response
GTN (μM)
Ctrl
1
10
100
1,000
B
EC50
Cranio-facial 7.3
Viable Malformed 16
Heart 50
Microphthalmia > 100
Percent response
GTN (μM)
Ctrl
1
10
100
1000

Figure 2.6 Effects of *ex-ovo* GTN treatment of the quail embryo. A) One side of a HH 9 embryo was treated with 44 μM GTN (Tr) the other with corn oil (NTr) and examined 18h later. B) Hematoxylin and eosin stained cross sectional analysis of the same embryo shows the NTr side with a developing lens (1) an invaginating optic vesicle (2). The Tr side eye field shows the failure of the lens to develop and the absence of an invaginating optic vesicle (40X).

Figure 2.6

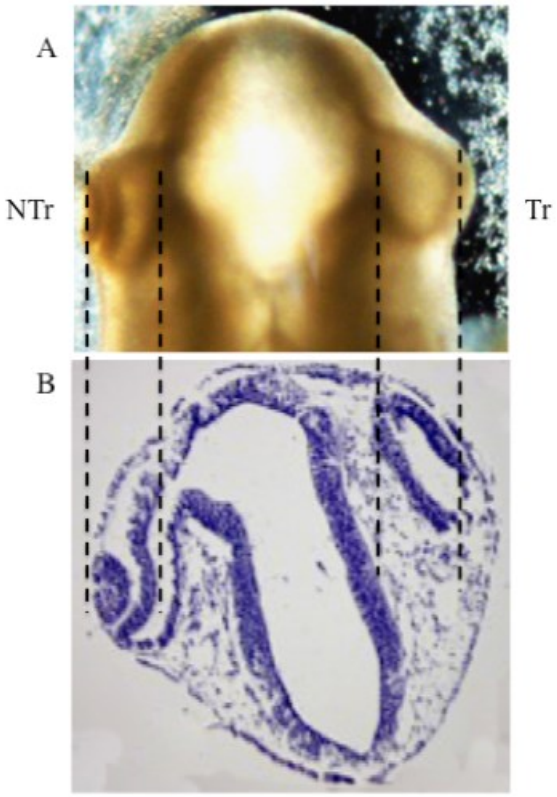

Figure 2.7 Effects of GTN treatment on protein nitration. HH 9 embryos were treated with GTN and examined 18 h later for the presence of nitrated proteins using Western blot analysis. Lanes MW (Nitrated Standards), A (Untreated embryo), B (vehicle treated), C (4.4 μM GTN), D (44 μM GTN) and E (440 μM GTN). An increase in the presence of nitrated proteins is seen by the increase in band intensities at 216 and 16 kDA.

Figure 2.7

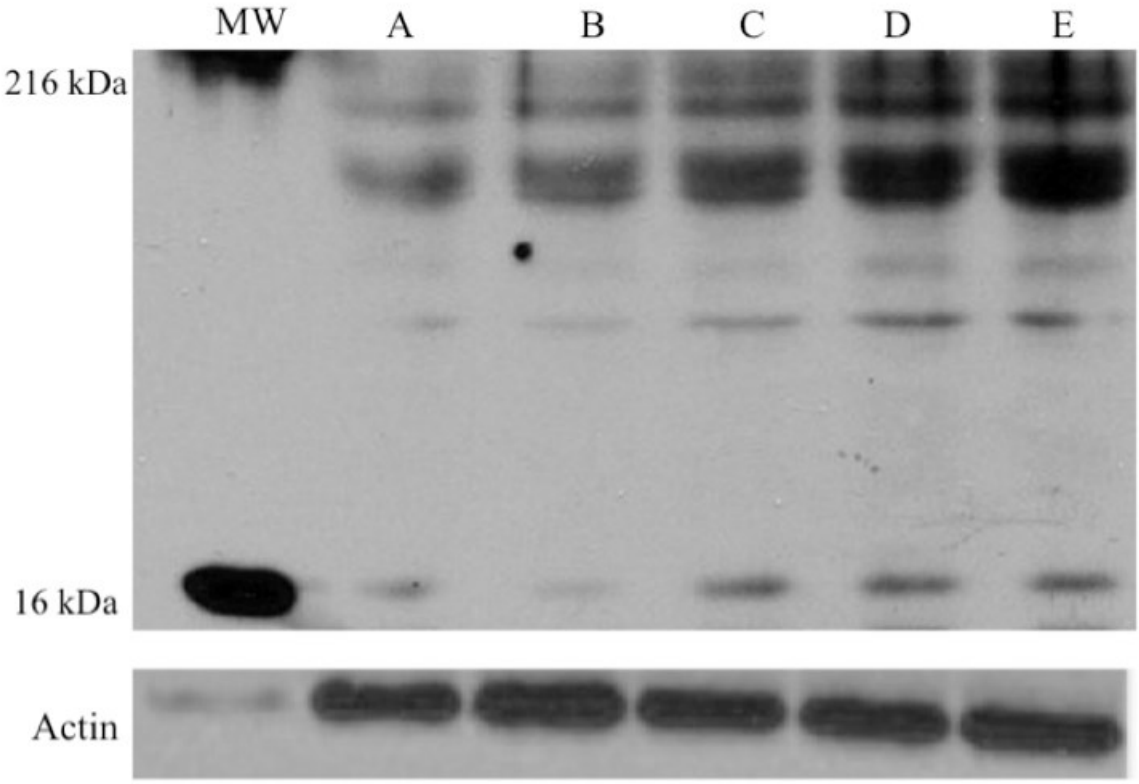

Connecting Text for Chapter 2 to Chapter 3

I have demonstrated that *in-ovo* exposure to GTN induced developmental toxicity in Japanese quail embryos; GTN increased mortality, decreased embryo growth, and increased the incidence of developmental defects that include a decrease in craniofacial, mesencephalon and eye size (Chapter 2). *Ex-ovo* exposure of quail embryos to GTN increases ocular malformations; these malformations were associated with a GTN dose-dependent increase in nitrated proteins. This increase in the presence of nitrated proteins suggested that the embryo has the ability to biotransform GTN. In Chapter 3 I tested the hypothesis that the quail embryo contains a GST-type enzyme(s) capable of metabolizing GTN.

CHAPTER 3: Glyceryl trinitrate metabolism in the quail embryo by the glutathione S-transferases leads to a perturbation in redox status and embryotoxicity

Ghalib K. Bardai, Barbara F. Hales and Geoffrey I. Sunahara†

Published in: *Comparative Biochemistry and Physiology Part B: Biochemistry and Molecular Biolology.*

Comp Biochem Physiol B Biochem Mol Biol.(2013) 165, 153-164.

Abstract

Exposure of stage 9 quail (*Coturnix coturnix japonica*) embryos to glyceryl trinitrate (GTN) induces malformations that were associated in previous studies with an increase in protein nitration. Increased nitration suggests metabolism of GTN by the embryo. The goals of this study were to characterize the enzymes and co-factors required for GTN metabolism by quail embryos, and to determine the effects of *in ovo* treatment with N-acetyl cysteine (NAC), a precursor of glutathione (GSH), on GTN embryotoxicity. GTN treatment of quail embryo resulted in an increase in nitrite, a decrease in total GSH, and an increase in the ratio of NADP+/NADPH, indicating that redox balance may be compromised in exposed embryos. Glutathione S-transferases (GSTs; EC 2.5.1.18) purified from the whole embryo (*K*m 0.84 mM; *V*max 36 μM/min) and the embryonic eye (*K*m 0.20 mM; *V*max 30 μM/min) had GTN-metabolizing activity (1436 and 34 nmol/min/mg, respectively); the addition of ethacrynic acid, an inhibitor of GST activity, decreased GTN metabolism. Peptide sequencing of the GST isozymes indicated that alpha- or mu-type GSTs in the embryo and embryonic eye had GTN metabolizing activity. NAC co-treatment partially protected against the effects of GTN exposure. Thus, GTN denitration by quail embryo GSTs may represent a key initial step in the developmental toxicity of GTN.

Key Words: Glutathione, Ethacrynic acid; Nitrated proteins; N-acetylcysteine, Redox homeostasis, Embryotoxicity.

Abbreviations: Glyceryl trinitrate, GTN; N-acetyl cysteine, NAC; Glutathione, GSH; Glutathione S-transferase, GST; Nitric oxide, NO; Nitrite, NO_2^-; Hamilton Hamburger stage, HH;

Introduction

Glyceryl trinitrate (GTN) is used to treat a variety of cardiovascular diseases, including coronary artery disease, congestive heart failure, and acute myocardial infarction. In addition, organic nitrates may be beneficial in several other diseases and conditions, such as osteoporosis (Wimalawansa et al., 1996) and cancer pain management (Lauretti et al., 2002). GTN is a pro-drug, thought to exert its action through the release of nitric oxide (NO) or nitrite (NO_2^-). While both NO and NO_2^- have pharmacologically beneficial effects, their chemical and biological reactivity may also lead to detrimental consequences to the organism. Nitric oxide is a free radical; its reaction with reactive oxygen species leads to the formation of peroxynitrite which interacts with lipids, DNA, and proteins via direct oxidative reactions or via indirect, radical-mediated mechanisms, leading to cytotoxicity (Radi, 2004). Although NO_2^- was thought to be a biologically inert molecule, it has been shown to act under physiological conditions as a signaling molecule and to post-translationally modify proteins independent of NO (Bryan et al., 2005; Veselik et al., 2008).

Despite the extensive use of GTN in therapeutics, relatively little is known about the possibility that GTN may induce embryotoxicity. It has been suggested that NO and the peroxynitrite pathway may contribute to the embryotoxicity of some teratogens (Kasapinovic et al., 2004). *In-ovo* exposure of Hamilton Hamburger (HH) stage 9 Japanese quail embryos to GTN increased mortality, decreased embryo growth, and increased the incidence of embryo defects; these included a decrease in craniofacial, mesencephalon, and eye sizes (Bardai et al.,

2011). *Ex-ovo* exposure of quail embryos to GTN increased ocular malformations; these malformations were associated with a GTN concentration-dependent increase in nitrated proteins (Bardai et al., 2011). This increase in the presence of nitrated proteins indicated that the embryo has the ability to biotransform GTN, releasing NO_2^- and/or NO and forming peroxynitrate. However, how the quail embryo metabolizes GTN is not known.

The enzymes implicated in the metabolism of GTN are mitochondrial aldehyde dehydrogenase (ALDH2) (Chen et al., 2002) and the cytosolic or microsomal glutathione S-transferases (GST) (EC 2.5.1.18) (Lau and Benet, 1990). High concentrations of the GSTs are present in the cytoplasm; indeed GSTs may constitute up to 10% of the cytosolic proteins (Board, 2007). The first and rate-limiting step in the release of NO_2^- from GTN is catalyzed by cytosolic GSTs (Kozlov et al., 2003); therefore, GSTs represent an important source of enzymatic GTN metabolizing activity and NO_2^- production (Lau et al., 1990). While GSTs are found in all species, seven classes of cytosolic GST are recognized in mammalian species and are designated alpha, mu, pi, sigma, theta, omega, and zeta based on their functional and structural properties (Hayes et al., 2005). Several hepatic glutathione S-transferases isozymes, including the alpha and mu forms, are capable of denitrating GTN into glyceryl dinitrate (GDN) and NO_2^- (Singhal et al., 1996); these GSTs are also present in avian species (Bardai et al., 2006; Dai et al., 1996; Hsieh et al., 1999). The ability of the GSTs to metabolize GTN is dependent upon the presence of glutathione (γ-glutamyl-cysteinyl-glycine or GSH); the reaction is thought to proceed as follows: GTN + 2GSH → NO_2^- + GSSG

(glutathione disulfide) (Needleman, 1976). In addition to their role in xenobiotic metabolism, GSTs are present in the squid and octopus eye as crystallins, where they play a structural role (Tomarev et al., 1991).

In addition to its role as a cofactor in the GST reaction, GSH constitutes the largest pool (up to 10 mM) of low molecular weight thiols in cells (Pallardó et al., 2009). Therefore, GSH plays a central role in controlling cellular thiol/disulfide redox state; the ratio of reduced $[GSH]^2$ to oxidized [GSSG] (the disulfide form) provides one estimate of redox status (Nkabyo et al., 2002). Proteins that are critical for embryo development contain redox-sensitive thiols, such as cysteine (Jones, 2008). These redox sensitive thiols control DNA replication, DNA repair, chromatin structure, transcription factor DNA binding, and cell proliferation (Chiu and Dawes, 2012). The proper functioning of redox sensitive thiols is dependent upon a finely tuned balance between their reduced and oxidized forms. Dysregulation of the redox equilibrium can severely hamper embryo development (Wells et al., 2005).

Quail embryos are an excellent model system for research because they develop *in-ovo* and, therefore, contributions from maternal metabolism are absent (Padgett and Ivey, 1959). Furthermore, these embryos can be cultured *ex-ovo*, allowing an examination of the effects of exposing specific areas of the embryos at one stage of development (Chapman et al., 2001). We hypothesize that the quail embryo contains a GST-type enzyme(s) capable of metabolizing GTN, using glutathione (GSH) as a required co-substrate. Furthermore, we postulate that GST-catalyzed metabolic activation of GTN plays a role in mediating its embryotoxicity in quail embryos. To test these hypotheses, we determined how the

quail embryo metabolizes GTN and whether manipulation of this pathway protects against the embryotoxicity of GTN.

Materials and methods

Chemicals and reagents

Nitroglycerin (GTN, CAS 118-96-7; 99.9% purity) in a corn oil solution (0.2 g/mL) was supplied by General Dynamics Ordnance and Tactical Systems - Canada (Valleyfield, QC, Canada). Analytical reference standards 1,2-glyceryl dinitrate (1,2- GDN), 1,3-GDN, 1-glyceryl mononitrate (GMN) and 2-GMN were purchased from Cerilliant (Round Rock, TX). Acetonitrile and acetone (high performance liquid chromatography, HPLC grade) were obtained from EM Science (Darmstadt, Germany). Reduced GSH, 1-chloro-2,4-dinitrobenzene (CDNB), ethacrynic acid (EA) and SNAP (S-nitroso-N-acetyl-D,L-penicillamine, CAS 67776-06-1) were purchased from Sigma Chemicals (Oakville, ON, Canada). Sephadex G-25 was purchased from Amersham Pharmacia Biotech (Uppsala, Sweden). All other chemicals and reagents were of the highest grades of purity available and were obtained from Sigma Chemicals (St. Louis, MO) and Anachemia (Milwaukee, WI).

Experimental animals

Fertilized Japanese quail (*Coturnix coturnix japonica*) eggs were obtained from a local breeder (Couvoir Simetin, Mirabel, QC, Canada). Eggs were incubated horizontally at 20°C for 2 h about their long axis, and were then placed in a forced draft incubator (Brinsea Octagon, Titusville, FL) at 37.7 ± 0.5°C (average $\pm$ SD)

and 55-60% relative humidity, for 3 d before embryo harvest. For the isolation of embryonic eyes, eggs were incubated for 5 d, and the whole eye was removed by dissection using a pair of fine scissors. For the N-acetylcysteine (NAC) rescue experiments, embryos were treated and analyzed as previously described (Bardai et al., 2011) with the following modifications. Eggs were incubated until HH stage 9, at which point they were first pre-treated *in-ovo* with NAC (10 mM) dissolved in phosphate buffered saline (PBS) (140 mM NaCl, 2.7 mM KCl, 10 mM Na_2HPO_4, 1.8 mM KH_2PO_4, pH 7.4) (Buffer A) or buffer alone; after 3 h they were injected with GTN (440 µM) or saline.

Ex ovo embryo cultures

Following incubation at 37.7 ± 0.5°C and 55-60% relative humidity, HH 9 embryos (from 29-33h post-fertilization) were processed as previously described (Chapman et al., 2001). Briefly, the yolk and the albumen over the blastoderm were removed in a glass Petri dish. A square of filter paper with a hole punched in the middle was placed over the embryo. After cutting through the vitelline membranes, the filter paper with the attached blastoderm was placed ventral side up in a Petri dish with an agar-albumen substrate. Any remaining yolk adhering to the filter paper was gently washed away. For GTN exposure, a GTN solution (5.7 µM in saline) or saline (control) was applied directly to the embryos using a pipette. Control and GTN-treated embryos (n = 3 embryos/group) were collected after 0, 0.5, 1, and 3 h to monitor GTN, nitrite, total GSH, and NADP/NADPH ratios. These

data were also used to analyze the Pearson product-moment correlation coefficient

GTN determinations

For GTN determinations, a Waters (Milford, MA) HPLC-UV chromatographic system composed of a Model 600 pump, a Model 717 Plus injector, a Model 2996 Photodiode-Array Detector (λ = 230 nm) and a temperature control module was used. A Supelcosil LC-CN (250 × 4.6 mm, 5 µm particles, Supelco, Bellefonte, PA) was used for separation with a column heater set at 35°C. The isocratic mobile phase consisted of methanol/water (30/70, v/v) delivered at 1.5 mL/min for 8 min. A linear gradient was then run (30% to 65%, v/v) over 12 min. Following this, the solvent ratio was returned to initial isocratic conditions over 5 min. These initial conditions were then held for another 5 min. The sample volume injected was 50 µL with a 25-min run time. The limit of quantification was 0.05 mg/L. Relative standard deviation for the instrument precision was < 1.3% for concentrations equal or higher than 0.5 mg/L, and 7.5% for a concentration of 0.05 mg/L.

Measurements of total GSH concentrations and NADP+/NADPH ratios

Total GSH was quantified by its reaction with Ellman's reagent (5,5'-dithiobis-2-nitrobenzoic acid (DTNB), according to the enzymatic method first reported by Tietze (1969), using a 96-well plate kit (Oxford Biomedical Research, Rochester Hills, MI). NADP+, NADPH, and the ratio of NADP+/NADPH were

assessed using a quantitation kit (K347-100, Biovision, Mountain View, CA), according to the manufacturer's instructions. Briefly, NADP(H) was quantified using the enzymatic recycling method that reads total NADP(H). The samples were then heated to 60ºC for 30 min to decompose NADP(+). The reactions were performed in a micro-plate and read at 450 nm. This method specifically recognizes NADP(H) and not NAD(H).

Electrochemical measurements of nitrite and NO

Nitrite was analyzed by reduction to nitric oxide prior to detection with an Apollo 4000 Free Radical Analyzer (World Precision Instruments, Sarasota, FL). Potassium iodide (0.1 mol/L) was used to reduce nitrite in the presence of sulfuric acid (0.1 mol/L). Calibration was carried out by adding different amounts of a standard potassium nitrite solution to the iodide solution and measuring the corresponding current change.

NO concentrations in quail embryo extracts following treatment with GTN dissolved in corn oil (440 μM) were measured by using a NO-specific sensor with a 2-mm-diameter tip (ISO-NOP sensor; World Precision Instruments, Sarasota, FL, USA) connected to an Apollo 4000 Free Radical Analyzer (World Precision Instruments, Sarasota, FL, USA), according to manufacturer's instructions. In brief, the NO sensor was calibrated prior to the experiment by using SNAP (0.09 mM) dissolved in PBS + EDTA in combination with a catalyst, copper sulfate, to generate known amounts of NO in solution. A similar calibration curve was also prepared using SNAP in combination with crude embryo homogenate. A

calibration curve was constructed by plotting the signal output (pA) vs. concentration (nM) of SNAP. The estimated limit of detection for NO was 100 nM. For the experiment, a reaction mixture was prepared in a 10-mL glass vial that contained 5-mL PBS and 250 μL of crude embryo homogenate. The previously calibrated NO sensor was introduced into the homogenate and allowed to stabilize. Once a steady baseline had been achieved, 20 μL of GTN dissolved in corn oil was added.

Determination of GTN biotransformation products with LC-MS

A Bruker bench-top ion trap mass analyzer attached to a Hewlett Packard 1100 Series HPLC system equipped with a DAD detector was used. Partially purified GST and GTN incubation mixtures were injected into a 5-mm pore size Zorbax™ SB-C18 capillary column (0.5 mm inner diameter × 150 mm length; Agilent, Mississauga, Ontario, Canada) at 25°C. The solvent system was composed of a CH_3CN/H_2O gradient (30 to 70% v/v) at a flow rate of 12 mL per min. For mass analysis, the negative electrospray ionization mode was used. The mass spectra of nitrate esters were characterized by the absence of the deprotonated molecular ions $[M–H]^-$ and the presence of the characteristic mass ion fragments *m*/*z* 62 (NO_3) and *m*/*z* 46 (NO_2). The mass range was scanned from 40 to 650 Da. The mass fragmentation data obtained were compared to the fragmentation data of pure 1,2- and 1,3-GDN standards.

Sample preparation and GST enzyme purification

Quail embryos (72 h old; n=120) were washed with ice-cold isotonic saline, pooled to final wet weight of 40 g and rapidly homogenized in 50 mL of ice-cold Buffer A using a Polytron tissue grinder (Brinkmann Instruments, Westbury, NY). The homogenate was centrifuged at 10 000 × *g* for 30 min, the supernatant was collected and further centrifuged at 100 000 × *g* for 60 min. The 100 000 × *g* supernatant (containing cytosol) was filtered through glass wool and used for further purification. All enzyme purification procedures, including fast protein liquid chromatography (FPLC®) (Amersham Pharmacia Biotech, Uppsala, Sweden), were performed as previously described (Bardai et al., 2006). Briefly, protein purification columns were pre-equilibrated in Buffer A (described above). A 50-mL aliquot of cytosol was then applied to a Pharmacia XK-50 desalting column. The desalted crude cytosolic fraction was passed three times through a XK-16 column containing 15 mL of GSH Sepharose at 1 mL/min. Following each pass of crude cytosol, the column was washed extensively with Buffer A, and the bound GST was eluted with Buffer B (50 mM Tris-HCl, pH 8.0, containing 10 mM GSH). Protein was monitored at 280 nm and the fractions with GST activity (i.e., those having high 1-chloro 2,4 dintrobenzene (CDNB) conjugating activity, as described below) were collected. Buffer B was then exchanged by Buffer A, and the protein was concentrated using Amicon centrifugal filter units (15 mL; 10 000 MW cut off) and stored at -80°C until further use. Protein concentration was determined with a bicinchoninic acid protein assay kit from Pierce Chemical Company (Rockford, IL)

using bovine serum albumin (BSA) as the standard. Purification of total GST from embryonic eye was carried out in the same manner.

Analysis of enzyme-catalyzed GTN metabolism

Enzyme-catalyzed GTN biotransformation assays for in-vitro embryo homogenates were run in triplicate using 6-mL glass septum-sealed vials, flushed with argon to create anaerobic conditions, with constant agitation in the dark at 37°C for 2 h. Each 1 mL sample contained: GTN (30 μmol), cytosol (5 mg protein) or enzyme preparation (0.50 mg protein), GSH (100 μM), enzyme inhibitor, either ethacrynic acid (200 μM), an α,β-unsaturated ketone that inhibits the enzyme by binding to the cysteinyl residue in the active site (Cameron et al., 1995; Bryant et al., 2011), or diphenyliodonium chloride (100 μM), an inhibitor of flavoenzymes (Bhushan et al., 2003) and Buffer A. Controls were prepared by omitting enzyme or GSH from the reaction mixture. The reaction was stopped with the addition of 1 mL acetonitrile, vortexed, and placed in the dark at 4°C for 1 h to allow for protein precipitation. The solution was subsequently filtered through a 0.45 μm membrane. GTN was measured by HPLC, as described below. Activity of the enzymatic biotransformation of GTN was expressed as micromoles nitrite per min per mg protein.

Analysis of GST isozymes using reverse phase HPLC

Affinity-purified embryo and embryonic eye GSTs were concentrated to 1 μg/μL and 100 μL was combined with 1 μL trifluoroacetic acid (TFA) prior to

injection onto a 150 mm × 4.6 mm × 5 µM C4 column (Grace Vydac, Hesperia, CA) using acetonitrile containing 0.1% TFA and water containing 0.08% TFA as the mobile phase solvents. The column flow rate was 0.7 mL/min, and gradients were developed in 20% acetonitrile that was increased to 40% in 10 min, followed by a linear increase to 60% acetonitrile over 1 h. Peaks were detected using a Waters diode array detector UV–Vis detector (λ = 210, 214, and 280 nm) and integrated using Empower (Waters, Columbia, MD) software. Eluted fractions containing the GST subunits were collected post-detection, separated by sodium dodecyl sulphate polyacrylamide gel electrophoresis (SDS-PAGE), silver stained, and identified by mass spectrometry.

Sodium dodecyl sulphate – polyacrylamide gel electrophoresis and mass spectrometry analysis of HPLC fractions

To confirm sample purity and determine molecular weights of the purified proteins, SDS–PAGE was done in 15% gels containing 0.1% SDS (Laemmli, 1970) using a BioRad Mini Protean II electrophoresis system. The loading volume was 10 µL (containing 1 µg protein) per well. Molecular weights were determined from R_f values of standard marker proteins (BioRad, Hercules, CA), and protein bands were visualized using a silver stain. Gel analysis was carried out using the BioRad Quantity One Analysis software.

After resolution by SDS-PAGE, the HPLC fractions corresponding to GST isozymes were excised from the acrylamide gel and prepared for mass spectrometry. Bands were first minced into 1 mm^3 gel pieces then transferred to a

96-well tray (each band was placed in separate well) and subjected to reduction, cysteine-alkylation, and in-gel tryptic digestion by automation using a MassPrep Workstation (Micromass, Manchester, UK), as previously described (Wasiak et al., 2002). Briefly, the gel sections were washed twice with 50 mM ammonium bicarbonate (NH_4HCO_3), dehydrated in acetonitrile, and finally dried under vacuum. Proteins were in-gel digested by adding 25 µL of trypsin (6 ng/µL in 50 mM NH_4HCO) and incubating for 30 min at room temperature followed by 4.5 h at 37°C. To extract peptides, 30 µL of a mix containing 1% formic acid and 2% acetonitrile was added and incubated 30 min at room temperature. Gel sections were rinsed twice in 50 µL of 5% acetonitrile in 0.1% TFA, followed by a wash in 50% acetonitrile in 0.1% TFA. Supernatants from each wash were collected and combined with the initial protein digest. Samples were then dried to 10–20 µL total volume under vacuum and stored at −80°C until analysis. Extracted peptides were then subjected to mass spectrometry analysis.

Samples were desalted and subsequently resolved on a 10 cm × 75 micron PicoFrit® column containing BioBasic™ C18 packing (Supelco, Bellefonte, PA, USA). Peptides were eluted from the column with a 30 min gradient of 10-95% acetonitrile (v/v) containing 0.1% formic acid (v/v) at a flow rate of 20 nL/min using an Agilent (Mississauga, ON, Canada) 1100 series NanoHPLC system. Precursor ion selection for subsequent tandem ms fragmentation analysis was done as follows. Briefly, up to three doubly, triply or quadruply charged ions of intensity greater than 2×10^6 counts per second (cps) from each enhanced-ms survey scan were selected for passage into a collision cell. Collision-induced dissociation was

facilitated by collision with nitrogen gas; fragment ions were trapped in Q3 and scanned. The peak listed data were then searched against a copy of the Universal Protein Resource (UniProt) data base (May 21, 2008) limited to the Galliformes taxonomy (taxon ID 8976) (9880 sequences; 3 554 051 residues).

Glutathione-S-transferase activity

The GST assays were done at room temperature using a 96-well microtiter plate reader (Biotek™; Molecular Devices Corp, Sunnyvale, CA) set at an absorbance of 340 nm. Activity was measured using CDNB as the substrate, and reduced GSH as the cofactor. The CDNB (20 mM) was prepared in anhydrous ethanol. Fresh solutions of GSH (20 mM) were prepared daily in 100 mM sodium phosphate buffer (pH 6.5). Each reaction mixture (250 µL) contained: 100 mM phosphate buffer, 1 mM GSH, and 1 mM CDNB. The ethanol concentration was less than 5%. The increase in absorbance was recorded for 5 min to ensure that the reaction went to completion (steady state). Non-enzymatic conjugation of GSH with CDNB was subtracted from all assays by including a blank (buffer only) consisting of all the assay components except the protein preparation. One unit of GST activity was defined as the initial rate of one micromole of the product (S-2,4-dinitrobenzene-glutathione) formed per min measured at 340 nm using an extinction coefficient of 9.6 mM^{-1} for the conjugate (Habig et al.,1974). Kinetic studies of the partially purified enzyme were done using varying concentrations of CDNB (from 0.02 to 5 mM) and GSH (from 0.07 to 5 mM); the apparent enzyme kinetic constants (app. V_{max} and app. K_m) were calculated according to the

Michelis-Menten equation. Specific activities were expressed as μmol/min/mg protein.

Statistical analyses

Differences between the test and control samples were considered significant at $p \leq 0.05$ using the Student's *t* test for paired data or one-way ANOVA with Tukey's multiple comparisons test, where appropriate. The Pearson product-moment correlation coefficient was used to analyze the association between all studied parameters and considered significant at $p \leq 0.05$. Statistical analyses were done using GraphPad Prism version 5.0 for Macintosh, GraphPad Software (San Diego, CA). The GST kinetic constants (*K*m and *V*max) were determined by Lineweaver-Burke plots and were compared to the *K*m and *V*max constants generated by the Michaelis–Menten equation using Kaleidagraph (Reading, PA).

Results

GTN, NO_2^-, total GSH, and NADP(H) concentrations after ex-ovo treatment of embryos with GTN

A GTN/saline solution (5.7 μM) was applied to embryos *ex-ovo* and GTN, NO_2^-, GSH, and $NADP^+$/NADPH concentrations were determined over different time intervals (0, 0.5, 1, and 1.5 h). There was a significant decrease in residual GTN when analyzed by ANOVA at all three time points (Fig. 3.1). Tukey's multiple comparison tests showed significant decreases in GTN between 0.5 and 1.0 h ($p \leq 0.05$) and between 1.0 and 1.5 h ($p \leq 0.01$). The decrease in the concentrations

of GTN remaining over time was associated with significant increases in both NO_2^- and the NADP+/NADPH ratio, and a decrease in total glutathione (GSH) when compared to paired controls treated with saline only (Fig. 3.2 A, B, and C). Tukey's post hoc test showed a significant increase in nitrite levels at 0.5 h ($p \leq 0.05$), 1 h ($p \leq 0.01$) and 3 h ($p \leq 0.001$), and in the NADP+/NADPH ratios at 1 h ($p \leq 0.001$) and 3 h ($p \leq 0.001$) when compared to their time-matched controls. Total GSH levels decreased significantly at 1 h and 3 h when compared to the time-matched controls.

A Pearson product-moment correlation coefficient was calculated to assess the relationship between metabolism of GTN over time (Fig. 3.1) and its subsequent biological effects on NO_2^-, NADP(H), and GSH. There was a significant inverse relationship for both NO_2^- and NADP(H), and a significant positive correlation for GTN and GSH (Fig 3.2 A, B, C inset). These data demonstrate that the embryo can metabolize GTN *ex ovo* by a denitration pathway, releasing nitrite; this was accompanied by a decrease in GSH and an increase in the ratio of NADP+/NADPH compared to time matched controls.

Enzyme-catalyzed GTN biotransformation

To further characterize the metabolism of GTN by embryos, time course studies were carried out using HPLC analyses of crude whole embryo cytosol to identify the GTN biotransformation products. Approximately 97% of the initial 30 µmol GTN added to the 1 mL samples was metabolized after 4 h of incubation (Fig. 3.3A). The rate of GTN disappearance was 0.060 ± 0.001 nmol/min/mg

protein based on the linear descending phase of GTN concentrations, i.e., from 0 to 1.5 h incubation. In control samples, the GTN concentration in the samples containing buffer only (i.e., with no cytosol added) showed little to no change in GTN concentrations, indicating the absence of detectable abiotic transformation. The cytosol-dependent decrease in GTN concentration (Fig. 3.3A) was accompanied by increases in the formation of nitrite (NO_2^-) and the denitrated metabolites, 1,2- or 1,3-GDN (Fig. 3.3B) that were maximal at 4 h, and decreased until the end of the 24 h study. The increase in nitrite levels and decrease in GTN levels were stochiometric in the first 2 h (1:1). However, after 2 h the increase in nitrite was not stoichiometric when compared to the decrease in GTN, indicating that further denitration of the 1,2-GDN or 1,3-GDN metabolites was occurring. At 4 h incubation, the amount of nitrite began to decrease (Fig. 3.3B), suggesting that the nitrite formed earlier was being sequestered by proteins. These *in-vitro* data confirm our *ex-ovo* data, and indicate that GTN is metabolized by quail embryo cytosol, as evidenced by the decrease in GTN concentrations and concomitant formation of GTN metabolites.

To identify the key enzymes involved in the metabolism of GTN in quail embryos, GTN metabolism studies were carried out using samples of crude whole cytosol containing 5 mg/mL protein and GTN, in the presence or absence of 200 μM GSH (Fig. 3.4). Ethacrynic acid (EA), a GST inhibitor (Cameron et al., 1995; Tew et al., 1997), was used as a biochemical tool to determine if quail embryo GSTs are involved in the *in-vitro* biotransformation of GTN. The GTN concentrations remained constant in the Group 1 abiotic control samples. Group 1

samples contained GTN, GSH, and ethacrynic acid (EA, 100 μM), and saline only. The purpose of this *in-vitro* treatment group was to determine if GTN spontaneously decomposed or if it reacted abiotically with GSH or EA. These results indicate that the addition of GSH and EA did not react abiotically with GTN. Group 2 samples included cytosol and GTN (i.e., no GSH or EA were added). The addition of cytosol led to a significant 67% decrease ($p \leq 0.001$) in GTN concentrations, from 28.4 ± 0.15 μM (Group 1) to 9.3 ± 0.4 μM (Group 2). The GTN concentration was decreased further when the whole cytosol was incubated with the addition of exogenous GSH (200 μM) (Group 3). The addition of EA to whole cytosol incubated with GTN led to a significant increase in residual GTN concentrations (17.0 ± 1.0 μM; Group 4) compared to cytosol samples incubated without EA (Group 2). Thus, EA significantly decreased ($p \leq 0.05$) the biotransformation of GTN in the crude cytosol of quail embryos. Addition of the flavoprotein inhibitor diphenyliodonium chloride (100 μM) (Group 5) did not inhibit GTN metabolism (Group 2 *vs.* Group 4), suggesting that flavoproteins are not involved in the metabolism of GTN. It should be noted that the studies described above used crude whole cytosol containing soluble proteins and co-factors. Taken together, these data show that a crude cytosolic preparation from the quail embryo contains the enzymatic activity required to metabolize GTN. Inhibition with EA indicates that this activity may be a GST isozyme. The addition of exogenous GSH only increased the metabolism of GTN by 9%, signifying that GTN metabolism is in fact enzymatic, and not simply dependent on the presence of thiol-containing compounds.

Enzyme purification of quail embryo GSTs

GSTs were purified from preparations of whole embryo or embryo eye using GSH-affinity chromatography. Table 3.1 summarizes of the activity profiles, comparing the GST activity (reflected by the metabolism of CDNB) and GTN metabolism (reflected by NO_2^- production) at the different purification steps of quail embryo GSTs. In preparations of quail whole embryo, the GST specific activity (nmol/min/mg), using CDNB as the substrate, increased from 0.12 in the crude homogenate to 15.52 in the affinity chromatography purified samples (Table 3.1), resulting in 129-fold purification. Based on the NO_2^- production rate in the different fractions, the GTN removal rate remained similar in the crude (0.29 nmol/min/mg) and 10 000 $\times$ *g* supernatant (0.26 nmol/min/mg), but increased in the 100 000 $\times$ *g* cytosol fraction (0.48 nmol/min/mg). Notably, the largest increase in the NO_2^- production rate was observed in the affinity-purified fraction (1436 nmol/min/mg) of quail whole embryos. This represents a 4951-fold increase in GTN metabolizing activity.

In embryonic eye preparations, the specific activity of GST (nmol/min/mg), using CDNB as the substrate, remained the same in the first three fractions (0.01, 0.02, and 0.02) increased to 1.25 in the affinity chromatography fractions (Table 3.1), resulting in 125-fold purification. The GTN removal rate, based on NO_2^- production rate in the different fractions, increased at each subsequent purification step (0.49, 0.77, and 0.90 nmol/min/mg) with the largest increase (34.2

nmol/min/mg) observed in the affinity purification step. This represented a 70- fold increase in GTN metabolizing activity.

To account for the differences observed in specific activities we carried out a series of kinetic studies on the embryo and embryonic eye GST-type enzyme fractions eluted from the affinity column. The calculated respective V_{max} (μM/min) and *K*m (mM) values were significantly different ($p = 0.03$; $p < 0.001$) for whole embryo (30.0 and 0.20), and embryo eye (35.9 and 0.8) (Supplemental Fig. S3.1A, B). These data suggest that the enzymes responsible for GTN biotransformation are GSTs with differing specific and kinetic activities. SDS-PAGE analysis of proteins from embryonic eye (Fig. 3.5, lane A) or whole embryo (Fig. 3.5, lane B) purified using the GSH affinity column were within the 22–29 kDa range; this is consistent with the range of molecular masses reported for avian GSTs (24-30 kDa) (Bardai et al., 2006; Cameron et al., 1995; Hsieh et al., 1999). Thus, the enzymes purified from whole embryo and embryonic eye using the GSH affinity column are GST-type enzymes.

Time course of GTN biotransformation in-vitro

GTN biotransformation studies were carried out using affinity purified whole embryo GST proteins. Metabolism of GTN did not occur or was negligible when incubated with buffer (PBS), cofactor (GSH) or EA alone (Fig. 3.6A). Metabolism of GTN occurred only when GTN was incubated in the presence of both purified enzyme and GSH (Fig. 3.6B), as evidenced by the complete disappearance of GTN after 15 min of incubation. The addition of EA inhibited GTN metabolism at

120 min incubation in samples containing partially purified GST and GSH, and gave results similar to studies using whole cytosol (Fig. 3.4). The incubation of GTN for 120 min in Buffer A with only GSH and no enzyme added, or with only enzyme (ENZ) and no GSH added, did not cause a significant disappearance of GTN compared to the time zero controls, or GTN samples incubated for 120 min without enzyme and GSH (Fig. 3.6A). Thus, GST partially purified from quail embryo can degrade GTN in the presence of GSH, confirming the studies with whole cytosol.

Time course studies were conducted using affinity purified GST to determine whether the observed metabolism of GTN *in-vitro* was also accompanied by the formation of GTN metabolites, including NO_2^-, 1,2- or 1,3-GDN (Fig. 3.6B). As anticipated, the complete disappearance of GTN after 15 min incubation with partially purified GST was accompanied by an increase in nitrite levels (31.5 ± 4.7 μM) and GTN metabolites (24.0 ± 2.5 μM) when compared to time zero control. The nitrite levels continued to increase significantly ($p < 0.001$) (44.9 ± 0.5 μM) from 30 to 60 min of incubation. However, during this time, the concentration of combined GTN metabolites (21.7 ± 0.4 μM) was not significantly changed. These results indicate that the dinitrated metabolites (1,2- and 1,3-GDN) may have continued to undergo further denitration to 1-glyceryl mononitrate (1-GMN), and 2-glyceryl mononitrate (2-GMN), metabolites that we were unable to resolve using our HPLC technique (Hashimoto and Kobayashi, 2003), leading to an increase in released nitrite, as shown in Fig. 3.6. Finally, the addition of EA completely inhibited the ability of the enzyme to biotransform GTN. These data

clearly show that GST is involved in the metabolism of GTN, and that GTN may undergo further metabolism to mono-denitrated products.

Biotransformation products identified with LC-MS

While HPLC data indicated the presence of GTN metabolites, it was not possible to distinguish between the 1,2- and 1,3-GDN metabolites. To identify the biotransformation products of GTN metabolism, we carried out LC-MS studies using purified embryo GST. Figure 3.7A is the total ion chromatogram (TIC) scanned from 40 to 650 Da. Three characteristic peaks (peak 1, 2, and 3, at 10.5, 11.5, and 21.5 min, respectively) were observed. Figures 3.7B, C, and D are the LC-MS data of the extracted ion chromatogram of Peaks 1, 2, and 3 detected at 62 Da. These peaks were identified as 1,3-GDN, 1,2-GDN, and GTN, respectively, based on comparisons to the fragmentation patterns obtained using pure 1,3- and 1,2-GDN standards. The adduct ion masses [M+Cl-]- m/z 262 and m/z 217 are the adduct ion masses of GTN and 1,2-GDN, respectively. The characteristic fragment m/z 47 (HNO_2) was not observed for 1,3-GDN. These characteristic fragmentation patterns were compared to fragmentation patterns of known control material.

NO assay

Since the quail embryo possesses the capacity to metabolize GTN to nitrite, and NO is a highly reactive pharmacological by-product of GTN metabolism, we sought to determine if the embryo further oxidizes the nitrite to NO. The addition of SNAP to crude embryo homogenates clearly showed that the probe was

capable of detecting NO (Fig. 3.8) with a limit of detection of 1.1 nM NO. However, NO was not detected in embryo homogenates to which GTN was added, suggesting that HH 9 embryo homogenates may not be capable of further oxidizing nitrite to NO.

GST subunit analysis by reverse phase HPLC

Reverse phase HPLC (RP-HPLC) was used to separate the GST isozymes from the partially purified enzyme preparation of embryonic eye (Fig. 3.9A) and whole embryo (Fig. 3.9B) to determine which of the GST isozymes were capable of metabolizing GTN *in vitro*. The RP-HPLC separation of embryonic eye affinity purified proteins revealed the presence three major peaks (Peaks 2, 6, and 8), and seven minor peaks (Peaks 1, 3, 4, 5, 7, 9, and 10; Fig. 3.9A). The resolution of whole embryo fractions (Fig. 3.9B) revealed the presence of four major peaks (Peaks 2, 6, 8, and 9) and five minor peaks (Peaks 1, 3, 4, 5, and 7). When the individual collected fractions from the RP-HPLC separation from both embryonic eye and embryo were subjected to SDS-PAGE followed by silver staining, all visible proteins eluted in the molecular weight range consistent with GSTs (*i.e.,* 23–27 kDa, inset Fig. 3.9A,B). This indicates that both the embryonic eye and embryo contain multiple GSTs that were resolved.

MS peptide sequencing and MALDI-TOF analyses

To determine the identity of the purified isozymes capable of metabolizing GTN from both the embryonic eye and embryo (Figs. 3.9A,B), we did BLAST

analysis of the peptide sequences obtained from the MS analysis of the trypsin-digested peaks using the Swiss-Prot and NCBI databases. Protein peaks 2, 3, 4, 5, 7, and 10 of embryonic eye GST subunits (Fig. 3.9A), contained α-like GSTs, whereas peaks 6, 8, and 9 had μ-like GSTs. A similar analysis of whole embryo GST subunits (Fig. 3.9B) indicated that peaks 2, 3, 4, 6, 7, 8, and 9 contained α-like GSTs, whereas peaks 1 and 5 contained μ-like GSTs.

NAC supplementation experiments

Since we have shown that GSTs metabolize GTN in the quail embryo and that GSH is required, our next goal was to determine the consequences of supplementation with NAC on the embryotoxicity of GTN in quail embryos. GTN treatment increased the mortality of quail embryos (35%) compared to that observed after treatment with either vehicle (Control, 8%) or NAC (4%) alone (Table 3.2). A 46% decrease in mortality was observed when embryos were pre-treated with NAC prior to administration of GTN. All viable embryos were evaluated using a one-way between subjects ANOVA followed by Tukey's multiple comparisons test for embryo length. There was a significant effect of treatment on embryo length among the four treatment groups (Control, NAC, GTN, and NAC + GTN) (Table 3.2). Post hoc comparisons using Tukey's multiple comparison test showed a significant decrease in body length following treatment with GTN (Control *vs.* GTN; $p \leq 0.0001$ or NAC *vs*. GTN; $p \leq 0.0001$). Co-treatment of GTN-exposed embryos with NAC (GTN *vs.* NAC + GTN) resulted in a significant

increase ($p \leq 0.001$) in body length. Finally, there was no significant difference between NAC and NAC + GTN treatment groups.

Because the sizes of craniofacial structures, such as the mesencephalon and the eye, were shown previously to be decreased significantly in embryos exposed to GTN 48-h post dose (Bardai et al., 2011), we measured these parameters in the present experiment. A one-way ANOVA revealed a significant effect on embryo craniofacial, mesencephalon, and eye perimeter measurements (Table 3.3). Tukey's multiple comparisons test showed a significant decrease in craniofacial ($p \leq 0.001$), mesencephalon ($p \leq 0.001$) and eye ($p \leq 0.001$) perimeters between either the Control or NAC (10 mM) treated embryos and those exposed to GTN (440 µM). Co-treatment of GTN-exposed embryos with NAC (GTN *vs.* NAC + GTN) resulted in a significant increase in craniofacial, mesencephalon and eye perimeter values ($p \leq 0.05$) towards control perimeters (Table 3.3). Together, these results indicate that NAC co-administration reduced the effects of GTN exposure on all parameters of GTN embryotoxicity.

Discussion

This study shows that the quail embryo metabolizes GTN. This action is observed *in-vitro* and *ex-ovo,* in the whole embryo and embryo eyes, and is catalyzed by alpha- and mu-type GSTs. During the metabolism of GTN, there is a decrease in total GSH concentrations and an increase in the ratio of NADP+/NADPH compared to time matched controls, suggesting that GTN affects

these measures of redox status in the *ex-ovo* developing embryo. The pre-supplementation of embryos with NAC offers a partial rescue from GTN treatment.

The first finding that the quail embryo metabolizes GTN, is supported by both *ex-ovo* and *in-vitro* experiments. Three hours following exposure to GTN we found that GTN levels decreased significantly in *ex-ovo* treated embryos followed by a corresponding increase in nitrite in exposed embryos compared to vehicle treated embryos. The small decrease in GTN concentrations after 0.5 h that corresponds to a significant increase in NO_2^- can be explained stochiometrically because for every molecule of GTN metabolized there is the release of three nitrites. Two major pathways have been proposed for the metabolism of GTN. The first is a “mechanism-based biotransformation” pathway that produces nitric oxide (NO) and contributes directly to vasodilation; the production of NO is accompanied by an excess of the 1,2-GDN metabolite relative to 1,3-GDN (Hashimoto and Kobayashi, 2003). The second has been termed a “clearance-based biotransformation or detoxification” since the NO_2^- that is produced has no apparent cardiovascular effect; in this pathway, equimolar amounts of both GTN metabolites are produced. In the LC/MS experiment, we observed the formation of equimolar quantities of 1,2- and 1,3- GDN and the presence of NO_2^-, but not NO. These data are consistent with the clearance-based pathway of GTN metabolism. The absence of NO was also observed in experiments using whole embryo homogenates. Thus, the GTN metabolized by the quail embryo proceeds by a clearance-based biotransformation that results in the production of NO_2^-. Therefore, the increase in nitrated proteins we observed previously (Bardai et al.,

2011) is mediated by a reaction of proteins with NO_2^- rather than an NO-mediated reaction. However, nitrite can be reduced to NO by nitrite reductase (Shiva et al., 2007). Whether nitrite reductase is present in the quail embryo or not is unknown.

The second finding that a GST-type enzyme metabolizes GTN, is supported by the *in-vitro*, protein purification, and kinetic studies. As the cytosolic fraction of the whole embryo homogenate can metabolize GTN, we investigated the role of GSTs in this metabolic process. Ethacrynic acid (EA) is an unsaturated ketone that binds to the active site of GSTs, and can inhibit both human and rat GSTs of the α-, μ- and π-classes (Lau and Benet, 1992; Ploemen et al., 1990). This GST inhibitor significantly decreased GTN metabolism in quail embryo homogenates, suggesting that a GST type of enzyme was involved in the denitration reaction. As the addition of EA did not completely inhibit the metabolism of GTN *in-vitro*, other enzymes may also be involved in the metabolism of GTN in the cytosolic fractions (Chen et al., 2002). However, GSTs are likely to play an important role in GTN metabolism. Our observations that EA significantly reduced GTN metabolism in crude cytosol and completely inhibited GTN metabolism in purified protein preparations indicate the presence a GST-type of enzyme. The fact that EA failed to completely inhibit GTN metabolism in the crude cytosol after 2h (Fig. 3.4), in contrast to the purified GST preparation (Fig. 3.6), can be explained based on the proposed mechanism of action of EA, whereby EA inhibits enzyme activity by binding to cysteinyl residues (Bryant et al., 2011). Therefore, in crude cytosol preparations, EA binds to the active site of GST and reacts with other biomolecules

that contain cysteinyl residues. Addition of excess EA may more specifically target the cysteinyl residues of the active sites in the purified GST preparation.

There is evidence in mammalian systems for the involvement of GSTs from the subcellular fractions of both the liver and vascular tissue in the metabolism of GTN (Kurz et al., 1993; Lau and Benet, 1990; Lau et al., 1992). Previously, we demonstrated that alpha- and mu-type GSTs present in the subcellular fractions of the adult quail liver were capable of metabolizing other nitro-containing compounds (Bardai et al., 2006); here, for the first time, we show that in the quail embryo both the alpha- and mu-types of GSTs are capable of GTN denitration. In the 24 h time course study, the amount of free nitrite present decreased dramatically, suggesting that the nitrite was irreversibly bound to proteins. This is supported by our earlier observation that embryos treated with GTN *ex-ovo* and examined 18 h later showed the presence of nitrated proteins (Bardai et al., 2011). This post-translational modification of proteins is a consequence of the formation of radical nitrating species such as NO, a free radical that is generated as a consequence of GTN metabolism and is capable of causing developmental pathologies (Wells et al., 2005). We analyzed the cytosolic fraction to which GTN had been added for the presence of NO but were unable to detect NO in these assays (data not shown).

Reverse phase HPLC and tandem mass spectrometry of purified protein preparations clearly indicated the presence of alpha- and mu- type GSTs in both the whole embryo and embryo eye. Surprisingly, the results also showed that the kinetic profiles of GSTs in the quail embryo differed significantly from those purified

from the eye. The specific activities obtained for the whole quail embryo GSTs were comparable to previous reports (Bardai et al., 2006; Dai et al., 1996). That we found similar ratios of CDNB/GTN specific activity in crude extracts and purified GSTs from both the whole embryo (0.03) and embryonic eye (0.01) indicates that all of the important GTN biotransformation activity was purified from the crude extract. However, differences in specific activity and *K*m values indicate that there are different GST isozymes present in the whole embryo and embryonic eye extracts. It is possible that the GSTs present in the quail embryonic eye have a multifunctional role in addition to detoxification. Multifunctional GSTs in the squid eye lens (S-crystallins), similar in sequence to rat Gsta-1, have been described (Piatigorsky, 2003) and found to have to 40X lower activity with CDNB than GSTs purified from squid liver extracts (Wistow and Piatigorsky, 1987; Piatigorsky, 2003). This is similar to the difference in activity we observed between GST purified from whole embryo and embryo eye (Table 3.1). Proteins similar to chicken and human class alpha GSTs were reported to be abundant in the chicken corneal epithelium and stroma (Cuthbertson et al., 1992). The presence of both Gsta and Gstm isozymes in the embryo and embryonic eye, and their apparent differences in activity suggest that the quail embryonic eye may contain crystalline type GSTs. The role of crystallin GSTs in the quail embryo eye is not known.

Our third finding that GTN metabolism by the embryo results in a change in embryo redox status, is supported by the *ex-ovo* data showing that over a period of 3 h, concurrent with a decrease in GTN, there is a decrease in total GSH and an increase in the NADP+/NADPH ratio in treated embryos compared to their

controls. NADPH is required as a cofactor for the regeneration of GSH from GSSG, catalyzed by glutathione reductase (Lu, 2009). In the quail embryo NADPH may be supplied by the pentose phosphate pathway and/or by two NADPH-producing cytosolic enzymes, namely NADP+-dependent malic enzyme and NADP+-dependent isocitrate dehydrogenase. Together, these data suggest that GTN exposure may disrupt the redox balance and/or the energy status in the developing embryo, leading to GSH depletion. GSH is a critical regulator of redox balance and is required for normal embryo development (Ufer et al., 2010; Yanes et al., 2010). Interestingly, exposure to buthionine sulfoximine, an inhibitor of glutamate cysteine ligase, the rate limiting enzyme in the synthesis of GSH, results in the development of embryos with multiple developmental defects (Hales and Brown, 1991; Shi et al., 2000).

Our fourth finding is that supplementation with NAC offers a partial rescue to *in-ovo* GTN treated. Pre-treatment with NAC, a precursor in the formation of GSH, decreased GTN-induced embryo mortality and growth retardation (Tables 3.2, 3.3). Previous studies have shown that the addition of NAC to the culture medium of gestation 9 day rat embryos diminished the growth retardation induced by high glucose concentrations added to mimic oxidative stress in diabetic pregnancies (Gäreskog and Wentzel, 2007). NAC may serve as a source of cysteine for the synthesis of GSH or may react directly with free radicals, serving as an antioxidant. It is also possible that NADPH depletion (Fig. 3.2) results in partial metabolic dysfunction of the pentose phosphate pathway, and that NAC may act by partially restoring energy homeostasis.

Our demonstration that the quail embryo can metabolize GTN, with the production of reactive nitrogen species and perturbations in cellular redox status, as assessed by total GSH and the ratio of NADP+/NADPH, suggests that more careful consideration is required when administering GTN during pregnancy. The possible involvement of other enzymatic systems capable of metabolizing GTN in the embryo needs to be further investigated to determine their role in mediating the developmental pathologies observed. Finally, GSTs in the embryonic eye differ in enzymatic activity from those in the whole embryo. It is not yet clear what role, if any, these GSTs within the eye may play in embryo development.

In summary, this study shows that the *ex-ovo* quail embryo possesses both α- and μ-type GSTs that can metabolize GTN to produce nitrite. The metabolism of GTN by *ex-ovo* quail embryo GSTs depletes total GSH and alters the ratio of NADP+ to NADPH, resulting in perturbation of the redox balance in the embryo. Because NAC administration provides partial protection to *in-ovo* GTN treated embryos, we propose that this pathway plays a role in mediating the embryotoxicity of GTN.

Supplementary data description

Supplementary data (Supp. Fig S3.1) depict the kinetic constants (Vmax and Km) of purified GSTs obtained from whole embryo and embryo eye.

Funding

G.B is the recipient of a Fonds de la recherché en Santé du Québec Doctoral Research Award. B.F. H. is a James McGill Professor of McGill University.

Acknowledgments

We thank General Dynamics Ordnance and Tactical Systems - Canada for providing the GTN, and Anna-Maria Halsz and Louise Paquet for the LC/MS and HPLC analyses.

References

Bardai, G.K., Halasz, A., Sunahara, G.I., Dodard, S., Spear, P.A., Grosse, S., Hoang, J., Hawari, J., 2006. In vitro degradation of hexanitrohexaazaisowurtzitane (CL-20) by cytosolic enzymes of Japanese quail and the rabbit. Environ. Toxicol. Chem. 25, 3221-3229.

Bardai, G.K., Hales, B.F., Sunahara, G.I., 2011. Developmental toxicity of glyceryl trinitrate in quail embryos. Birth Defects Res. A Clin. Mol. Teratol. 91, 230-240. Bhushan, B., Paquet, L., Spain, J.C., Hawari, J., 2003. Biotransformation of 2,4,6,8,10,12-hexanitro-2,4,6,8,10,12-hexaazaisowurtzitane (CL-20) by denitrifying *Pseudomonas sp*. strain FA1. Appl. Environ. Microbiol. 69, 5216-5221.

Board, P.G., 2007. The use of glutathione transferase-knockout mice as pharmacological and toxicological models. Expert Opin. Drug Metab. Toxicol. 3, 421-433.

Bryan, N.S., Fernandez, B.O., Bauer, S.M., Garcia-Saura, M.F., Milsom, A.B., Rassaf, T., Maloney, R.E., Bharti, A., Rodriguez, J., Feelisch, M., 2005. Nitrite is a signaling molecule and regulator of gene expression in mammalian tissues. Nat. Chem. Biol. 1, 290-297.

Bryant, Z.E., Janser, R.F., Jabarkhail, M., Candelaria-Lyons, M.S., Romero, B.B., Slambrouck, S.V., Steelant, W.F., Janser, I., 2011. Inhibitory effects of ethacrynic acid analogues lacking the α,β-unsaturated carbonyl unit and para-acylated phenols on human cancer cells. Bioorganic Medicinal Chemistry Letters. 21, 912-915.

Cameron, A.D., Sinning, I., L'Hermite, G., Olin, B., Board, P.G., Mannervik, B., Jones, T.A., 1995. Structural analysis of human alpha-class glutathione transferase A1-1 in the apo-form and in complexes with ethacrynic acid and its glutathione conjugate. Structure. 3, 717-727.

Chapman, S.C., Collignon, J., Schoenwolf, G.C., Lumsden, A., 2001. Improved method for chick whole-embryo culture using a filter paper carrier. Dev. Dyn. 220, 284-289.

Chen, Z., Zhang, J., Stamler, J.S., 2002. Identification of the enzymatic mechanism of nitroglycerin bioactivation. Proc. Natl. Acad. Sci. U S A. 99, 8306-8311.

Chiu, J., Dawes, I.W., 2012. Redox control of cell proliferation. Trends Cell Biol. 22, 592-601.

Cuthbertson, R.A., Tomarev, S.I., Piatigorsky, J., 1992. Taxon-specific recruitment of enzymes as major soluble proteins in the corneal epithelium of three mammals, chicken, and squid. Proc. Natl. Acad. Sci. U S A. 89, 4004-4008.

Dai, H., Edens, F.W., Roe, R.M., 1996. Glutathione S-transferases in the Japanese quail: tissue distribution and purification of the liver isozymes. J. Biochem. Toxicol. 11, 85-9

Gäreskog, M., Wentzel, P., 2007. N-Acetylcysteine and alpha-cyano-4-hydroxycinnamic acid alter protein kinase C (PKC)-delta and PKC-zeta and diminish dysmorphogenesis in rat embryos cultured with high glucose in vitro. J. Endocrinol. 192, 207-214.

Habig, W.H., Pabst, M.J., Jakoby, W.B., 1974. Glutathione S-transferases. The first enzymatic step in mercapturic acid formation. J. Biol. Chem. 249, 7130-7139.

Hales, B.F., Brown, H., 1991. The effect of in vivo glutathione depletion with buthionine sulfoximine on rat embryo development. Teratology. 44, 251-257.

Hashimoto, S., Kobayashi, A., 2003. Clinical pharmacokinetics and pharmacodynamics of glyceryl trinitrate and its metabolites. Clin. Pharmacokinet. 42, 205-221.

Hayes, J.D., Flanagan, J.U., Jowsey, I.R., 2005. Glutathione transferases. Annu. Rev. Pharmacol. Toxicol. 45, 51-88.

Hsieh, C.H., Liu, L.F., Tsai, S.P., Tam, M.F., 1999. Characterization and cloning of avian-hepatic glutathione S-transferases. Biochem. J. 343 Pt 1, 87-93.

Jones, D.P., 2008. Radical-free biology of oxidative stress. Am. J. of Physiol. - Cell Physiol. 295, C849-C868.

Kasapinovic, S., McCallum, G.P., Wiley, M.J., Wells, P.G., 2004. The peroxynitrite pathway in development: phenytoin and benzo[a]pyrene embryopathies in

inducible nitric oxide synthase knockout mice. Free Radic. Biol. Med. 37, 1703-1711.

Kozlov, A.V., Dietrich, B., Nohl, H., 2003. Various intracellular compartments cooperate in the release of nitric oxide from glycerol trinitrate in liver. Br. J. Pharmacol. 139, 989-997.

Kurz, M.A., Boyer, T.D., Whalen, R., Peterson, T.E., Harrison, D.G., 1993. Nitroglycerin metabolism in vascular tissue: role of glutathione S-transferases and relationship between NO. and NO2- formation. Biochem. J. 292 (Pt 2), 545-550.

Laemmli, U.K., 1970. Cleavage of structural proteins during the assembly of the head of bacteriophage T4. Nature. 227, 680-685.

Lau, D.T., Benet, L.Z., 1990. Nitroglycerin metabolism in subcellular fractions of rabbit liver. Dose dependency of glyceryl dinitrate formation and possible involvement of multiple isozymes of glutathione S-transferases. Drug Metab. Dispos. 18, 292-297.

Lau, D.T.W., Benet, L.Z., 1992. Effects of sulfobromophthalein and ethacrynic acid on glyceryl trinitrate relaxation. Biochem. Pharmacol. 43, 2247-2254.

Lau, D.T., Chan, E.K., Benet, L.Z., 1992. Glutathione S-transferase-mediated metabolism of glyceryl trinitrate in subcellular fractions of bovine coronary arteries. Pharm. Res. 9, 1460-1464.

Lauretti, G.R., Perez, M.V., Reis, M.P., Pereira, N.L., 2002. Double-blind evaluation of transdermal nitroglycerine as adjuvant to oral morphine for cancer pain management. J. Clin. Anesth. 14, 83-86.

Lu, S.C., 2009. Regulation of glutathione synthesis. Mol Aspects Med. 30, 42-59.

Needleman, P., 1976. Organic nitrate metabolism. Annu. Rev. Pharmacol. Toxicol. 16, 81-93.

Nkabyo, Y.S., Ziegler, T.R., Gu, L.H., Watson, W.H., Jones, D.P., 2002. Glutathione and thioredoxin redox during differentiation in human colon epithelial (Caco-2) cells. Am. J. Physiol. Gastrointest. Liver Physiol. 283, G1352-G1359.

Padgett, C.A., Ivey, W.D., 1959. Coturnix quail as a laboratory research animal. Science. 129, 267-268.

Pallardó, F.V., Markovic, J., García, J.L., Viña, J., 2009. Role of nuclear glutathione as a key regulator of cell proliferation. Mol. Aspects Med. 30, 77-85.

Piatigorsky, J., 2003. Crystallin genes: specialization by changes in gene regulation may precede gene duplication. J. Struct. Funct. Genomics. 3, 131-137.

Ploemen, J.H., van Ommen, B., van Bladeren, P.J., 1990. Inhibition of rat and human glutathione S-transferase isoenzymes by ethacrynic acid and its glutathione conjugate. Biochem. Pharmacol. 40, 1631-1635.

Radi, R., 2004. Nitric oxide, oxidants, and protein tyrosine nitration. Proc. Natl. Acad. Sci. U S A. 101, 4003-4008.

Shi, Z.Z., Osei-Frimpong, J., Kala, G., Kala, S.V., Barrios, R.J., Habib, G.M., Lukin, D. J., Danney, C.M., Matzuk, M.M., Lieberman, M.W., 2000. Glutathione synthesis is essential for mouse development but not for cell growth in culture. Proc. Natl. Acad. Sci. U S A. 97, 5101-5106.

Shiva, S., Huang, Z., Grubina, R., Sun, J., Ringwood, L. A., MacArthur, P. H., Xu, X., Murphy, E., Darley-Usmar, V. M. and Gladwin, M. T., 2007. Deoxymyoglobin is a nitrite reductase that generates nitric oxide and regulates mitochondrial respiration. Circ Res. 100, 654-661.

Singhal, S.S., Piper, J.T., Srivastava, S.K., Chaubey, M., Bandorowicz-Pikula, J., Awasthi, S., Awasthi, Y.C., 1996. Rabbit aorta glutathione S-transferases and their role in bioactivation of trinitroglycerin. Toxicol. Appl. Pharmacol. 140, 378-386.

Tew, K.D., Dutta, S., Schultz, M., 1997. Inhibitors of glutathione S-transferases as therapeutic agents. Adv. Drug. Deliv. Rev. 26, 91-104.

Tietze F.,1969. Enzymic method for quantitative determination of nanogram amounts of total and oxidized glutathione: Applications to mammalian blood and other tissues. Anal. Biochem. 27, 502–522.

Tomarev, S.I., Zinovieva, R.D., Piatigorsky, J., 1991. Crystallins of the octopus lens. Recruitment from detoxification enzymes. J. Biol. Chem. 266, 24226-24231.

Ufer, C., Wang, C.C., Borchert, A., Heydeck, D., Kuhn, H., 2010. Redox control in mammalian embryo development. Antioxid. Redox. Signal. 13, 833-875.

Veselik, D.J., Divekar, S., Dakshanamurthy, S., Storchan, G.B., Turner, J.M., Graham, K. L., Huang, L., Stoica, A., Martin, M.B., 2008. Activation of estrogen receptor-alpha by the anion nitrite. Cancer. Res. 68, 3950-3958.

Wasiak, S., Legendre-Guillemin, V., Puertollano, R., Blondeau, F., Girard, M., de Heuvel, E., Boismenu, D., Bell, A.W., Bonifacino, J.S., McPherson, P.S., 2002. Enthoprotin: a novel clathrin-associated protein identified through subcellular proteomics. J. Cell. Biol. 158, 855-862.

Wells, P.G., Bhuller, Y., Chen, C.S., Jeng, W., Kasapinovic, S., Kennedy, J.C., Kim, P.M., Laposa, R.R., McCallum, G.P., Nicol, C.J., Parman, T., Wiley, M.J., Wong, A.W., 2005. Molecular and biochemical mechanisms in teratogenesis involving reactive oxygen species. Toxicol. Appl. Pharmacol. 207**,** 354-366.

Wimalawansa, S.J., De Marco, G., Gangula, P., Yallampalli, C., 1996. Nitric oxide donor alleviates ovariectomy-induced bone loss. Bone. 18, 301-304.

Wistow, G., Piatigorsky, J., 1987. Recruitment of enzymes as lens structural proteins. Science. 236, 1554-1556.

Yanes, O., Clark, J., Wong, D.M., Patti, G.J., Sánchez-Ruiz, A., Benton, H.P., Trauger, S. A., Desponts, C., Ding, S., Siuzdak, G., 2010. Metabolic oxidation regulates embryonic stem cell differentiation. Nat. Chem. Biol. 6, 411-417.

TABLES

Table 3.1. Purification of quail embryo and embryonic eye glutathione *S*-transferases

Purification Steps	Total Protein (mg)	Total Activity (U)	GST Specific activity [a]	NO_2^- Specific Activity [b]	Purification (-fold GST)	Purification (-fold NO_2^-)	Recovery [c] (%)
Quail – Embryo							
1. Crude Homogenate	500	6.0	0.12	0.29	1	1	
2. 10,000 × g supernatant	341	4.7	0.14	0.26	1.2	0.9	78
3. Cytosol	208	3.3	0.16	0.48	1.3	1.7	55
4. GST-Affinity Chromatography	0.04	0.58	15.52	1436	129	4951	9.7
Quail – Embryonic eye							
1. Crude Homogenate	120	1.38	0.01	0.49	1	1	
2. 10,000 × g supernatant	78	1.18	0.02	0.77	2	1.6	86
3. Cytosol	63	1.13	0.02	0.90	2	1.8	82
4. GST-Affinity Chromatography	0.24	0.29	1.25	34.2	125	70	21

[a] Specific activity measured according to Habig et al. (1974), using 1-chloro-2,4-dinitrobenzene (CDNB) as substrate (U/mg protein).

[b] Specific activity of NO_2^- production (nmol/min/mg protein).

[c] % Recovery calculated as: 100X(Total activity of the purification step / Total Activity of the Crude Homogenate).

Table 3.2. Effects of *in-ovo* NAC supplementation following GTN treatment of quail embryos.

Group[a]	n[b]	Mortality (%)	Crown Rump Length (mm)[c]
Control	30	8	14.2 ±1.1
NAC (10 mM)	30	4	13.9 ± 1.1[d]
GTN (440 µM)	30	35	11.5 ± 1.5[e,f]
NAC (10 mM) + GTN (440 µM)	30	16	13.2 ± 1.7[g]

[a] Injection volume = 20 µL. Abbreviations used: NAC (N-acetyl cysteine), GTN (glyceryl trinitrate)
[b] Number of eggs treated
[c] Mean ± SD
[d] Not significantly different from Ctrl and NAC + GTN
[e,f] Significantly different from Ctrl and NAC ($p \leq 0.0001$)
[g] Significantly different from GTN (440 µM) treatment alone ($p \leq 0.01$), using Tukey's multiple comparison test

Table 3.3. Effects of *in-ovo* NAC supplementation following GTN treatment on cranio-facial and mesencephalon perimeter and eye diameter.

Treatment[a]	Craniofacial perimeter (mm)[b]	Mesencephalon perimeter (mm)[b]	Eye diameter (mm)[b]
Control	8.3 ± 0.56	4.0 ± 0.29	3.0 ± 0.37
NAC (10 mM)	8.5 ± 0.72 [c,d]	3.9 ± 0.38 [c,e]	2.8 ± 0.39 [c,f]
GTN (440 µM**)**	7.0 ± 0.89[g,h]	3.2 ± 0.36[g,h]	2.2 ± 0.39[g,h]
GTN +NAC	7.7 ± 0.96[i,j]	3.6 ± 0.42[i,j]	2.5 ± 0.49[i,j]

[a] Injection volume = 20µL. Abbreviations used: NAC (N-acetyl cysteine), GTN (glyceryl trinitrate)

[b] Mean ± SD, (N=30)

[c] Not significantly different from Ctrl

[d] Significantly different from NAC + GTN (**$p \leq 0.01$)

[e] Significantly different from NAC + GTN (*$p \leq 0.05$)

[f] Not significantly different from NAC + GTN

[g,h] Significantly different from either Ctrl or NAC treatment alone (***$p \leq 0.001$) using Tukey's post-hoc test

[i,j] Significantly different from GTN (*$p \leq 0.05$) and NAC treatment alone (*$p \leq 0.05$) using Tukey's post-hoc test

Figure Legends:

Figure 3.1 Time course of the metabolism of glyceryl trinitrate (GTN, 5.7 μM) by quail embryos *ex-ovo* (mean ± SD; n= 3 embryos/group). Asterisks denote a significant difference (*p < 0.05; **p < 0.01, one-way ANOVA followed by a post hoc Tukey's test).

Figure 3.1

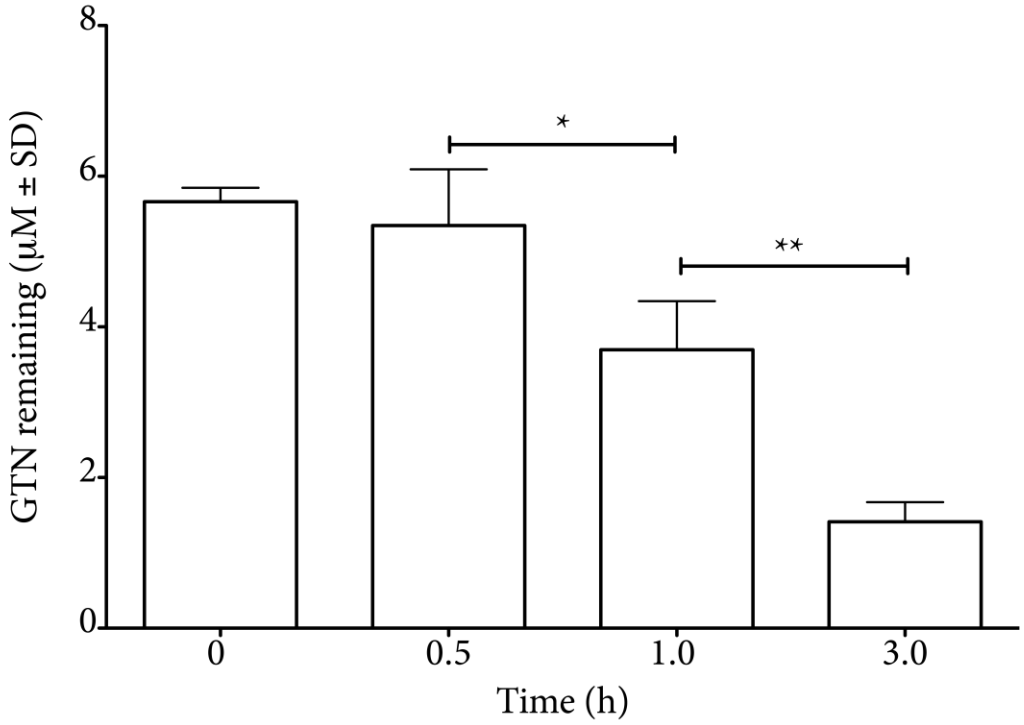

Figure 3.2 Nitrite (A), total GSH (B) and the ratio of NADP+/NADPH (C) in quail embryos treated *ex-ovo* with saline (control, Ctrl) or glyceryl trinitrate (GTN, 5.7 μM, treated) (mean ± SD; n= 3 embryos/group). Asterisks denote a significant difference from time-matched controls (* $p < 0.05$; ** $p < 0.01$; *** $p < 0.001$, one-way ANOVA followed by a post hoc Tukey's test). The insets show the Pearson correlation coefficient (r), and the statistical significance.

Figure 3.2

Figure 3.3 *In-vitro* time course studies of GTN (5.7 μM) biotransformation in whole quail embryo cytosol. Symbols used in 3A (-◆- buffer; -●- whole quail embryo cytosol) indicate the concentration of remaining GTN; In 3B symbols (-▲- nitrite (NO_2^-) (-■- 1,2- or 1,3-GDN) indicate the appearance of GTN metabolites. Incubation conditions: 37°C. Data are the means of triplicates; error bars represent SD.

Figure 3.3

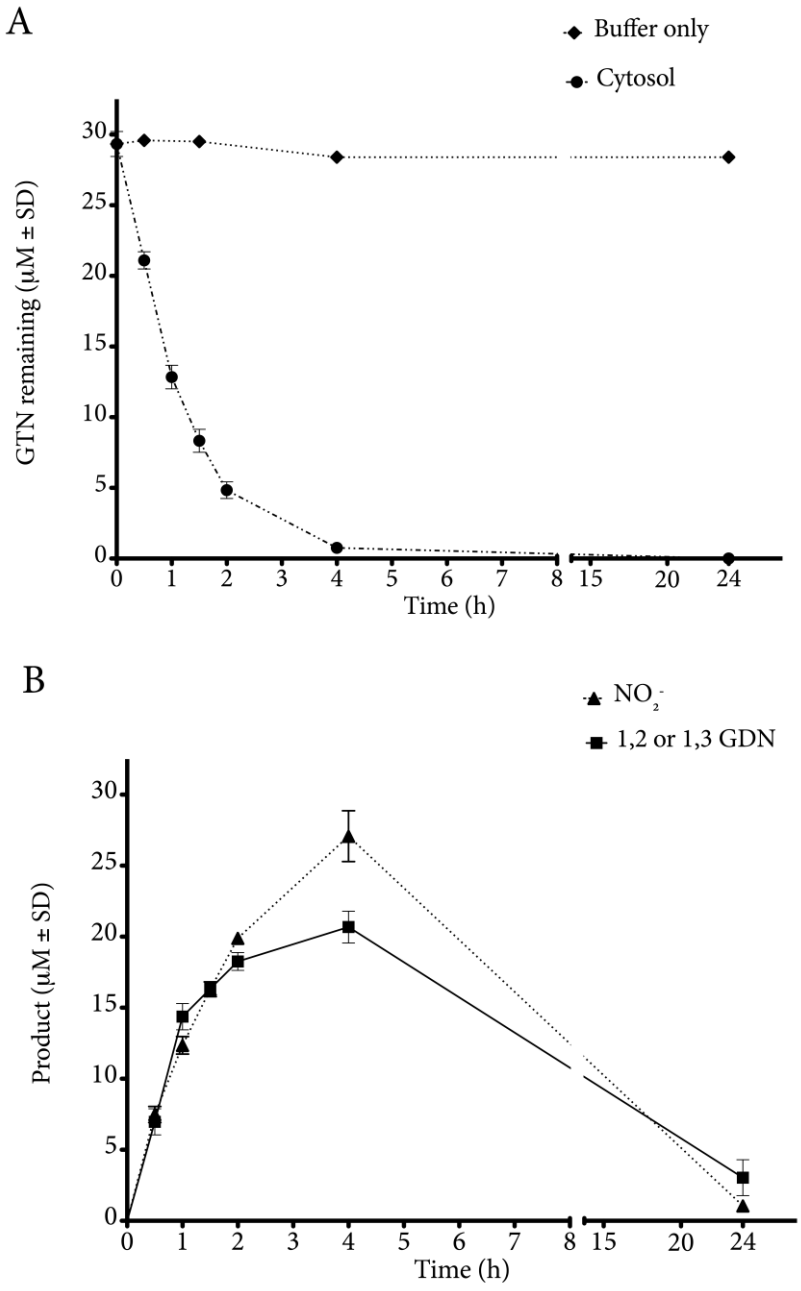
A
Buffer only
Cytosol
GTN remaining (μM ± SD)
30
25
20
15
10
5
0
0 1 2 3 4 5 6 7 8 15 20 24
Time (h)
B
NO_2^-
1,2 or 1,3 GDN
Product (μM ± SD)
30
25
20
15
10
5
0
0 1 2 3 4 5 6 7 8 15 20 24
Time (h)

Figure 3.4 The enzyme dependent biotransformation of glyceryl trinitrate (GTN, 5.7 μM) by quail embryo cytosol is inhibited by ethacrynic acid (EA, 100 μM) but not diphenyliodonium chloride (DPI, 100 μM). Bars represent the concentration of GTN remaining. Incubation conditions (at 37°C for 2 h under anaerobic conditions) are shown in the table below the graph. Data are the means of triplicates; error bars represent SD. Asterisks denote a significant difference (* $p < 0.05$; ** $p < 0.01$; *** $p < 0.001$, one-way ANOVA followed by a post hoc Tukey's test).

Figure 3.4

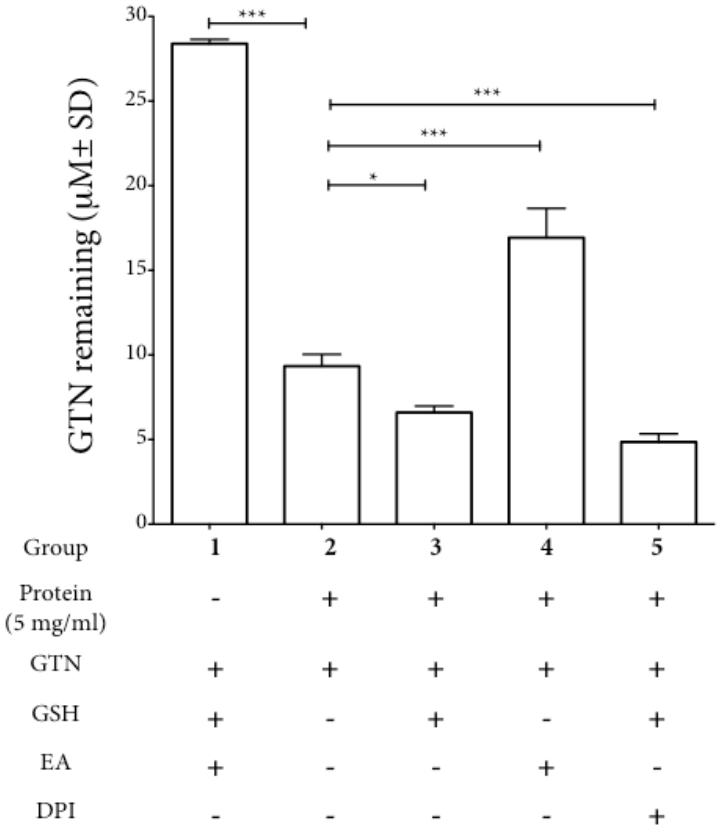
GTN remaining (μM± SD)
30
25
20
15
10
5
0
***
***
***
*
Group 1 2 3 4 5
Protein (5 mg/ml) - + + + +
GTN + + + + +
GSH + - + - +
EA + - - + -
DPI - - - - +

Figure 3.5 SDS-PAGE of GSH affinity column purified quail embryonic eye and whole embryo cytosolic GTN degrading enzymes. The gel was silver stained. Lane A: eye proteins; Lane B: whole embryo proteins; Lane C: molecular weight markers (97 kDa Phosphorylase b, 66 kDa Serum albumin, 45 kDa Ovalbumin, 31 kDa Carbonic anhydrase, 21.5 kDa Trypsin, 14.4 kDa Lysozyme).

Figure 3.5

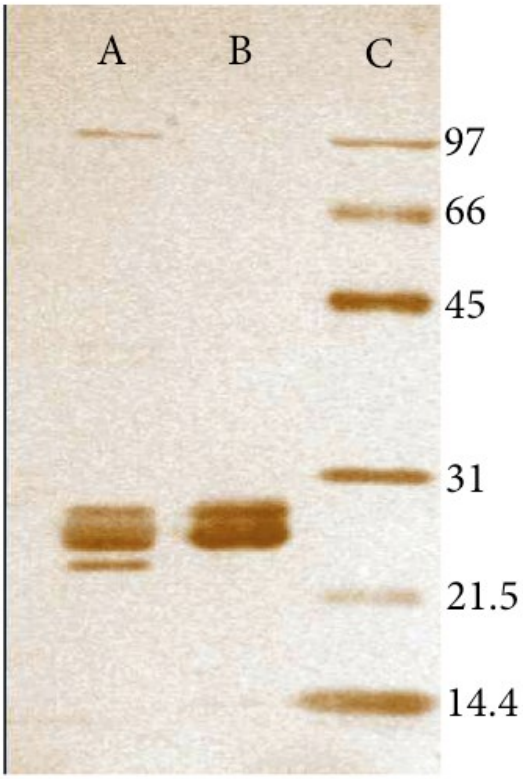

Figure 3.6 Time course of the biotransformation of GTN at 37°C under differing incubation conditions, as shown in the table below the graph. Data are the means of triplicates and error bars represent SD. PBS (phosphate buffered saline); ENZ (partially purified enzyme preparation; 0.5 mg protein); GSH (glutathione; 100 μM); and EA (ethacrynic acid; 200 μM). Asterisks denote a significant difference (*** $p < 0.001$, one-way ANOVA followed by a post hoc Tukey's test).

Figure 3.6

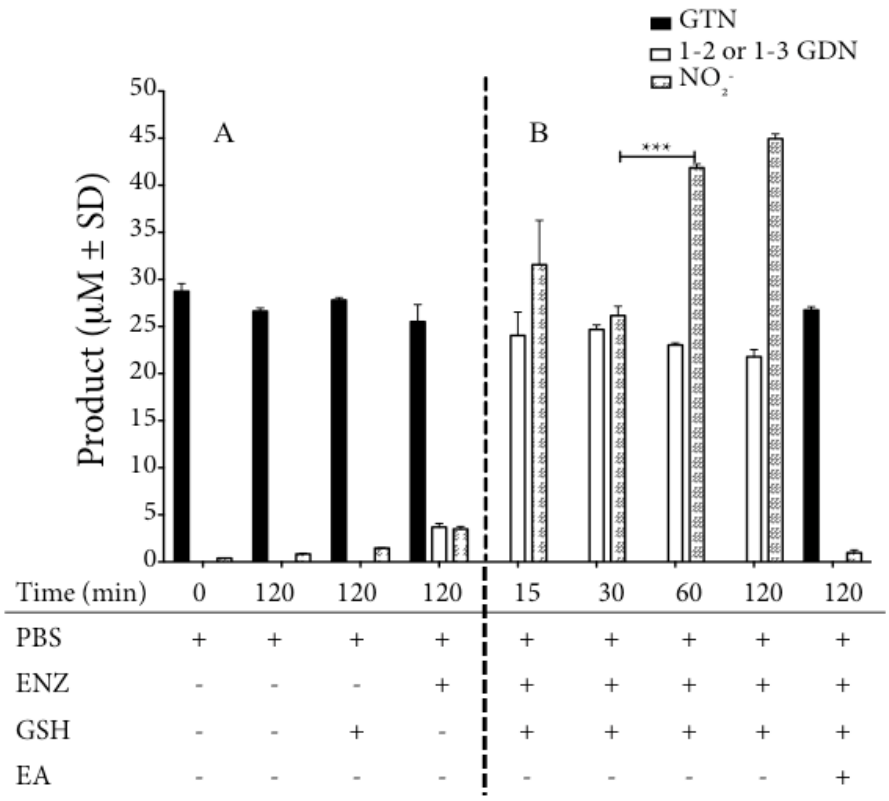
GTN
1-2 or 1-3 GDN
NO_2^-
Product (μM ± SD)
50
45
40
35
30
25
20
15
10
5
0
A
B
***
Time (min) 0 120 120 120 15 30 60 120 120
PBS + + + + + + + + +
ENZ - - - + + + + + +
GSH - - + - + + + + +
EA - - - - - - - - +

Figure 3.7 Mass spectrometry of GTN and its metabolites. Total Ion Chromatograph (A) showing GTN (peak 3) and its intermediates 1,3-GDN (peak 1) and 1,2-GDN (peak 2). Extracted ion chromatograms of GTN (D) and its intermediates 1,3-GDN (B) and 1,2-GDN (C) were obtained using LC-MS. GTN was incubated for 20 min with GSH and affinity purified enzyme GST preparations from (72 h old; n=120) quail embryos.

Figure 3.7

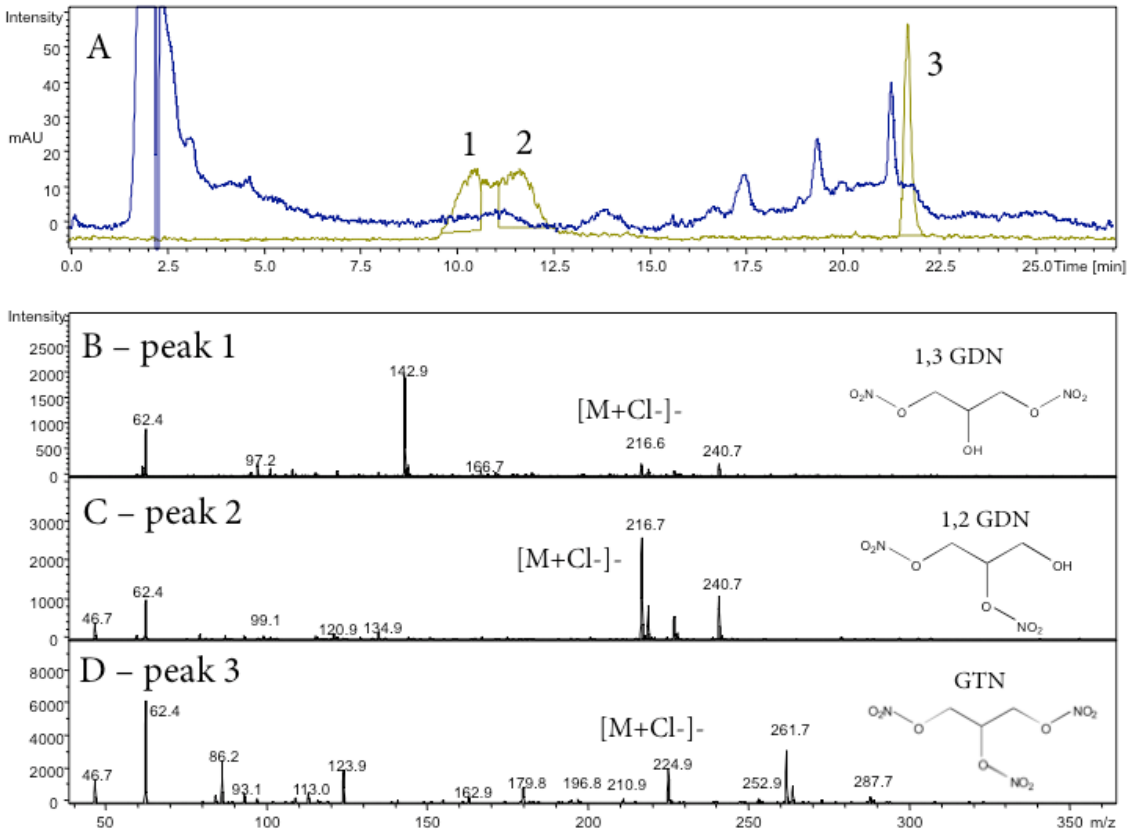
A
1
2
3
Intensity
mAU
Time [min]
B – peak 1
1,3 GDN
[M+Cl-]-
142.9
62.4
97.2
166.7
216.6
240.7
C – peak 2
1,2 GDN
[M+Cl-]-
216.7
240.7
62.4
46.7
99.1
120.9
134.9
D – peak 3
GTN
[M+Cl-]-
62.4
261.7
86.2
123.9
46.7
93.1
113.0
162.9
179.8
196.8
210.9
224.9
252.9
287.7
m/z

Figure 3.8 Analysis of quail embryonic eye and whole embryo GST subunits by reverse phased HPLC. 8A a representative chromatogram of embryonic eye affinity-purified GST separated by RP-HPLC, reveals three major and at least seven minor protein peaks absorbing at 224 nm. Mass spectrometer identified peaks 2, 3, 4, 5, 7, and 10 are alpha-like; peaks 6, 8, and 9 are identified as mu-like. Inset shows SDS-PAGE silver staining of protein fractions eluted by HPLC. 8B, a representative chromatogram of whole embryo affinity-column purified GST separated by reverse phase HPLC, reveals four major and at least five minor protein peaks absorbing at 224 nm. Peaks 2, 3, 4, 6, 7, 8, and 9 are identified as alpha-like, while peak 1 and 5 contain mu-like isozymes. The inset shows SDS-PAGE silver staining of protein fractions eluted by HPLC with the molecular weight markers described in Fig. 3.5.

Figure 3.8

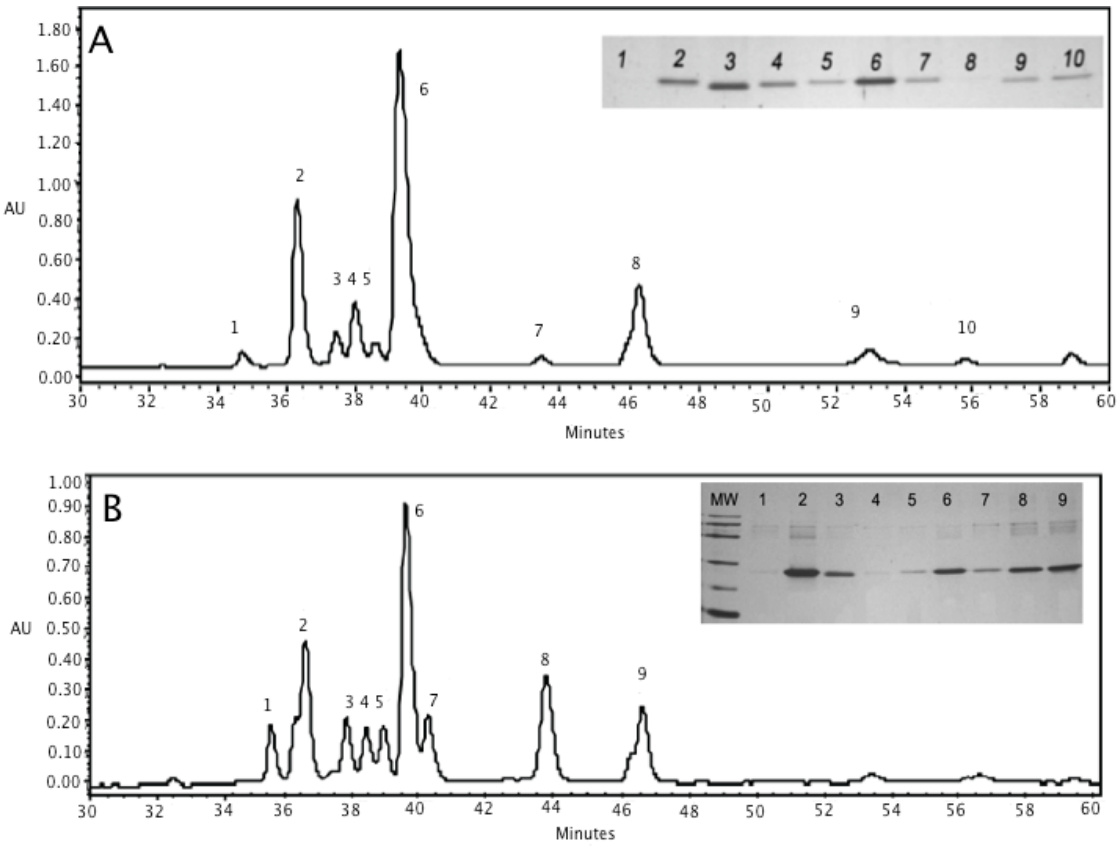
A
AU
Minutes
1
2
3 4 5
6
7
8
9
10
1 2 3 4 5 6 7 8 9 10
B
AU
Minutes
1
2
3 4 5
6
7
8
9
MW 1 2 3 4 5 6 7 8 9

Figure 3.9 In-vitro NO production by H.H stage 9 quail embryos. Arrows indicate the addition of SNAP (-●-) and GTN (440 μM) dissolved in corn oil (-■-, GTN-O) or PBS (-▲-, GTN-W) to whole embryo homogenates (250 μL) in 5 mL PBS. The final concentration of NO (nM) detected in homogenates to which SNAP has been added is indicated.

Figure 3.9

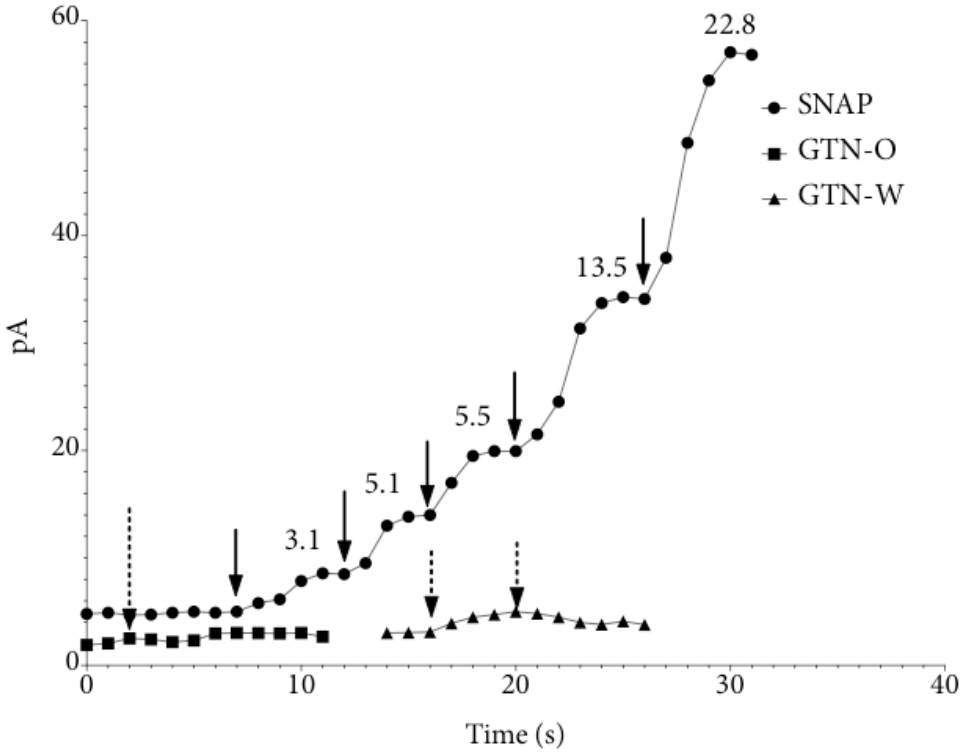

Supplementary Figure 3.1 Determination of the kinetic constants V_{max} and K_m. of purified GST obtained from whole embryo (Fig. S1A) and embryo eye (Fig. S1B). The inset shows the Lineweaver-Burk substrate velocity data.

Supplementary Figure 3.1

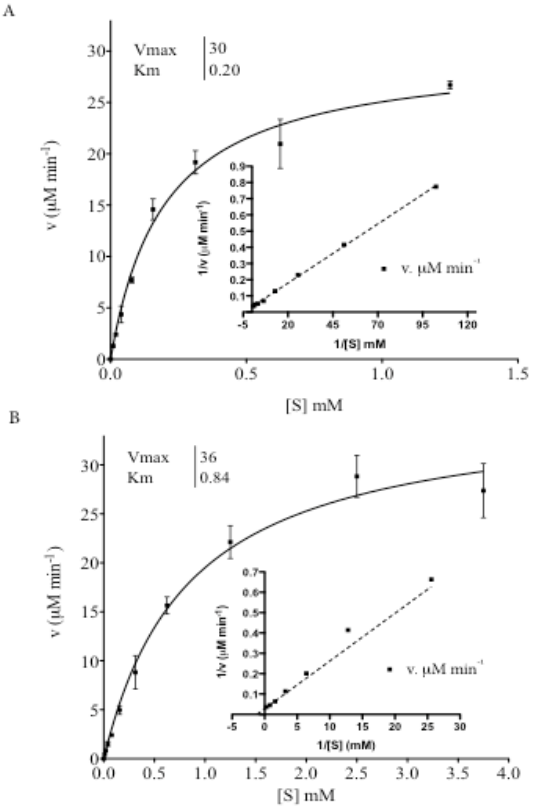

Connecting text for Chapter 3 to Chapter 4

I have demonstrated in my previous studies that the quail embryo has the ability to biotransform GTN to produce nitrite. This biotranformation comes at a cost. The metabolism of GTN by *ex-ovo* quail embryo GSTs depletes total GSH and alters the ratio of NADP+ to NADPH, resulting in perturbation of the redox balance in the embryo; NAC administration provides partial protection to *in-ovo* GTN treated embryos. The role of GSH in the maintenance of nuclear homeostasis, DNA synthesis, and cell proliferation has been documented. I hypothesize that GTN treatment may disrupt redox dependent gene expression in the quail embryo.

CHAPTER 4: Effects of Glyceryl Trinitrate on the Gene Expression Profile in Quail Embryos

Ghalib K. Bardai[*†], Barbara F. Hales[*], Geoffrey I. Sunahara[†]

[*]Department of Pharmacology and Therapeutics

McGill University, Montreal, Quebec, Canada, H3G 1Y6.

[†]Biotechnology Research Institute, National Research Council of Canada,

Montreal, Quebec, Canada, H4P 2R2

ABSTRACT

Our previous studies have shown that glyceryl trinitrate (GTN) is a developmental toxicant in Hamilton Hamburger stage 9 (HH9) quail embryos *ex-ovo*. The goal of this study was to evaluate changes in the expression of genes that might contribute to the developmental pathologies observed. Pooled RNA samples (n = 6-8/treatment group) isolated from vehicle and GTN treated HH 9 embryos after 15 h of exposure were analyzed using the 44K Agilent chicken whole genome microarrays. Gene lists generated by fold change (>1.5) and p -value (≤ 0.05) included 498 up- and 892 down-regulated differentially expressed genes in GTN-treated embryos compared to the control embryos. Ingenuity pathway analysis suggested that the EIF2, mTOR and WNT/β-CATENIN signaling pathways are most affected by GTN exposure. Further investigation of differentially expressed genes within these pathways may contribute to a basic understanding of the molecular mechanisms involved in the developmental toxicity of GTN.

Key Words: Quail embryo; GTN; Microarray; Gene expression

4.1. Introduction

Glyceryl trinitrate (GTN) is the pharmacological agent of choice to treat a variety of the cardiovascular diseases currently afflicting 9 million individuals in the United States (Roger et al., 2012). In addition, clinical trials indicate that this organic nitrate may be of beneficial use for several other diseases and conditions, such as pain management (Lauretti et al., 2002) and osteoporosis treatment (Jamal et al., 2006), via modulation of cytokine (IL-1β, TNF-α, and IFN-γ)-induced effects on osteoblast function.

GTN is also considered as a tocolytic therapy in preterm labor to reduce infant morbidity and mortality (Berkman et al., 2003; Black et al., 1999; Smith et al., 1999; Smith et al., 2007). GTN crosses the placenta (David et al., 2000) and is metabolized (Bustard et al., 2002). In addition, GTN may disrupt signaling pathways (Bryan et al., 2005; Veselik et al., 2008) which affect the energy status of biological systems (Cao et al., 2009; Garcia et al., 2010), modify proteins (Perlman et al., 2009), and form both reactive oxygen and nitrogen species (Münzel et al., 1995). Considering the emerging diverse possible therapeutic uses of GTN, notably its possible use during pregnancy, and the ability of GTN to disrupt critical signaling pathways, there are surprisingly few studies on the effects of GTN exposure during organogenesis.

We have shown that the exposure of Japanese quail embryos undergoing organogenesis (Hamilton Hamburger [HH] stage 9) to GTN decreases embryo growth and increases both mortality and the incidence of craniofacial,

mesencephalic, ocular, and cardiac defects in a dose dependent manner (Bardai et al., 2011). Further studies showed that glutathione S transferase enzymes in the quail embryo metabolize GTN to produce nitrite, with the consumption of GSH and changes in the ratio of oxidized to reduced co-factors such as NADPH (NADP+/NADPH). Additionally, co-treatment of GTN exposed embryos with N-acetyl cysteine (NAC), a readily cellular transportable derivative of L-cysteine and a precursor in GSH formation, partially rescued GTN-treated quail embryos (Bardai et al., 2013). We hypothesize that the developmental toxicity of GTN in the quail embryo is associated with the disturbances in the expression of genes that are important in pattern formation during organogenesis. The aim of this study was to characterize changes in global gene expression in control compared to GTN-treated quail embryos to delineate the major cellular pathways that are dysregulated in the quail embryo in response to a teratogenic dose of GTN during organogenesis.

Microarray technology provides unbiased data on all gene networks, including members of gene families, ligands, receptors, and transcription factors, and may lead to the discovery of genes and/or pathways that previously were not known to be involved in mediating the induction of specific developmental malformations. we used 44 K chicken DNA microarrays in the current study to identify system-wide differences in transcriptome response of quail embryos to GTN treatment. Our data show that GTN exposure has a significant impact on the gene expression profile in quail embryos.

4.2. Materials and Methods

4.2.1. Chemicals

Glyceryl trinitrate (GTN, CAS 118-96-7; 99.9% purity) in a corn oil solution (0.2 g/mL) was supplied by General Dynamics Ordnance and Tactical Systems - Canada (Valleyfield, Quebec, Canada).

4.2.2 Experimental animals

Fertilized Japanese quail (*Coturnix coturnix japonica*) eggs were obtained from a local breeder (Couvoir Simetin, Mirabel, Quebec, Canada). Eggs were incubated horizontally at 20°C for 2 h about their long axis to allow blastoderm to be positioned close to the topmost point on the yolk and to avoid trauma from the introduction of the needle. During this time, embryo development was paused. Embryos were treated with GTN as previously described (Bardai et al., 2011), with the following modifications. Eggs (n = 120) were incubated until HH stage 9, at which point they were injected *in-ovo* with GTN (440 µM) dissolved in corn oil or corn-oil only and were then placed in a forced draft incubator (Brinsea Octagon, Titusville, FL) at 37.7 ± 0.5°C (average $\pm$ SD) and 55-60% relative humidity for 15 h. Following the 15 h incubation, the yolk was placed into a glass Petri dish and the embryos were dissected out by cutting around the developing embryo. To remove any adhering yolk, embryos were rinsed in ice-cold Hanks balanced salt solution and then frozen in a dry ice/ethanol bath. Embryos were then stored at -80^{o}C.

4.2.3 Total RNA isolation and quantification

RNA was isolated from both control and GTN-treated embryos (n = 8 groups with 6-8 embryos per group) in accordance with the PARIS protocol (Ambion, Austin, Tx, USA). The integrity, quantity, and purity of total RNA was assessed with an Agilent Bioanalyzer 2100 and RNA 6000 Nano LabChip Kit (Agilent Technologies, Palo Alto, CA, USA). The RNA Integrity Numbers (RINs) for the samples ranged from 8-9.

4.2.4 Microarray hybridization

Fluorescently labeled complementary RNA (cDNA) for microarray hybridization was prepared by reverse transcribing 20 µg of RNA using Superscript III Reverse Transcriptase (Invitrogen Life Technologies, Carlsbad, CA, USA) and oligo(dT)21 in the presence of Cy3- or Cy5-dCTP (Invitrogen). Template RNA was degraded using 2.5 units' RNase H (USB) and 1 µg RNase A (Pharmacia) incubated at 37°C for 30 min. Labeled cDNA was purified with a Qiagen RNeasy Mini Kit (Qiagen, Valencia, CA, USA). Equal amounts (825 ng) of the Cy3 and Cy5 labeled cDNA probes were hybridized on 4 × 44 K Agilent chicken oligo microarrays (n = 2) (design ID: 015068; Agilent Technologies Inc.). Therefore, N=8 different pooled embryo samples were assayed on 2 arrays. The hybridization was carried out with 1X Gex Hyb Buffer (HI-RPM) (Agilent Technologies Inc.) at 65°C for 18 h in a hybridization oven with regular agitation. The slides were washed twice in 1.0% SSC (0.15 M NaCl and 0.015 M sodium

citrate) with 0.2% SDS at 42°C for 5 min; once in 0.1% SSC with 0.2% SDS at 42°C for 3 min; and once in 0.1% SSC at 24°C for 90 seconds. The microarray slides were then air-dried prior to analyses.

4.2.5 Microarray data collection and analyses

A multiple dye swap design was used to analyze gene expression data (Kerr, 2003). Each microarray experiment (n = 2) using independent biological replicates was scanned at 5 μm resolution using a ScanArray microarray scanner (Perkin Elmer, Wellesley, MA, USA). The signal intensity of all features on each image was quantified by Imagene 8.0 software (BioDiscovery, El Segundo, CA, USA) using global normalization based on local polynomial regression (loess) to remove effects that due to undesirable systematic variations in microarray experiments (rather than due to biological differences). The average values of the resulting normalized expression values in replicate hybridization sets were considered in the subsequent analyses. The microarray data were analyzed in GeneSpring® using an unpaired *t* -test with a Benjamini–Hochberg multiple comparison correction to compare differences between the control and GTN treated embryos. Pathway analysis was conducted using the Fischer Exact test in the IPA™ software (Qiagen). Venny v2.0.2, a free online tool, was used to create the Venn diagrams and lists of EIF2, WNT/β-CATENIN and mTOR overlapping and unique targets (Oliveros, 2007–2015). Data from all other experiments were log transformed then tested using 1-way or 2-way ANOVA,

followed by a Bonferroni *post-hoc* multiple comparison correction to detect statistical differences among the control and GTN treated groups.

4.2.6 Bioinformatic Analyses

The previously normalized microarray data were then analyzed using GeneSpring GX 11.5® (Silicon Genetics, Redwood, CA, USA) for statistical and gene expression pattern analyses. To derive human and mouse phenotypes both the Mouse Genome Informatics Database (MGID) (Eppig et al., 2015) and Online Mendelian Inheritance in Man database (OMIM) website were used. The Search Tool for the Retrieval of Interacting Genes (STRING) database v10 (Szklarczyk et al., 2015) was used to construct a Protein–Protein Interaction (PPI) network of pathways perturbed by GTN exposure.

4.3. Results

4.3.1 Differentially expressed genes

The Agilent chicken gene expression microarrays were used to identify changes in gene transcription in HH Stage 9 quail embryos exposed for 15 h to 400 uM GTN (n = 8) relative to a vehicle control group. Data were first filtered to remove all spots corresponding to bright and dark corners on the arrays, leaving only gene probes (n = 43603) to be considered in all further analyses. Next, the intensity values of the probes were filtered between the 20-90th percentile, thereby avoiding saturated probes and probes biased by background. These data were then considered for statistical analyses. Genes were identified as differentially expressed based on fold changes (> 1.5), both up and down, and p - values (≤ 0.05). Hierarchical clustering using the differentially expressed gene set was performed in GeneSpring GX. The expression profile of each sample was clustered based on gene expression and treatment. Cluster analysis clearly separated vehicle-treated embryos from GTN-treated embryos (Figure 4.1). Data filtration and analysis of statistical differences revealed that the expression of 1360 transcripts showed differential expression > 1.5-fold ($p < 0.05$) in GTN-exposed embryos relative to the control corn oil-treated embryos. Among these, 498 genes were upregulated and 862 were downregulated (Figure 4.2).

The gene with highest fold change increase in expression was Charged multivesicular body protein 4c (*CHMP4C)*; expression of this transcript was 3.9-fold higher in GTN-treated embryos compared to vehicle-treated embryos. We also observed an increase in the *CHMP4C* predicted functional partner,

CHMP2A. The largest overall decrease in expression in GTN-exposed embryos was observed for DNA-directed RNA polymerase III subunit RPC3 mRNA (*POLR3C*).

4.3.2 Cellular pathways perturbed by GTN exposure

We did pathway analysis on the microarray data using IPA software to elucidate the cellular pathways that were perturbed in the developing embryo in response to GTN. The most significantly activated pathways in quail embryos exposed to GTN were the EIF2, WNT (wingless-type MMTV integration site family)/β-CATENIN and mTOR signaling pathways (Figure 4.3). Interestingly, closer analysis of these pathways showed that there was considerable overlap in genes between the EIF2 and mTOR pathways (Table 4.1). In contrast, the WNT/β-CATENIN pathway did not show any overlap of common targets with the EIF2 pathway and only two genes overlapped between the WNT/β-CATENIN and mTOR pathways (Figure 4.4 and Table 4.1).

4.3.3 Genes in cellular pathways perturbed by GTN exposure mapping to observed phenotypes

To examine the relationship of the genes with altered expression to the phenotypes observed in quail embryos exposed to GTN (cardiovascular, craniofacial, growth/body size and vision/eye defects) we mapped the unique genes as indicated in the Venn diagram analysis to the Mouse Genome Informatics Database (MGID) (Eppig et al., 2015) for the mouse homologs of the

human gene and their phenotypes (Figure 4.4 a, b and c) with those in Table 4.2a, b and c. This database shows the phenotypic outcome of mice when a gene of interest is overexpressed, under-expressed or completely silenced. Interestingly the data show that in mice 45% of the genes in the EIF2 signaling pathway are associated with a phenotype that is like the one observed in quail embryos exposed to GTN (Table 4.2a). In the WNT/β-CATENIN pathway, 68% of the genes mapped to a phenotype similar to the one we observed. The mTOR pathway had the lowest number of genes, 42%, that were associated with a phenotype related to the defects associated with quail embryo GTN exposure. Interestingly, genes with functions as transcriptional regulators, G-protein coupled receptors and kinases were over represented as being involved in the observed phenotypes (Table 4.2a, b and c).

4.3.4 Construction of a Protein–Protein Interaction (PPI) network of pathways perturbed by GTN exposure

While functional analyses and canonical pathway mapping provide useful information, it is ultimately the functional partnerships and interactions that occur between gene products that are at the core of cellular processing. Their systematic characterization helps to provide context to gene array experiments. To perform this characterization, we have used the STRING database v10 (Search Tool for the Retrieval of Interacting Genes) (Szklarczyk et al., 2015) with protein names of the prioritized genes from the perturbed pathways for construction of protein-protein interaction (PPI) networks (Figure 4.4a, b and c).

The EIF2 and mTOR signaling pathways share many ribosomal proteins (RPs) (Fig. 4.4a and b) and these proteins are clearly over represented. Considering that RPs are over represented, and that impeding ribosomal biogenesis generates ribosomal stress that activates *p53* (Zhang and Lu, 2009), we determine if the expression of *TP53* (transformation–related protein 53 or tumor suppressor protein 53) or its downstream targets was altered. The expression of both tumor protein p53-inducible nuclear protein 11 (*TP53I1*; fold change -1.9 and p=0.0006) and tumor protein p53-inducible nuclear protein 2 (*TP53INP2*; fold change - 2.0 and p=0.00002) were downregulated in embryos exposed to GTN.

The WNT/β-CATENIN pathway contains a high number of transcription regulators (*HDAC1*, *SOX3*, *SOX10*, *SOX11* and *TCF3*) (Table 4.2a, b and c). In comparison to the EIF2 and mTOR pathways, the WNT/β-CATENIN pathway also contains the highest number of genes that code for G-protein coupled receptors (*FZD1, FZD2, FZD3, FZD5, FZD7* and *SMO*). Importantly, 68% of the genes within the WNT/β-CATENIN signaling pathway matched the phenotypes observed in quail embryos exposed to GTN, while 45 and 42% matched the EIF2and mTOR pathways, respectively. Pathway analysis also revealed that the second largest subset of genes with perturbed expression were the frizzled (*FZD*) receptors, including the smoothened (*SMO*) frizzled class receptor (Table 4.2c and Fig. 4.6c).

4.4. Discussion

This study demonstrated that the treatment of quail embryos with GTN during organogenesis induced a dysregulation of the expression of a number of genes, many from developmentally important signaling pathways. The highest fold change increase in expression (3.9-fold greater in GTN-treated compared to vehicle-treated embryos) observed was the transcript for Charged multivesicular body protein 4c (*CHMP4C)*. *CHMP4C* is thought to be a probable core component of the ubiquitin mediated endosomal sorting complexes required for transport to the lysosome; these complexes are conserved throughout all major eukaryotic taxa (Williams and Urbé, 2007). Membrane traffic within this system flows along highly organized directional routes where biomolecules are synthesized and assembled in the endoplasmic reticulum (ER), then transported to the Golgi complex for further processing and maturation, and finally moved through the cytoplasm to fuse with the cell surface. Therefore, the product of this gene is critical in regulating the delivery of newly synthesized proteins, carbohydrates, and lipids to the cell surface, a necessity for growth and homeostasis (Lippincott-Schwartz et al., 2000). However, changes in its expression have not been reported to date to be associated with any known human disease or mouse phenotype.

The largest overall decrease in expression in the GTN treatment group compared to the control, approximately six-fold, was observed for DNA-directed

RNA polymerase III subunit RPC3 mRNA (*POLR3C*). Eukaryotes contain three distinct DNA-dependent RNA polymerases (Pol I, Pol II, and Pol III) (Roeder & Rutter, 1969) that share the task of transcribing the information contained in genes. Pol III transcribes a diverse group of small untranslated RNAs that participate in the regulation of transcription, splicing, and translation (Dumay-Odelot et al. 2010). After transcription, Pol III transcripts are either directly degraded or modified for participation in the regulation and execution of processes in the nucleus and cytoplasm (i.e., transcription regulation, RNA processing, ribosome assembly, and translation) that ultimately lead to protein synthesis (Ream et al., 2009). Loss of *POLR3C*, therefore, can clearly affect the expression of genes in the developing embryo.

Pathway analyses showed that the EIF2, mTOR, and WNT/β-CATENIN signaling pathways are the most perturbed pathways. However, both the EIF2 and mTOR pathways share common genes within their pathways (eukaryotic translation initiation factors and ribosomal proteins) (Fig. 4.4, 4.6a. 4.6b and Table 4.1). The EIF2 signaling pathway integrates many stress-related signals to regulate both global and specific mRNA translation. Interestingly, the ribosomal proteins (RPs) in both the EIF2 and mTOR signaling pathways are overrepresented among the genes with significant changes in expression; furthermore, three of the RPs, RPL5, 15 and 21 are specific only to the EIF2 signaling pathway (Table 4.1 and Fig. 4.5a) and have been linked to phenotypes observed in GTN-exposed quail embryos (Bardai et al. 2013).

The mammalian ribosome is a macromolecular assembly of 4 RNA species and approximately 80 different proteins, including RPL5 (Kenmochi et al., 1998). A group of human disorders, collectively referred to as “ribosomopathies”, have genetic alterations in components of the ribosome machinery (including RPs); one example is Diamond-Blackfan anemia (Gazda et al. 2008). Mutations in several different RPs have been associated with bone marrow failure and congenital birth defects, such as malformations in limb, face, heart, and kidney development, suggesting that RPs play an important role during embryonic development (Ganapathi & Shimamura, 2008).

Ribosomal stress, induced by impeding ribosomal biogenesis, also activates the TP53 signaling pathway and arrests cell growth (Zhang and Lu, 2009). While the TP53 signaling pathway was not identified as a target of GTN-exposure in quail embryos, the expression of two downstream genes were affected; the expressions of *TP53I1* and *TP53INP2* were downregulated. While the function of *TP53I11* is not clear, it has shown to be up-regulated or down regulated, depending on the cell type, by chemopreventive agents. (Liu et al. 2009). However, *TP53INP2* (ENSGALT00000001836) an uncharacterized protein in *Gallus*, when blasted using UniProt against *Homo sapiens*, returns a 65% sequence similarity to *TP53INP2*. One interesting possibility is that perturbed RPs/ribosomal stress may directly activate the expression of these genes.

As a signaling pathway that plays a crucial role during embryogenesis, WNT/β-CATENIN is tightly regulated; expression of the WNT proteins and WNT

antagonists is restricted both temporally and spatially during development (Najdi et al., 2012). Deregulated WNT signaling has detrimental consequences for the developing embryo, including skeletal defects and neural tube closure defects such as spina bifida (Logan and Nusse, 2004). During embryo development, the WNT signaling pathway and, specifically, the WNT/β-CATENIN signaling pathway modulates cellular differentiation, proliferation, movement, and polarity (Logan and Nusse, 2004). WNT signaling pathways are a group of signal transduction pathways made of proteins that pass signals into a cell through cell surface receptors. Three WNT signaling pathways have been characterized: the canonical WNT pathway, the noncanonical planar cell polarity pathway, and the noncanonical WNT/calcium pathway. All three pathways are activated by binding a WNT-protein ligand to the N-terminal extra-cellular cysteine-rich domain of the FZ receptor family in the presence of the low-density lipoprotein-related receptor (LRP), resulting in a tripartite complex (He et al., 2004). In our microarray data, we only observed the down regulation of the wnt soluble protein 8 transcript (*WNT8*) (Table 4.1.). *WNT8* protein binds to FZD5 and FZD7 and may play an important role in the development and differentiation of certain forebrain structures, notably the hippocampus (Holmen et al., 2002). The FZ protein is a seven-transmembrane-span protein with topological homology to G-protein coupled receptors (Schulte and Bryja, 2007). In this study, we observed the downregulation of the *FZD2, FZD5*, and *FZD7* receptors transcripts in quail embryos after GTN exposure (Table 4.2c). These receptors have been reported to cause craniofacial, cardiovascular, and abnormal growth and body size

phenotypes in mice. These phenotypes have been observed in our studies (Bardai et al. 2013). In addition to the binding of wnt soluble proteins to the frizzled receptor, to activate the WNT pathways, the interaction of co-receptors such as the low-density-lipoprotein-related protein5/6 (LRP5/6) is required to mediate the canonical WNT signal (He et al., 2004). Two LRP proteins (LRP2 and LRP4) were observed to be downregulated in GTN-exposed quail embryos. This suggest the ability to bind wnt soluble proteins is dramatically decreased leading to a decrease in the expression of Wnt responsive genes.

β-CATENIN is central to the WNT signaling pathway. In the absence of canonical WNT proteins, β-CATENIN is bound to AXIN and phosphorylated by glycogen synthase kinase (GSK)-3β at the amino terminal, followed by polyubiqitination and degradation by the proteasome (Behrens et al., 1998). When the FZ is bound by canonical WNTs, the Dishevelled protein is recruited to the receptor complex, phosphorylated and inhibits (GSK)-3β (Niehrs, 2012). This prevents phosphorylation of β-CATENIN , which is then free to translocate to the nucleus and form complexes with the T-cell factor/leukemia enhancer factor (Tcf/Lef) family members (Daniels and Weis, 2005) activating or repressing various WNT target genes. Since *AXIN* transcripts are downregulated in our microarray, and β-CATENIN has shown no significant change, which suggests normal expression, it is possible the stability of β-CATENIN may be compromised in GTN treated embryos due to downregulation of AXIN (Table 4.1). Clearly, quantification of *AXIN* transcript numbers and β-CATENIN breakdown products

in both GTN-treated and control embryos would help to determine if this is occurring.

The data from this study raises interesting questions as to the effects of GTN on embryo development via the disruption of the WNT/β-CATENIN pathway. Clearly the next steps should be to quantify and validate the expression of the transcripts in this pathway, and to determine if there are any differences in β-CATENIN degradation products between control and GTN-treated embryos. Further, to our previous work it would be interesting to test the hypothesis if a change in redox status can, in fact, perturb the WNT/β-CATENIN pathway.

FUNDING

G. B. is a recipient of a Fonds de la recherché du Québec en Santé Doctoral Research Award. B. H. is a James McGill Professor of McGill University.

ACKNOWLEDGEMENTS

We thank General Dynamics Ordnance and Tactical Systems Canada for providing the GTN and Nazem El Husseini for help with Ingenuity Pathway analysis.

References

Ashburner, M., Ball, C.A., Blake, J.A., Botstein, D., Butler, H., Cherry, J.M., Davis, A.P., Dolinski, K., Dwight, S.S., et al. (2000). Gene ontology: tool for the unification of biology. The Gene Ontology Consortium. Nat Genet *25*, 25-29

Bardai, G. K., Hales, B. F., Sunahara, G.I. (2011). Developmental toxicity of glyceryl trinitrate in quail embryos. *Birth Defects Res A Clin Mol Teratol 91*, 230-240.

Bardai, G. K., Hales, B. F., Sunahara, G.I. (2013). Glyceryl trinitrate metabolism in the quail embryo by the glutathione S-transferases leads to a perturbation in redox status and embryotoxicity. Comp Biochem Physiol B Biochem Mol Biol 153-164.

Behrens J., Jerchow B. A., Würtele M., Grimm J., Asbrand C., Wirtz R., Kühl M., Wedlich D., Birchmeier W. (1998). Functional interaction of an axin homolog, conductin, with beta-catenin, APC, and GSK3beta. Science 280, 596–599.

Berkman, N.D., Thorp, J.M., Lohr, K.N., Carey, T.S., Hartmann, K.E., Gavin, N.I., Hasselblad, V., and Idicula, A.E. (2003). Tocolytic treatment for the management of preterm labor: a review of the evidence. Am J Obstet Gynecol *188*, 1648-659

Black, R.S., Lees, C., Thompson, C., Pickles, A., and Campbell, S. (1999). Maternal and fetal cardiovascular effects of transdermal glyceryl trinitrate and intravenous ritodrine. Obstet Gynecol *94*, 572-76.

Bonifacino, J.S., and Hierro, A. (2011). Transport according to GARP: receiving retrograde cargo at the trans-Golgi network. Trends Cell Biol *21*, 159-167.

Bryan, N.S., Fernandez, B.O., Bauer, S.M., Garcia-Saura, M.F., Milsom, A.B., Rassaf, T., Maloney, R.E., Bharti, A., Rodriguez, J., and Feelisch, M. (2005). Nitrite is a signaling molecule and regulator of gene expression in mammalian tissues. Nat Chem Biol *1*, 290-97

Bustard, M.A., Farley, A.E., and Smith, G.N. (2002). The pharmacokinetics of glyceryl trinitrate with the use of the in vitro term human placental perfusion setup. Am J Obstet Gynecol *187*, 187-190.

Cao, Z., Bell, J.B., Mohanty, J.G., Nagababu, E., and Rifkind, J.M. (2009). Nitrite enhances RBC hypoxic ATP synthesis and the release of ATP into the vasculature: a new mechanism for nitrite-induced vasodilation. Am J Physiol Heart Circ Physiol *297*, H1494-1503.

Chapman, G., Remiszewski, J. L., Webb, G. C., Schulz, T. C., Bottema, C. D. K., Rathjen, P. D. (1997). The mouse homeobox gene, Gbx2: genomic organization and expression in pluripotent cells in vitro and in vivo. Genomics *46*, 223-233.

Daniels D. L., Weis W. I. (2005). Beta-catenin directly displaces Groucho/TLE repressors from Tcf/Lef in Wnt-mediated transcription activation. Nat. Struct. Mol. Biol. 12, 364–371.

David, M., Walka, M.M., Schmid, B., Sinha, P., Veit, S., and Lichtenegger, W. (2000). Nitroglycerin application during cesarean delivery: plasma levels, fetal/maternal ratio of nitroglycerin, and effects in newborns. Am J Obstet Gynecol *182*, 955-961.

Diaz Vivancos, P., Wolff, T., Markovic, J., Pallardó, F.V., and Foyer, C.H. (2010). A nuclear glutathione cycle within the cell cycle. Biochem J *431*, 169-178.

Dumay-Odelot, H., Durrieu-Gaillard, S., Da Silva, D., Roeder, R.G., and Teichmann, M. (2010). Cell growth- and differentiation-dependent regulation of RNA polymerase III transcription. Cell Cycle *9*, 3687-699

Eppig, J.T., Richardson, J.E., Kadin, J.A., Smith, C.L., Blake, J.A., Bult, C.J.; MGD Team. (2015). Mouse Genome Database: From sequence to phenotypes and disease models. Genesis 53, 458-73.

Feinstein, M., Flusser, H., Lerman-Sagie, T., Ben-Zeev, B., Lev, D., Agamy, O., Cohen, I., Kadir, R., Sivan, S., Leshinsky-Silver, E., Markus, B., Birk, O. S. (2014). VPS53 mutations cause progressive cerebello-cerebral atrophy type 2 (PCCA2). J Med Genet *51, 303-308*.

Ganapathai, K.A. and Shimamura, A. (2008). Ribosomal dysfunction and inherited marrow failure. Br. J. Haematol 141, 376–387.

Garcia, J.I., Seabra, A.B., Kennedy, R., and English, A.M. (2010). Nitrite and nitroglycerin induce rapid release of the vasodilator ATP from erythrocytes: Relevance to the chemical physiology of local vasodilation. J Inorg Biochem *104*, 289-296.

Gazda, H. T., Sheen, M. R., Vlachos, A., Choesmel, V., O'Donohue, M.-F.,Schneider, H., Darras, N., Hasman, C., Sieff, C. A., Newburger, P. E., Ball, S. E., Niewiadomska, E., and 9 others: (2008). Ribosomal protein L5 and L11 mutations are associated with cleft palate and abnormal thumbs in Diamond-Blackfan anemia patients. Am. J. Hum. Genet 83, 769-780.

Go, Y.M., and Jones, D.P. (2010). Redox control systems in the nucleus: mechanisms and functions. Antioxid Redox Signal *13*, 489-509.

Hamada F., Tomoyasu Y., Takatsu Y., Nakamura M., Nagai S., Suzuki A., Fujita F., Shibuya H., Toyoshima K., Ueno N., et al. (1999). Negative regulation of Wingless signaling by D-axin, a Drosophila homolog of axin. Science 283, 1739–1742.

Haw, R., and Stein, L. (2012). Using the reactome database. Curr Protoc Bioinformatics *Chapter 8*, Unit8.7.

He X, Semenov M, Tamai K, Zeng X. (2004). LDL receptor-related proteins 5 and 6 in Wnt/beta-catenin signaling: arrows point the way. Development. 131, 1663–1677.

Holmen, S.L., Salic, A., Zylstra, C.R., Kirschner, M.W., and Williams, B.O.(2002). A novel set of wnt-frizzled fusion proteins identifies receptor components that activate beta-catenin-dependent signalling. J. Biol. Chem. 277, 34727–34735.

Kenmochi, N., Kawaguchi, T., Rozen, S., Davis, E., Goodman, N., Hudson, T. J., Tanaka, T., Page, D. C.:(1998). A map of 75 human ribosomal protein genes. Genome Res 8, 509-523.

Liu, X.M., Xiong, X.F., Song, Y., Tang, R.J., Liang, X.Q., and Cao, E.H. (2009). Possible roles of a tumor suppressor gene PIG11 in hepatocarcinogenesis and As2O3-induced apoptosis in liver cancer cells. Journal of gastroenterology 44, 460-69

Logan C. Y., Nusse R. (2004). The Wnt signaling pathway in development and disease. Annu. Rev. Cell Dev. Biol. 20, 781–810.

Jamal, S.A., Hamilton, C.J., Black, D., and Cummings, S.R. (2006). The effects of organic nitrates on osteoporosis: a randomized controlled trial [ISRCTN94484747]. Trials *7*, 10.

Kamburov, A., Pentchev, K., Galicka, H., Wierling, C., Lehrach, H., and Herwig, R. (2011). ConsensusPathDB: toward a more complete picture of cell biology. Nucleic Acids Res *39*, D712-17.

Kayang, B.B., Fillon, V, et al. (2006). Integrated maps in quail (Coturnix japonica) confirm the high degree of synteny conservation with chicken (Gallus gallus) despite 35 million years of divergence. BMC Genomics *7*, 101.

Kerr, M.K. (2003). Design considerations for efficient and effective microarray studies. Biometrics *59*, 822-28.

Kondrashov, N., Pusic, A., Stumpf, C.R., Shimizu, K., Hsieh, A., Xue, S., Ishijima, J., Shiroishi, T., and Barna, M. (2011). Ribosome-Mediated Specificity in Hox mRNA Translation and Vertebrate Tissue Patterning. Cell *145*, 383-397.

Lauretti, G.R., Perez, M.V., Reis, M.P., and Pereira, N.L. (2002). Double-blind evaluation of transdermal nitroglycerine as adjuvant to oral morphine for cancer pain management. J Clin Anesth *14*, 83-86.

Li, X., Chiang, H.I., Zhu, J., Dowd, S.E., and Zhou, H. (2008). Characterization of a newly developed chicken 44K Agilent microarray. BMC Genomics *9*, 60.

Lippincott-Schwartz, J., Roberts, T.H., and Hirschberg, K. (2000). Secretory protein trafficking and organelle dynamics in living cells. Annu Rev Cell Dev Biol *16*, 557-589.

MacPherson, H., Noble, B.S., and Ralston, S.H. (1999). Expression and functional role of nitric oxide synthase isoforms in human osteoblast-like cells. Bone *24*, 179-185.

Mallo M, Alonso CR. (2013). The regulation of Hox gene expression during animal development. Development, *140*, 3951–63.

Markovic, J., García-Gimenez, J.L., Gimeno, A., Viña, J., and Pallardó, F.V. (2010). Role of glutathione in cell nucleus. Free Radic Res *44*, 721-733.

Millet, S., Campbell, K., Epstein, D. J., Losos, K., Harris, E., Joyner, A. L. (1999). A role for Gbx2 in repression of Otx2 and positioning the mid/hindbrain organizer. Nature *401*, 161-164.

Murrell, W. (1879). Nitro-glycerine as a remedy for angina pectoris. The Lancet *113*, 225-27.

Münzel, T., Sayegh, H., Freeman, B.A., Tarpey, M.M., and Harrison, D.G. (1995). Evidence for enhanced vascular superoxide anion production in nitrate tolerance. A novel mechanism underlying tolerance and cross-tolerance. J Clin Invest *95*, 187-194.

Najdi R., Proffitt K. D., Sprowl S., Kaur S., Yu J., Covey T. M., Virshup D. M., Waterman M. L. (2012). A uniform human Wnt expression library reveals a shared secretory pathway and unique signaling activities. Differentiation 84, 203–213.

Niehrs C. (2012). The complex world of WNT receptor signalling. Nat. Rev. Mol. Cell Biol. 13, 767–779.

Oliveros, J. C. (2007–2015). Venny. An interactive tool for comparing lists with Venn's diagrams. http://bioinfogp.cnb.csic.es/ tools/venny/index.html.

Perlman, D.H., Bauer, S.M., Ashrafian, H., Bryan, N.S., Garcia-Saura, M.F., Lim, C.C., Fernandez, B.O., Infusini, G., McComb, M.E., et al. (2009). Mechanistic insights into nitrite-induced cardioprotection using an integrated metabolomic/proteomic approach. Circ Res *104*, 796-804.

Ream, T.S., Haag, J.R., Wierzbicki, A.T., Nicora, C.D., Norbeck, A., Zhu, J.K., Hagen, G., Guilfoyle, T.J., Pasa-Tolic, L., Pikaard, C.S. (2009). Subunit Compositions of the RNA-Silencing Enzymes Pol IV and Pol V Reveal Their Origins as Specialized Forms of RNA Polymerase II. Mol Cell 33, 192–203.

Reimand, J., Arak, T., and Vilo, J. (2011). g: Profiler--a web server for functional interpretation of gene lists (2011 update). Nucleic Acids Res *39*, W307-315.

Roeder, R.G., Rutter, W.J. (1969). Multiple forms of DNA-dependent RNA polymerase in eukaryotic organisms. Nature 5216, 234–237.

Roger, V.L., Go, A.S., Lloyd-Jones, D.M., Benjamin, E.J., Berry, J.D., Borden, W.B., Bravata, D.M., Dai, S., Ford, E.S., et al. (2012). Heart disease and stroke statistics--2012 update: a report from the American Heart Association. Circulation *125*, e2-e220.

Schindler, C., Chen, Y., Pu, J., Guo, X., Bonifacino, J. S. (2015). EARP is a multisubunit tethering complex involved in endocytic recycling. Nature Cell Biol *17, 639-650*.

Schulte G, Bryja V. (2007). The Frizzled family of unconventional G-protein-coupled receptors. Trends Pharmacol Sci 28, 518–525.

Smith, G.N., Walker, M.C., and McGrath, M.J. (1999). Randomised, double-blind, placebo controlled pilot study assessing nitroglycerin as a tocolytic. Br J Obstet Gynaecol *106*, 736-39.

Smith, G.N., Walker, M.C., Ohlsson, A., O'Brien, K., Windrim, R., and Canadian Preterm Labour Nitroglycerin Trial Group (2007). Randomized double-blind placebo-controlled trial of transdermal nitroglycerin for preterm labor. Am J Obstet Gynecol *196*, 37. e1-e8.

Szklarczyk, D., Franceschini, A., Wyder, S., Forslund, K., Heller, D., Huerta-Cepas, J., Simonovic, M., Roth, A., Santos, A., et al. (2015). STRING v10: protein-protein interaction networks, integrated over the tree of life. Nucleic Acids Res *43*, D447-452.

Veselik, D.J., Divekar, S., Dakshanamurthy, S., Storchan, G.B., Turner, J.M., Graham, K.L., Huang, L., Stoica, A., and Martin, M.B. (2008). Activation of estrogen receptor-alpha by the anion nitrite. Cancer Res *68*, 3950-58.

Williams, R.L., and Urbé, S. (2007). The emerging shape of the ESCRT machinery. Nat Rev Mol Cell Biol *8*, 355-368.

Xiong, X.F., Li, H., and Cao, E.H. (2007). PIG11 protein binds to DNA in sequence-independent manner in vitro. Biochem Biophys Res Commun 358, 29-34.

Zhang, Y. and Lu, H. (2009). Signaling to p53: ribosomal proteins find their way. Cancer Cell 5, 369-377.

Table 4.1. Genes present in pathways most affected by GTN exposure

Pathway	Genes
EIF2	*EIF2AK4, EIF3A, EIF4A2, EIF4G1, EIF4G2, HNRNPA1, IGF1R, INS, INSR, PABPC1, PIK3R2, PTBP1, RPL5, RPL6, RPL8, RPL13 RPL15, RPL21, RPL38, RPL27A, RPL7A, RPLP1, RPS2, RPS12 RPS13, RPS14, RPS20, RPS21, RPS23, RPS28, RPS15A, RPSA SREBF1*
mTOR	*EIF3A, EIF4A2, EIF4G1, EIF4G2, HMOX1, INS, INSR, PIK3R2, PPP2R2B, PRKAB2, PTPA, RHOA, RND2, RPS2, RPS12, RPS13, RPS14, RPS20, RPS21, RPS23, RPS28, RPS15A, RPSA, ULK1*
WNT/β-CATENIN	*AXIN1, BCL9, CDH3, CSNK2A2, FRZB, FZD1, FZD2, FZD3, FZD5 FZD7, GNAQ, HDAC1, ILK, PPP2R2B, PTPA, SMO, SOX3, SOX10, SOX11, TAB1, TCF3, WNT8A*
Single underline denotes similar genes found between the EIF2 and mTOR pathways. Double underline signifies similar genes between the mTOR and WNT/β-CATENIN pathways.	

Table 4.2a, b and c. List of genes, fold change, location and function found in each pathway that has been associated with phenotypes in mice that are similar to those observed in this study.

4.2a. EIF2 Signaling pathway

Symbol	Description	Fold Change	P-value	Function
EIF4A2	eukaryotic translation initiation factor 4A2	1.542	0.010	kinase
EIF4G1	eukaryotic translation initiation factor 4 gamma 1	-1.675	0.004	translation regulator
EIF4G2	eukaryotic translation initiation factor 4 gamma 2	1.67	0.022	translation regulator
HNRNPA1	heterogeneous nuclear ribonucleoprotein A1	-1.545	0.014	enzyme
IGF1R	insulin like growth factor 1 receptor	1.567	0.004	transmembrane receptor
INS	insulin	-2.226	0.007	
INSR	insulin receptor	-1.973	0.037	kinase
PIK3R2	phosphoinositide-3-kinase regulatory subunit 2	-1.544	0.008	kinase
PTBP1	polypyrimidine tract binding protein 1	-2.113	0.001	enzyme
RPL5	ribosomal protein L5	1.893	0.004	
RPL15	ribosomal protein L15	1.585	0.020	
RPL21	ribosomal protein L21	-1.93	0.017	
RPL27A	ribosomal protein L27a	1.79	0.030	
RPSA	ribosomal protein SA	1.949	0.004	translation regulator
SREBF1	sterol regulatory element binding transcription factor 1	-2.138	0.001	transcription regulator

4.2b. mTOR Signaling pathway

Symbol	Description	Fold Change	P-value	Function
EIF4G1	eukaryotic translation initiation factor 4 gamma 1	-1.675	0.004	translation regulator
EIF4G2	eukaryotic translation initiation factor 4 gamma 2	1.67	0.022	translation regulator
HMOX1	heme oxygenase 1	2.335	0.030	enzyme
INS	insulin	-2.226	0.007	
INSR	insulin receptor	-1.973	0.037	kinase
PIK3R2	phosphoinositide-3-kinase regulatory subunit 2	-1.544	0.008	kinase
PPP2R2B	protein phosphatase 2 regulatory subunit Bbeta	-1.571	0.014	phosphatase
PRKAB2	protein kinase AMP-activated non-catalytic subunit beta 2	-1.696	0.017	kinase
RPSA	ribosomal protein SA	1.949	0.004	translation regulator
ULK1	unc-51 like autophagy activating kinase 1	-1.51	0.016	kinase

4.2c. WNT/β-CATENIN Signaling pathway

Symbol	Description	Fold Change	P-value	Function
AXIN1	axin 1	-1.527	0.04	
CDH3	cadherin 3	-2.465	0.033	
FZD2	frizzled class receptor 2	-2.062	0.038	G-protein coupled receptor
FZD5	frizzled class receptor 5	1.548	0.029	G-protein coupled receptor
FZD7	frizzled class receptor 7	-1.798	0.015	G-protein coupled receptor
GNAQ	G protein subunit alpha q	2.228	0.0005	enzyme
HDAC1	histone deacetylase 1	-1.746	0.0002	transcription regulator
ILK	integrin linked kinase	-1.807	0.013	kinase
PPP2R2B	protein phosphatase 2 regulatory subunit Bbeta	-1.571	0.014	phosphatase
SMO	smoothened, frizzled class receptor	-2.605	0.001	G-protein coupled receptor
SOX3	SRY-box 3	-1.649	0.002	transcription regulator
SOX10	SRY-box 10	1.562	0.0001	transcription regulator
SOX11	SRY-box 11	-2.849	0.01	transcription regulator
TAB1	TGF-beta activated kinase 1 (MAP3K7) binding protein 1	-1.502	0.004	enzyme
TCF3	transcription factor 3	-1.93	0.003	transcription regulator

Table 4.3a, b and c. Functional enrichments of biological process within the Protein interaction network of pathways perturbed by GTN exposure

4.3a. Functional enrichment of biological pathways perturbed and their FDR rates in the eFI2 protein interaction pathways

#pathway ID	pathway description	observed gene count	false discovery rate
GO.0006413	translational initiation	25	3.04E-39
GO.0000184	nuclear-transcribed mRNA catabolic process, nonsense-mediated decay	22	5.82E-39
GO.0000956	nuclear-transcribed mRNA catabolic process	23	1.38E-37
GO.0006614	SRP-dependent cotranslational protein targeting to membrane	20	4.45E-35
GO.0019083	viral transcription	20	8.08E-35
GO.0019080	viral gene expression	20	3.56E-34
GO.0006415	translational termination	20	3.51E-31
GO.0006414	translational elongation	20	1.96E-30
GO.0019058	viral life cycle	20	2.54E-28
GO.0016032	viral process	24	2.00E-26

4.3b. Functional enrichment of biological pathways perturbed and their FDR rates in the mTOR protein interaction pathways

#pathway ID	pathway description	observed gene count	false discovery rate
GO.0006413	translational initiation	14	4.79E-18
GO.0000184	nuclear-transcribed mRNA catabolic process, nonsense-mediated decay	11	1.29E-15
GO.0000956	nuclear-transcribed mRNA catabolic process	12	1.29E-15
GO.0006614	SRP-dependent cotranslational protein targeting to membrane	10	3.70E-14
GO.0019083	viral transcription	10	3.70E-14
GO.0044270	cellular nitrogen compound catabolic process	13	3.70E-14
GO.0046700	heterocycle catabolic process	13	3.70E-14
GO.0019439	aromatic compound catabolic process	13	3.98E-14
GO.0019080	viral gene expression	10	6.46E-14
GO.1901361	organic cyclic compound catabolic process	13	9.31E-14

4.3c. Functional enrichment of biological pathways perturbed and their FDR rates in the WNT/B-cantenin protein interaction pathways

#pathway ID	pathway description	observed gene count	false discovery rate
GO.0060070	canonical Wnt signaling pathway	9	1.57E-12
GO.0016055	Wnt signaling pathway	9	4.39E-09
GO.0060429	epithelium development	13	4.39E-09
GO.0002009	morphogenesis of an epithelium	10	1.67E-08
GO.0009887	organ morphogenesis	12	1.67E-08
GO.0009790	embryo development	12	3.87E-08
GO.0048598	embryonic morphogenesis	10	1.16E-07
GO.2000026	regulation of multicellular organismal development	13	2.91E-07
GO.0009888	tissue development	13	3.02E-07
GO.0009653	anatomical structure morphogenesis	14	5.92E-07

Figure Legends:

Figure 4.1 Hierarchical clustering of expression profiles of HH 9 quail embryos exposed to 400 μM GTN and corn oil vehicle control. Clustering was based on 2031 differentially expressed genes (fold change >1.5, $p < 0.05$).

Figure 4.1

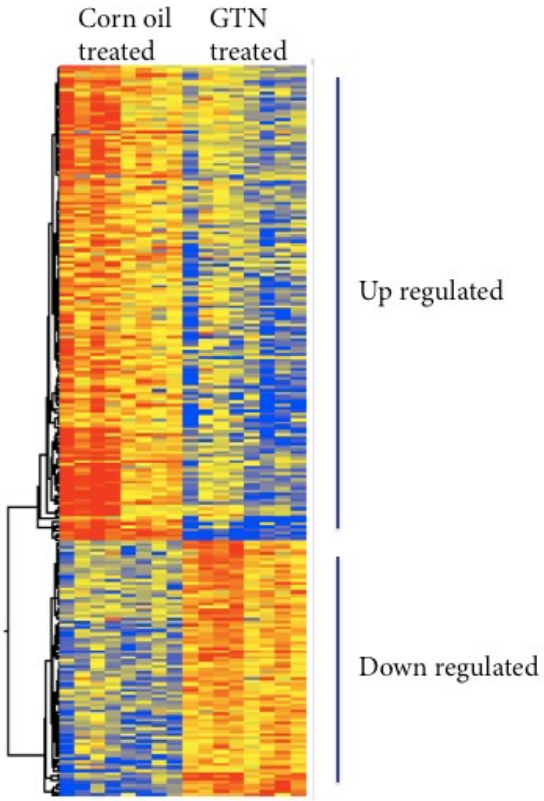

Figure 4.2 Bar graph of probes that were significantly upregulated or downregulated (expressed based on fold change) (> 1.5) both up and down and p -value (≤ 0.05) in response to GTN treatment in HH9 quail embryos.

Figure 4.2

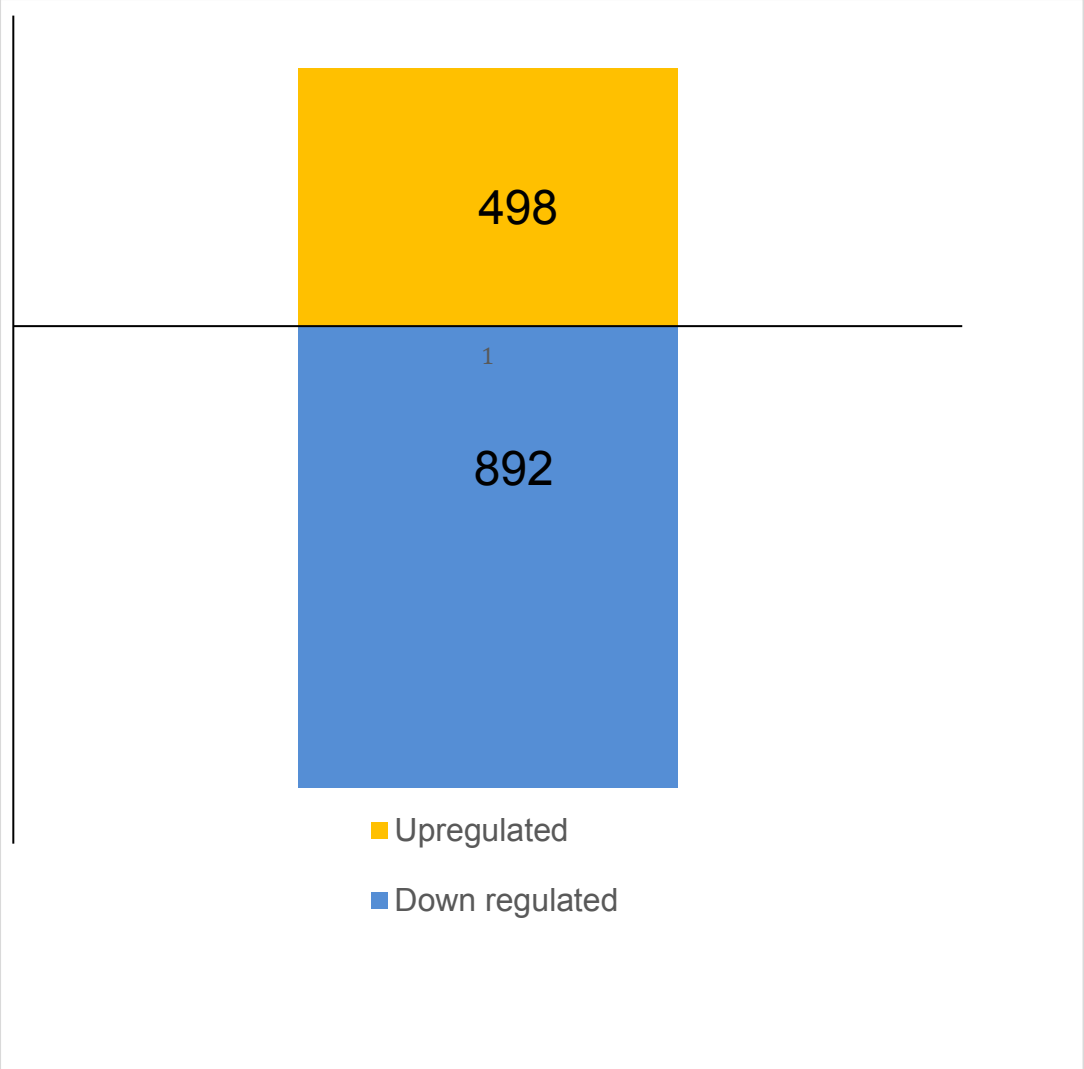

Figure 4.3 Predicted molecular pathways that were most affected by GTN exposure using the Ingenuity Pathway Analysis (IPA). Horizontal bars indicate the level of significance of each pathway indicated by –Log P-value and the ratio between detected genes in the microarray and total number of known genes in the database for that pathway. Statistical analysis was conducted with the IPA software.

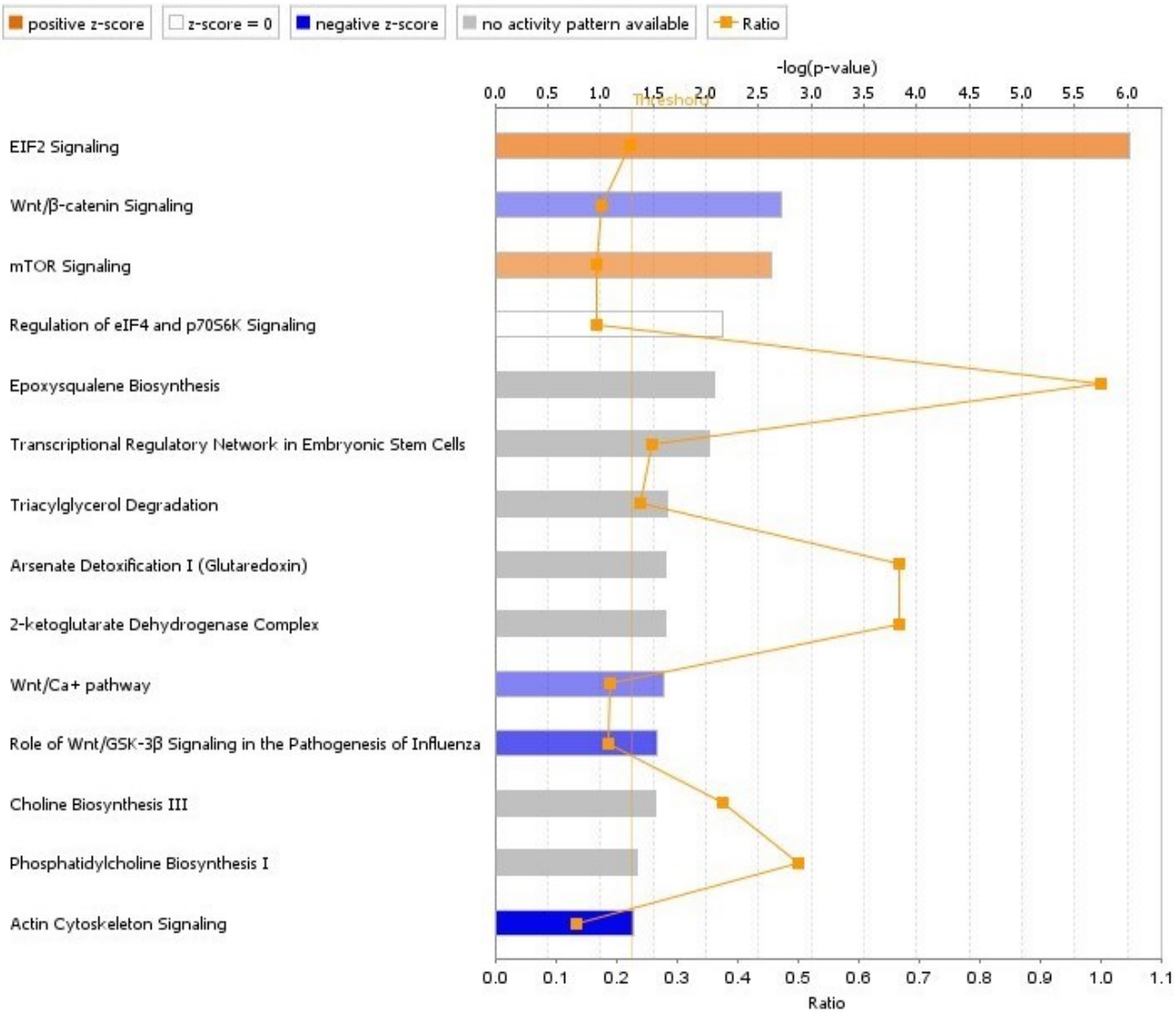
positive z-score
z-score = 0
negative z-score
no activity pattern available
Ratio
-log(p-value)
0.0 0.5 1.0 1.5 2.0 2.5 3.0 3.5 4.0 4.5 5.0 5.5 6.0
Threshold
EIF2 Signaling
Wnt/β-catenin Signaling
mTOR Signaling
Regulation of eIF4 and p70S6K Signaling
Epoxysqualene Biosynthesis
Transcriptional Regulatory Network in Embryonic Stem Cells
Triacylglycerol Degradation
Arsenate Detoxification I (Glutaredoxin)
2-ketoglutarate Dehydrogenase Complex
Wnt/Ca+ pathway
Role of Wnt/GSK-3β Signaling in the Pathogenesis of Influenza
Choline Biosynthesis III
Phosphatidylcholine Biosynthesis I
Actin Cytoskeleton Signaling
0.0 0.1 0.2 0.3 0.4 0.5 0.6 0.7 0.8 0.9 1.0 1.1
Ratio

Figure 4.4 Venn diagram of the number of common and unique genes associated with the EIF2, Wnt/B-catenin and mTOR signaling pathways.

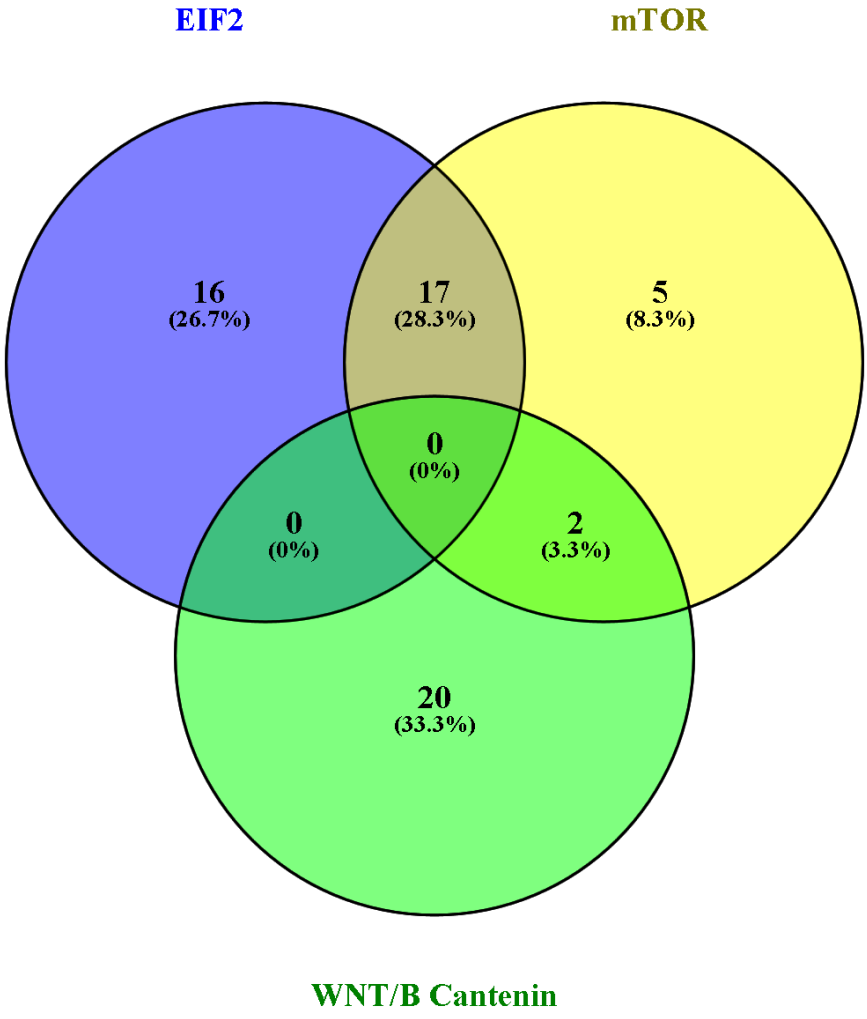
EIF2
mTOR
16
(26.7%)
17
(28.3%)
5
(8.3%)
0
(0%)
0
(0%)
2
(3.3%)
20
(33.3%)
WNT/B Cantenin

Figure 4.5 a, b and c. Matrix of the genes in the signaling pathways associated with phenotypes in both human and mouse.

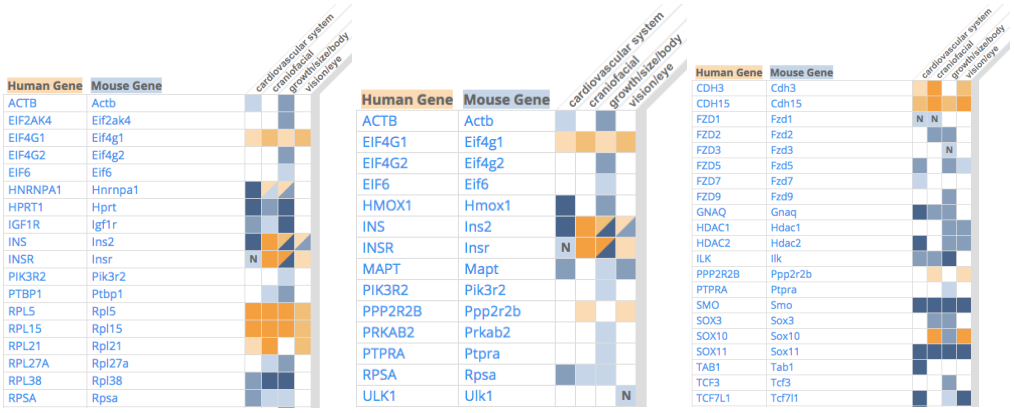

A B C

Terms are annotated to genes in human (orange) and mouse (dark blue). Darker colors indicate more annotations. (A) EIF2, (b) mTOR and (C) Wnt/B-cantenin.

Figure 4.6 a, b and c. Protein interaction network of pathways perturbed by GTN exposure

4.6a EIF2 Signalling pathway

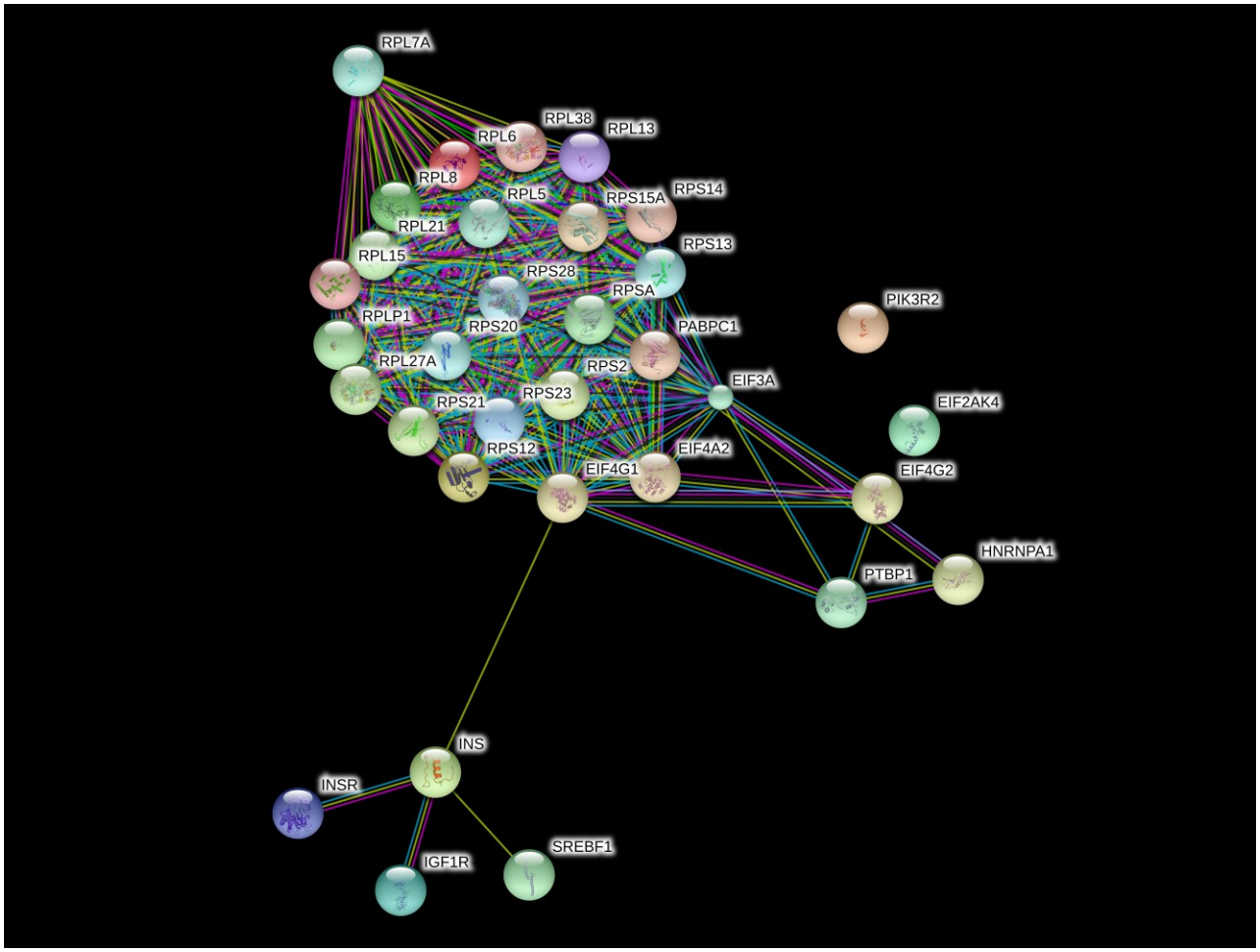

4.6b mTOR Signalling pathway

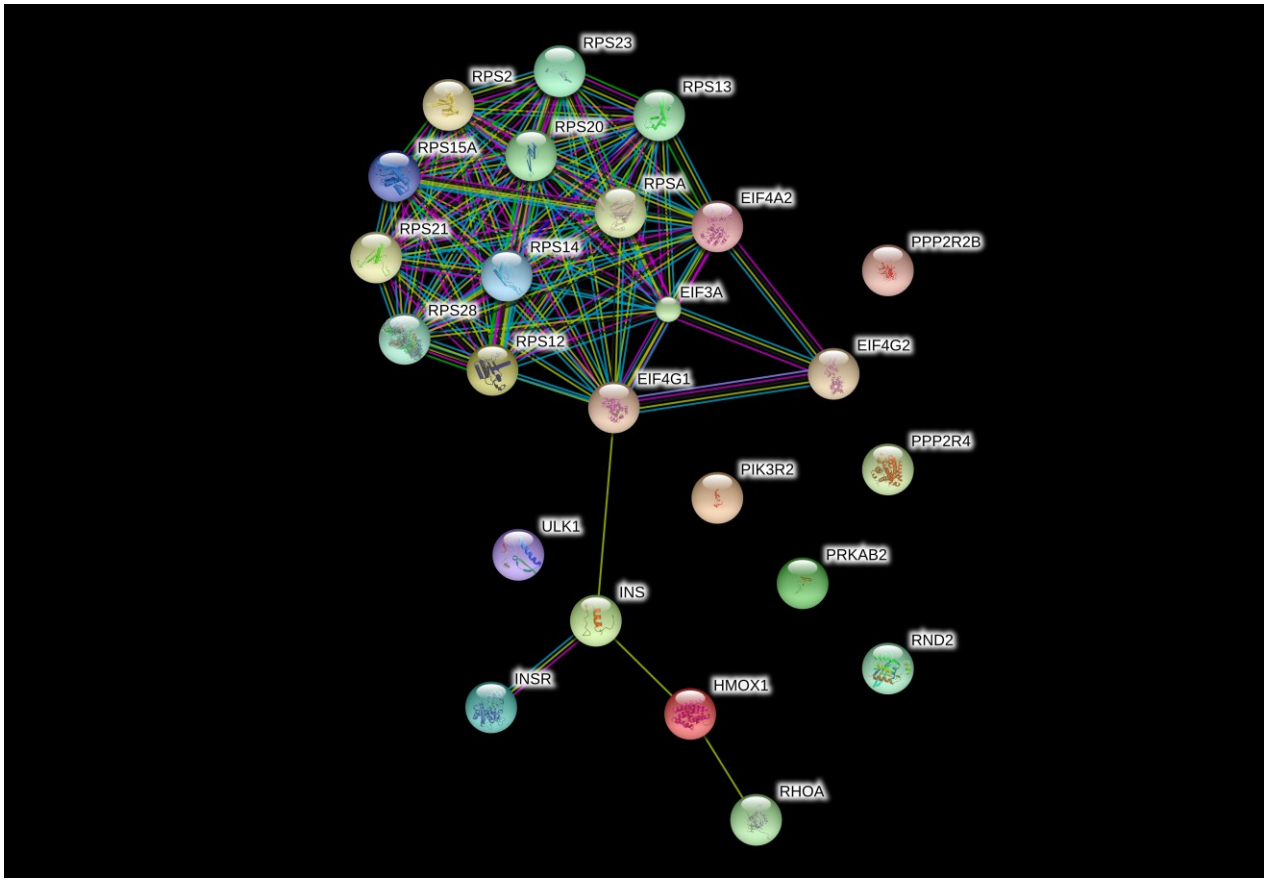

4.6c WNT/B-cantenin Signalling pathway

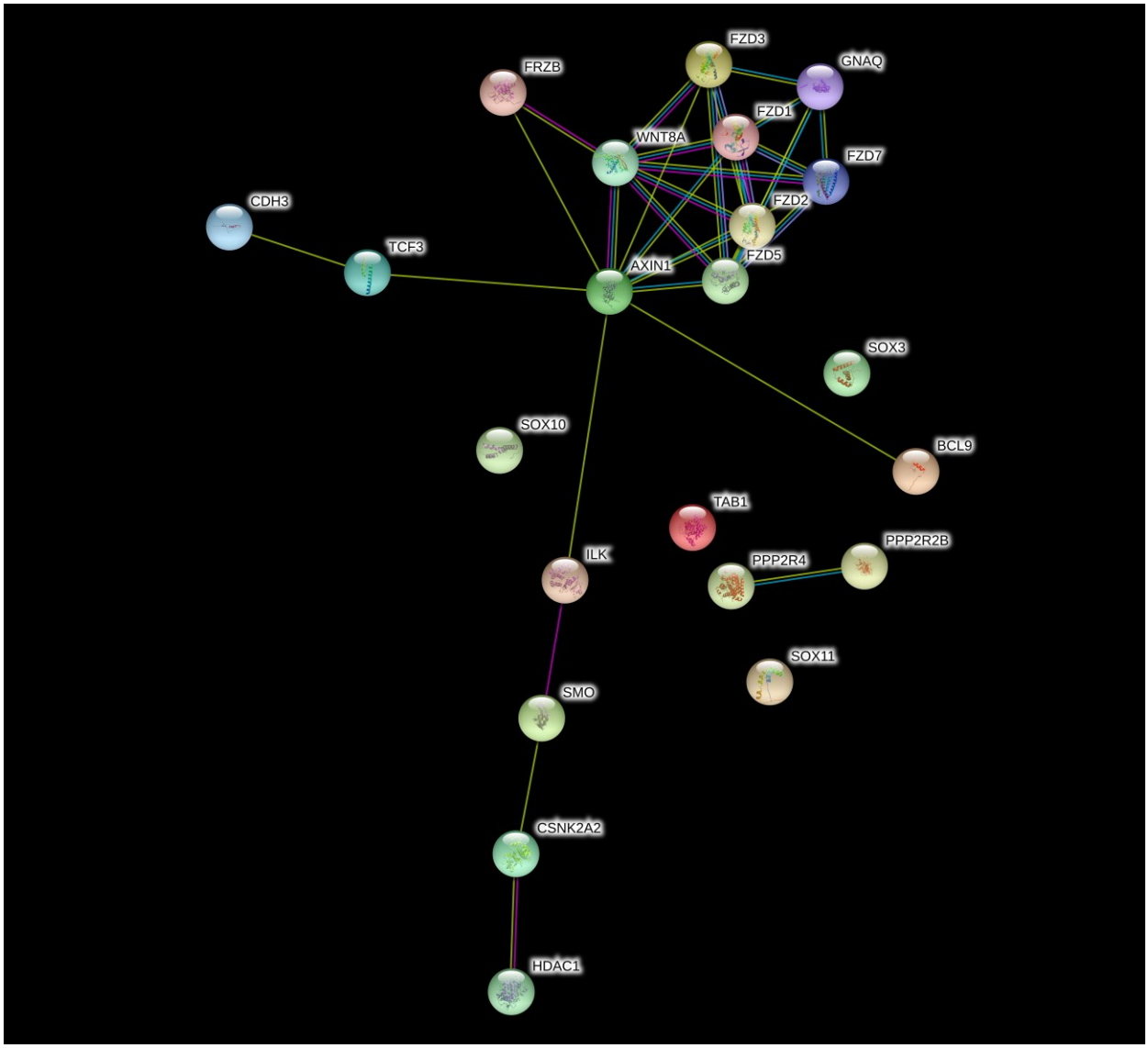

CHAPTER 5 – ORIGINAL CONTRIBUTIONS TO KNOWLEDGE, GENERAL DISCUSSION, CONCLUSION, AND FUTURE PERSPECTIVES

5.1 Original Contributions to Knowledge

Within this thesis, I presented my primary hypothesis that GTN is a developmental toxicant as well as formulated three research objectives. To investigate the developmental toxicity of GTN in a biological model that is representative of mammalian development, the Japanese quail embryo (*Cotournix cotournix japonica*); (2) determine the ability of the embryo to biotransform GTN; and 3) elucidate the effects of GTN on global gene expression. Each objective allowed me to gain new knowledge and make original contributions. These contributions are:

(1) GTN is highly embryotoxic to early stage quail embryos; the embryo lethality of GTN is greater in HH0 embryos than in HH 9 and 19 stage embryos.

(2) GTN exposure results in numerous malformations in quail embryos, including craniofacial, heart, and neural tube defects, and microphthalmia.

(3) Exposure to GTN produces an increase in protein nitration.

(4) The embryo and the embryonic eye can metabolize GTN, releasing nitrite and the metabolites 1,2- or 1,3-GDN and requiring GSH as an obligate cofactor.

(5) The metabolism of GTN results in a decrease in total GSH and an increase in the ratio of NADP+/NADPH.

(6) The major enzymes within the embryo responsible for the metabolism of GTN are the GST isozymes.

(7) The embryo and embryonic eye contain both α and μ type GSTs.

(8) Kinetic profiles of GSTs in the quail embryo differ significantly from those

purified from the eye.

(9) Presupplementation of embryos with NAC decreases GTN-induced embryo mortality and growth retardation.

(10) GTN treatment of HH 9 embryos results in the up-regulation and down-regulation of 498 and 892 genes, respectively.

(11) The highest fold increase in gene expression is observed in *Chmp4c* (Charged multivesicular body protein 4c) while the largest decrease in expression is in polymerase (RNA) III (DNA directed) polypeptide C (*POLR3C*).

(12) Ingenuity pathway analyses showed that the pathways most significantly disrupted by GTN exposure include EIF2A, mTOR, and WNT/B-cantenin signaling pathways.

(13) EIF2 and mTOR signaling pathways show significant overlap in the number of genes present in both pathways. WNT/B-cantenin shows no overlap with EIF2 and only two gene overlap with the mTOR pathway.

(14) Sixty-eight percent of the genes within the WNT/B-cantenin signaling match the observed phenotypes in this study; 45 and 42 % match the EIF2and mTOR pathways, respectively.

(15) Genes with functions as transcriptional regulators, G-protein coupled receptors, and kinases are over-represented as being involved in causing the expression of the observed phenotypes

5.2 **General Discussion**

This study enabled us to identify GTN as a developmental toxicant with the quail embryo as a model species, using both an *in-ovo* and *ex-ovo* exposure paradigms to determine the actions of the embryo on the drug, and to examine GTN-induced changes in global gene expression that may help to elucidate the mechanism of toxicity.

Data in the literature were conflicting with respect to the role of GTN as a developmental toxicant. In the few animal studies performed, isosorbide mononitrate treatment caused significant increases in the prolongation of gestation, prolonged parturition, stillbirth, and neonatal death in rats at doses of 500mg/kg/day (Wyeth-Ayerst Laboratories, 1993a); doses 35 and 150 times the maximum recommended human dose produced dose-related embryo toxicity in rabbits (Wyeth-Ayerst Laboratories, 1993b). Studies conducted with GTN in rats and rabbits, however, showed no adverse fetal effects (Hazardous Substances Databank). These incomplete and ambiguous data, taken together with the fact that the predominant metabolite of GTN, nitrite, is a biologically active molecule, warranted this study.

To address the central question of the developmental toxicity of GTN we used the quail embryo as our model. To our knowledge, our study is one of the first to be published, to demonstrate that *in ovo* GTN exposure was highly embryotoxic to early stage embryos and induced a dose dependent increase in the number of malformed viable quail embryos (Bardai et al., 2011). Our results clearly differ from those described above. One possible reason for these

divergent results could be due to the limitations of the avian biological model involved. The maternal drug metabolizing system represents the major source of the intra and interspecies variation in response to teratogens. The quail embryo is devoid of the maternal metabolic influences, i.e. the metabolism, pharmacokinetics, and accessibility of the drug is markedly different in the quail model. The avian embryo clearly does not possess a maternal drug metabolizing system. However, it does possess a drug metabolizing capacity that occurs from day 2 of incubation onwards, well after the dosing period in this study. While devoid of maternal metabolic influences, the quail embryo model affords a unique opportunity for investigating the direct interaction of GTN with the developing embryo. Clearly, a similar study using the metabolites of GTN would help to further elucidate the role of drug metabolism. I hypothesized that protein nitration may be the possible cause of the observed defects given that GTN has as a backbone a glycerol moiety with three nitrite ions. Nitrite ions have been shown to be biologically active (Bryan et al., 2005; Cao et al., 2009; Garcia et al., 2010), and nitrated proteins have been associated with hind limb defects (Fantel 1999). I sought to determine if protein nitration was associated with the increase in developmental defects observed after GTN exposure. Indeed, an increase in nitrated proteins was observed in the whole embryo and, more specifically, in the developing eye region of embryos exposed e*x-ovo* to GTN. Thus, my data indicate that GTN is in fact a developmental toxicant in this animal model and that nitrite may be involved in the mechanism of GTNs developmental toxicity (Bardai et al., 2013). Further

investigation into the role of nitrite is warranted since reports have described that GTN, or its nitrite metabolite, cause immediate spikes in adenosine triphosphate levels (Garcia et al., 2010). Extracellular adenosine triphosphate and the its first breakdown product, adenosine diphosphate, can act at the purinergic receptors P2Y1, P2Y12 and P2Y13 that are expressed in early embryo, while adenosine, a later product in the extracellular catabolic cascade, may act at four distinct G-protein-coupled receptors (Burnstock and Dale, 2015; Masse and Dale, 2012). Expression studies have demonstrated the presence of P2X, P2Y and adenosine receptors from gastrulation stages, suggesting that ATP, ADP and adenosine may also play a role during very early phases of development (Meyer et al., 1999). The increase of nitrated proteins after GTN treatment suggested that the embryo can biotransform GTN, although how the embryo metabolizes GTN is unknown. We investigated the mechanism of nitrite release from GTN by the embryo. Of the enzymes implicated in the metabolism of GTN, GSTs represent the single largest pool of detoxification enzymes present (Board et al., 2007), are found in adult quail (Bardai et al., 2006), and are the first and rate-limiting step in the release of NO_2^- from GTN catalyzed by cytosolic GSTs (Kozlov et al., 2003). Recently, we have found that adult type mu GSTs can, in fact, also metabolize polycyclic nitramine explosives (Bardai et al., 2006). In addition to their role in xenobiotic metabolism, GSTs are present in the squid and octopus eye as crystallins where they play a structural role (Tomarev et al., 1991; Zinovieva et al., 1993). Therefore, I hypothesized that the quail embryo contains GST-type enzyme(s) capable of metabolizing

GTN. We purified total GST's from the whole embryo and the embryo eye. This study showed that GSTs from both the whole embryo and embryo eye had the ability to metabolize GTN, releasing nitrite. Furthermore, we elucidated that the whole embryo and embryo eye contain multiple types of GSTs. However, we were unable to ascertain if all the forms of GST isolated in our study could metabolize GTN. Although these results enabled us to determine that nitrite is formed following denitration by embryo GSTs, they also revealed that GSH is a critical cofactor in the metabolism of GTN by embryo GSTs. While GSTs have been implicated in the metabolism of GTN other studies have shown a role for aldehyde dehydrogenase 2 (ALDH2), a mitochondrial isoform of the ALDH superfamily, in the bioactivation of GTN (Chen et al., 2002; Beretta et al., 2008). GAPDH, a key enzyme in glycolysis, has also been been identified as a enzyme capable of metabolizing GTN (Seabra et al., 2013). While all three of these enzymes have specified roles it is interesting to note that all these enzyme systems catalyze GTN biotransformation by a thiol-dependent enzymatic process and produce the same product profile following GTN metabolism, indicating that the thiol moiety is critical in both proper enzyme function and in the formation of a thiol radical.

Glutathione is the most abundant antioxidant defense molecule and is an obligatory cofactor for GSTs (Hayes et al. 2005). It is required for embryonic development because a knockout of GSH synthase (Gss) is embryonic lethal and Gss-null mice fail to undergo gastrulation (Winkler et al., 2011). The analysis of cofactor consumption revealed that there was a decrease in total

GSH. Furthermore, oxidation of GSH drives the formation of glutathione disulfide (GSSG), which can then be directly recycled to GSH through the enzyme glutathione disulfide reductase (GR), a reaction requiring NADPH (Lu et al., 2009). We also examined levels of NAPDPH; our studies revealed that NADPH was oxidized. Taken together, these results suggest that GTN exposure may disrupt the redox balance and/or the energy status in the developing embryo, leading to GSH depletion.

GSH and NADPH together play central roles in controlling cellular thiol/disulfide redox state. Proteins critical for embryo development contain redox-sensitive thiols, such as cysteine (Jones et al., 2008), that control DNA replication, DNA repair, chromatin structure, transcription factor DNA binding, and cell proliferation (Chiu et al., 2012). Another process with important implications for embryonic development is the interaction between GSH and epigenetic programming. It has been suggested that there are discrete pools of both nuclear and cytoplasmic GSH and the transport of GSH between these intracellular compartments is critical to the regulation of cell proliferation and, therefore, gene expression levels (Diaz Vivancos et al., 2010; Markovic et al., 2010). The cysteine peptide in GSH is synthesized from the same pool of homocysteine that is used for the synthesis of S adenosylmethionine (SAM), which serves as a cofactor for the methylation of DNA and histones (Hitchler et al., 2007). It is possible that GTN could induce a negative feedback loop whereby depletion of GSH, and therefore an imbalance in redox, could signal a need for increased synthesis of GSH. This could result in the shuttling of

metabolites that would be used for DNA methylation to GSH synthesis and thereby impair DNA methylation (Gowher et al., 2001), cumulating in the disruption of proper gene expression levels. Therefore, I hypothesized that the embryotoxic effects of GTN may be mediated by the dysregulation of gene expression. Our microarray study showed there was significant disruption in three pathways. One of the pathways, WNT/β-Cantenin, is clearly important in embryo development. Clearly, further studies are required to quantify these differences in gene expression levels.

5.3 Conclusion

In conclusion, GTN may be teratogenic to the developing quail embryo. It is also evident that the embryo can metabolize GTN. The detrimental consequences of GTN treatment also include perturbations in the normal gene expression of embryo development. The findings of this study unveil possible mechanisms and, therefore, the generation of interesting hypotheses by which GTN may disrupt gene expression, leading to unwanted outcomes during embryo development. This study creates a framework within which to experimentally examine pathways of normal and abnormal embryo development, from the microarray studies to examining the impact of GTN on the physiology of the embryo.

5.4 Future Perspectives

An understanding of the mechanisms of GTN's embryotoxic effects can help to open new areas of research on the effects of this widely-used therapeutic agent. While there is a clear dysmorphic embryo phenotype following GTN treatment, questions remain regarding the effect of GTN. Is GTN solely responsible for the teratogenic effects seen or is there an effect of the metabolites? Such questions would still have to be tested using a similar dose-response study. Regarding GSH specifically, a number of questions remain to be addressed. Are GSH levels affected *in-ovo* and, more importantly, are there discrete nuclear and cytoplasmic GSH pools present in the embryo? Are these pools affected following a challenge from GTN or the metabolites? It is known that GSH movement from the cytosol to the nucleus is an important factor in the control of the mammalian cell cycle because GSH recruitment into the nucleus is a very early event in the mammalian cell cycle (Markovic et al., 2007).

As was only briefly described in our studies, the role of NADPH also requires further investigation. The reduced forms of glutathione are regenerated by enzymes that require the reducing power of NADPH. This means that any imbalance in the reduced to oxidized ratio of pyridine nucleotides could alter the redox ratio of GSH to GSSG. Further investigation is also needed to determine if RPs are affected in any way by changes in the redox status of cells. Finally, my gene array studies have raised many interesting questions or hypotheses that might be tested. For example, it would

be interesting to study the changing distribution patterns of gene expression using both pathway and interactome analysis.

References

Bardai, G.K., Halasz, A., Sunahara, G.I., Dodard, S., Spear, P.A., Grosse, S., Hoang, J., Hawari, J., (2006). In vitro degradation of hexanitrohexaazaisowurtzitane (CL-20) by cytosolic enzymes of Japanese quail and the rabbit. Environ. Toxicol. Chem. 25, 3221-3229.

Bardai, G.K., Hales, B.F, et al. (2011). Developmental toxicity of glyceryl trinitrate in quail embryos. Birth Defects Res A Clin Mol Teratol *91*, 230-240.

Bardai, G.K., Hales, B.F, et al. (2013). Glyceryl trinitrate metabolism in the quail embryo by the glutathione S-transferases leads to a perturbation in redox status and embryotoxicity. Comp Biochem Physiol B Biochem Mol Biol *165*, 153-164.

Beretta, M., Gruber, K, et al. (2008). Bioactivation of nitroglycerin by purified mitochondrial and cytosolic aldehyde dehydrogenases. J Biol Chem *283*, 17873-880.

Board, P.G. (2007). The use of glutathione transferase-knockout mice as pharmacological and toxicological models. Expert Opin Drug Metab Toxicol *3*, 421-433.

Bryan, N.S., Fernandez, B.O, et al. (2005). Nitrite is a signaling molecule and regulator of gene expression in mammalian tissues. Nat Chem Biol *1*, 290-97.

Burnstock, G., and Dale, N. (2015). Purinergic signalling during development and ageing. Purinergic Signal. *3*, 277-305.

Cao, Z., Bell, J.B, et al. (2009). Nitrite enhances RBC hypoxic ATP synthesis and the release of ATP into the vasculature: a new mechanism for nitrite-induced vasodilation. Am J Physiol Heart Circ Physiol *297*, H1494-1503.

Chen, Z., Zhang, J, et al. (2002). Identification of the enzymatic mechanism of nitroglycerin bioactivation. Proc Natl Acad Sci U S A *99*, 8306-311.

Chiu, J., Dawes, I.W., (2012). Redox control of cell proliferation. Trends Cell Biol 22, 592-601.

Diaz Vivancos, P., Wolff, T., Markovic, J., Pallardó, F.V., and Foyer, C.H. (2010). A nuclear glutathione cycle within the cell cycle. Biochem J *431*, 169-178.

Fantel, A.G., Stamps, L.D., Tran, T,T., Mackler, B., Person, R.E., and Nekahi, N. (1999). Role of free radicals in the limb teratogenicity of L-NAME (N(G)-nitro-(L)-arginine methylester): a new mechanistic model of vascular disruption. Teratology. *60*, 151-60.

Garcia, J.I., Seabra, A.B., Kennedy, R., and English, A.M. (2010). Nitrite and nitroglycerin induce rapid release of the vasodilator ATP from erythrocytes: Relevance to the chemical physiology of local vasodilation. J Inorg Biochem *104*, 289-296.

Gowher, H., and Jeltsch, A. (2001). Enzymatic properties of recombinant Dnmt3a DNA methyltransferase from mouse: the enzyme modifies DNA in a non-processive manner and also methylates non-CpG [correction of non-CpA] sites. J Mol Biol *309*, 1201-08

Kozlov, A.V., Dietrich, B, et al. (2003). Various intracellular compartments cooperate in the release of nitric oxide from glycerol trinitrate in liver. Br J Pharmacol *139*, 989-997.

Lu, S.C., (2009). Regulation of glutathione synthesis. Mol Aspects Med. 30, 42-59.

Markovic, J., Borrás, C, et al. (2007). Glutathione is recruited into the nucleus in early phases of cell proliferation. J Biol Chem *282*, 20416-424.

Markovic, J., García-Gimenez, J.L, et al. (2010). Role of glutathione in cell nucleus. Free Radic Res *44*, 721-733.

Massé K., and Dale, N. (2012). Purines as potential morphogens during embryonic development. Purinergic Signal *3*, 503-21

Mayer, B., and Beretta, M. (2008). The enigma of nitroglycerin bioactivation and nitrate tolerance: news, views and troubles. Br J Pharmacol *155*, 170-184.

Meyer, M.,P., Clarke, J.,D., Patel, K., Townsend-Nicholson, A., and Burnstock ,G. (1999). Selective expression of purinoceptor cP2Y1 suggests a role

for nucleotide signalling in development of the chick embryo. Dev Dyn *214*, 152–158.

Seabra, AB., Ouellet, M., Antonic, M., Chretien, M.N., and English A.M. (2013). Catalysis of nitrite generation from nitroglycerin by glyceraldehyde-3-phosphate dehydrogenase (GAPDH). Nitric Oxide *35*, 116–122,

Tomarev, S.I., Zinovieva, R.D., Piatigorsky, J., (1991). Crystallins of the octopus lens. Recruitment from detoxification enzymes. J. Biol. Chem. 266, 24226-24231.

Winkler, A., Njålsson, R., Carlsson, K., Elgadi, A., Rozell, B., Abraham, L., Ercal, N., Shi, Z.Z., Lieberman, M.W., et al. (2011). Glutathione is essential for early embryogenesis--analysis of a glutathione synthetase knockout mouse. Biochem Biophys Res Commun *412*, 121-26

Wyeth-Ayerst Laboratories: Product information. Ismo. (1993a).

Wyeth-Ayerst Laboratories: Product information. Isordil. (1993b).

Zinovieva, R.D., Tomarev, S.I., and Piatigorsky, J. (1993). Aldehyde dehydrogenase-derived omega-crystallins of squid and octopus. Specialization for lens expression. J Biol Chem *268*, 11449-455